Hyperpolarizability contributions to the second Kerr-effect virial coefficients of non-dipolar molecules

by

Mbukeni Mzwandile Mhlongo

Submitted in partial fulfilment of the requirements for the degree of Master of Science in Physics in the School of Chemistry and Physics, University of KwaZulu-Natal.

School of Chemistry and Physics

University of KwaZulu-Natal

Private Bag X01, Pietermaritzburg

Scottsville 3209, South Africa

Supervisor: Dr V W Couling

2020

Abstract

The molecular theory of the second Kerr-effect virial coefficient, B_{K}, describing the effects of interacting pairs of molecules on the molecular Kerr constant for molecules with non-linear symmetry is reviewed, and then extended to include second hyperpolarizability contributions in the molecular interactions. The classical long-range dipole–induced-dipole model is used to describe the interactions between pairs of molecules.

This investigation has been limited to non-dipolar species, where the permanent electric quadrupole moment is the leading multipole moment, since for dipolar species, the hyperpolarizability contributions will likely be masked by the generally much-larger contributions arising from the permanent electric dipole moment. The resulting expressions for contributions to B_K are evaluated numerically (using Gaussian quadrature) for nitrogen (N_2), carbon dioxide (CO_2) and ethene (C_2H_4), these molecules having measured data against which to assess the theoretical predictions.

N_2 and CO_2 are axially-symmetric molecules, while C_2H_4 is of lower symmetry, belonging to the D_{2h} point group. Previous attempts to approximate the molecular properties of C_2H_4 to axial symmetry in calculations of B_{K} have produced theoretical results which significantly underestimate the measured data. Inclusion of the full molecular symmetry has been shown to be essential if the molecular-tensor theory

is to yield reasonable agreement with experimental data.

For CO_2 the quadrupole–induced-dipole contribution dominates, and the interaction-induced hyperpolarizability contribution to B_{K} is only 0.3% at 200 K rising to 1.5% at 500 K. For the N_2 and C_2H_4 molecules, the collision-induced hyperpolarizability contributes just under 2% at 200 K, rising to 4% at 500 K for N_2, and 5.5% for C_2H_4. These contributions are non-negligible, and are hence worth refining in future work through full *ab initio* quantum mechanical computation of the interaction-induced hyperpolarizability contribution where dispersion force and electron cloud overlap effects can be included.

Declaration

I, Mbukeni Mzwandile Mhlongo, declare that

1. The research reported in this thesis, except where otherwise indicated, is my original research.

2. This thesis has not been submitted for any degree or examination at any other university.

3. This thesis does not contain other persons' data, pictures, graphs or other information, unless specifically acknowledged as being sourced from other persons.

4. This thesis does not contain any other persons' writing, unless specifically acknowledged as being sourced from other researchers. Where other written sources have been quoted, then:

   (a) their words have been rewritten but the general information attributed to them has been referenced;

   (b) where their exact words have been used, their writing has been placed inside quotation marks, and referenced.

5. This thesis does not contain text, graphics or tables copied and pasted from the internet, unless specifically acknowledged, and the source being detailed in the thesis and in the References sections.

Signed .....  .....

on this 13th day of March 2020

I hereby certify that this statement is correct.

Signed .....  .....

V W Couling

Supervisor

Acknowledgements

I would love to take this opportunity to thank the people who helped me through this project.

Firstly, I would like to thank Dr Couling for the opportunity he gave me to work with him and for his constant help and support throughout this project. As my teacher and mentor, he has taught me more than I could ever give him credit for here. He has shown me, by his example, what a good scientist, and person, should be.

Nobody has been more important to me in the pursuit of this project than the members of my family. I would like to thank my parents, whose love and guidance are with me in whatever I pursue even when it was hard for them to understand, but I'm grateful for the life they gave me and for allowing me to do this work.

This year has been so hard, and I would like to dedicate this achievement to my late mother Welephi Mhlongo: I want to thank you for the drive and confidence you have instilled in me which helped me to pursue this work. This is all for you and dad, wishing you were here as well to celebrate with us but I'm sure you are.

This work would not have been possible without the financial support I obtained from the CSIR IBS Bursary for which I am grateful.

I am grateful to everyone who has been in my life for the support and all types of encouragement they have given me.

Contents

List of Tables

List of Abbreviations

CC3	iterative approximate coupled cluster singles, doubles, and triples
CCSD	coupled cluster method with single and double replacements
CH_3F	fluoromethane
CH_2F_2	difluoromethane
CHF_3	trifluoromethane
CO_2	carbon dioxide
C_2H_4	ethene
C_2H_6	ethane
$(CH_3)_2O$	dimethyl ether
CH_3COCH_3	acetone
DID	dipole–induced-dipole
ESHG	electric-field-induced second-harmonic generation
H_2	hydrogen
H_2S	hydrogen sulphide
N_2	nitrogen
NLO	nonlinear optics
QID	quadrupole−induced-dipole
SCF	self-consistent field
SO_2	sulphur dioxide
t-aug-cc-pVTZ	triply-augmented correlation-consistent polarized valence triple zeta

Chapter 1

Review and Introduction

1.1 Review

In 1875, the Reverend John Kerr reported his observation that upon placing an isotropic medium in a strong uniform electric field, the medium generally becomes birefringent [1]. This project is concerned with the Kerr effect in gaseous media, where the application of a uniform static electric field induces anisotropy in the molecular distribution through two possible mechanisms, namely (i) the anisotropy which is induced in the molecules due to the applied electric field itself, and (ii), in the case of molecules which possess a permanent dipole moment, through the intrinsic anisotropy in the individual molecules, since the electric field will exert a torque on a dipolar molecule, resulting in partial alignment of the molecules.

Kerr-effect measurements in gases permit the determination of molecular polarizabilities and hyperpolarizabilities, and if measurements are carried out over a sufficiently large range of gas densities, the second Kerr-effect virial coefficients can also be obtained. Extraction of these properties from experimental data requires mathematical relationships between the macroscopic experimental observables and the molecular-property tensors of the individual molecules [2–4].

In 1955, Buckingham and Pople developed a molecular-tensor theory to account for the Kerr-effect in ideal gases of atoms or axially-symmetric molecules [5]. Buckingham then developed a statistical-mechanical theory of the Kerr constant to account for the density-dependence of the Kerr effect in real gases of atoms or axially-symmetric molecules [6]. In 1969, this theory was refined by Buckingham and Orr to calculate values of the second Kerr-effect virial coefficient B_{K} for difluoromethane (CH_2F_2), fluoromethane (CH_3F) and trifluoromethane (CHF_3) [7]. Here, they included additional effects of polarizability and angle-dependent repulsive forces, but their calculated B_{K} only yielded approximate agreement with their measured value for CH_3F, while the calculated B_{K} for CHF_3 was far too small. Attributing this to the effects of short-range interactions on the polarizability and potential energy, they posited that measurements of B_{K} for gases of dipolar molecules would probably not provide useful information about the nature of intermolecular forces. This discrepancy between experiment and theory for the fluoromethanes was resolved in 1983, when Buckingham, Galwas and Fan-Chen included the collision-induced polarizability in the theory, finding that it was the predominant contribution to B_{K} [8]. Using a simple Stockmayer-type potential, they obtained reasonable agreement with the measured B_{K} data for the fluoromethanes over the experimental range of temperature, although the large uncertainty of around 50% in the experimental values was a limitation on the test of the new theory.

Buckingham's theory was extended by Couling and Graham to include gases of dipolar molecules with nonlinear (and higher) symmetry, and also to include higher-order molecular-interaction terms to ensure convergence to a meaningful result [9]. Calculations for the dipolar molecules CH_3F, CH_2F_2, CHF_3, sulphur dioxide (SO_2), dimethyl ether ($(CH_3)_2O$), acetone (CH_3COCH_3) and hydrogen sulphide (H_2S) over a range of temperatures generally are within the uncertainty limits of the available literature experimental values [9–11]. Quadrupole and field gradient contributions

were neglected, being assumed to be negligible for molecules with large permanent dipole moments, but these contributions need not be negligible in the case of non-dipolar molecules. Couling and Naidoo included quadrupole−induced-dipole (QID) molecular-interaction contributions in 2017, and calculations of B_{K} for the non-dipolar molecules CO_2, C_2H_4 and ethane (C_2H_6) yielded reasonably good agreement with the measured data [12]. Those molecules which possess a relatively large quadrupole moment and polarizability anisotropy were found to have QID interaction contributions which can exceed those arising from the pure polarizability terms.

1.2 Interaction-induced hyperpolarizabilities

The question which arises is whether the hitherto-ignored collision-induced second-hyperpolarizability contribution $\gamma^{\mathrm{K}}(-\omega;\omega,0,0)$ to B_{K} for non-dipolar molecules is indeed sufficiently small that it may be safely neglected. The aim of this project has been to attempt an answer to this question. It is profitable, though, to first review any related investigations in the literature.

Donley and Shelton have measured the effects of molecular interactions on dc electric-field-induced second-harmonic generation (ESHG) molecular hyperpolarizabilities $\gamma^{\mathrm{ESHG}}(-2\omega;\omega,\omega,0)$ for the non-dipolar atoms and molecules helium (He), H_2, N_2 and argon (Ar) [13]. They compared their measured pair-interaction contributions with values obtained from a classical dipole–induced-dipole (DID) model, and found that their model underestimated the magnitude of the density dependence of the hyperpolarizability by around two times, and had the opposite sign. Buckingham, Concannon and Hands subsequently investigated the effect of dipolar interaction on the independent components of the hyperpolarizability of a pair of spehrical atoms (also using a classical DID model) for five different nonlinear-optical (NLO) phenom-

ena, including ESHG and the Kerr effect [14, 15]. They showed that Donley and Shelton's expression for the DID contribution to the pair hyperpolarizability differs from the original expression derived by Hunt [16], and this led to the correction of Donley and Shelton's expression by a numerical factor of $76/(5\times48)$ [17].

Concannon has also performed *ab initio* SCF calculations of the polarizability and second hyperpolarizability for interacting pairs of atoms at various internuclear separations [14]. The DID model employs the long-range theory of intermolecular interactions, where the molecules retain their separate identities even for short-range interactions where the electron clouds (and wavefunctions) actually begin to overlap [18]. The *ab initio* quantum mechanical calculations show that for interacting helium atoms, for long-range interatomic separations of 0.35 nm and greater, the calculated classical and quantum mechanical interaction-induced effects on the second hyperpolarizability are in excellent agreement, but for short-range separations of less than 0.35 nm, the classical model predicts larger interaction-induced effects since it neglects the electron overlap effects which are accounted for in the SCF calculations [14].

There have been various subsequent investigations of collision-induced hyperpolarizabilities between pairs of atoms, and occasionally between pairs of small molecules (such as hydrogen (H_2)), for example in references [19–26]. The *ab initio* computations have become increasingly accurate, but there remain restrictions on extending the calculations to polyatomic molecules of low symmetry, arising principally from the computational demands. What emerges is that the classical long-range DID model for interaction-induced hyperpolarizabilities is less effective than that for interaction-induced polarizabilities, which supports the notion that hyperpolarizabilities are greatly determined by the electronic structure of the outer reaches of the electron cloud [14, 27], making the collision-induced hyperpolarizability very

sensitive to the overlap of the electronic wavefunctions of the interacting atoms or molecules [14, 19, 20]. This necessitates the use of large basis sets with diffuse basis functions if accurate *ab initio* results for interaction-induced hyperpolarizabilities are to be obtained, which increases the computational demands considerably.

1.3 The aim of this project

In this project, the molecular-tensor theory of the Kerr effect is extended to include, in the classical DID long-range model, the contributions to B_{K} arising from the optical-frequency second hyperpolarizability $\gamma^{\mathrm{K}}(-\omega;\omega,0,0)$. This should provide a useful estimate of the order of magnitude of the hyperpolarizability contributions, and indicate whether they are completely negligible, or whether they are sizeable enough to warrant future investigation at the quantum mechanical level, where inclusion of dispersion force and electron cloud overlap effects will refine the accuracy and precision of our knowledge of their contribution.

The permanent multipole moments of a molecule (e.g. its electric dipole and quadrupole moments) are fundamental properties which describe the molecular charge distribution, while the molecular (hyper)polarizabilities describe the distortion of the molecular charge distribution by applied fields or the fields arising from the permanent moments of neighbouring molecules [28–31]. These permanent multipole moments and polarizabilities provide key insight into molecular structure and intermolecular forces, and are crucial to the development of the molecular-tensor theory of the Kerr effect. Hence they are now reviewed in sufficient detail to permit the subsequent development of the Kerr effect theory, which is presented in Chapter 2.

1.4 The multipole expansion

The description of two interacting molecules can be simplified provided the separation of the molecules is sufficiently large, allowing for the expansion of the electrostatic potential of a molecule about an arbitrary origin which is close to the charges. The resulting series of moments of charge provide a useful characterization of the molecule.

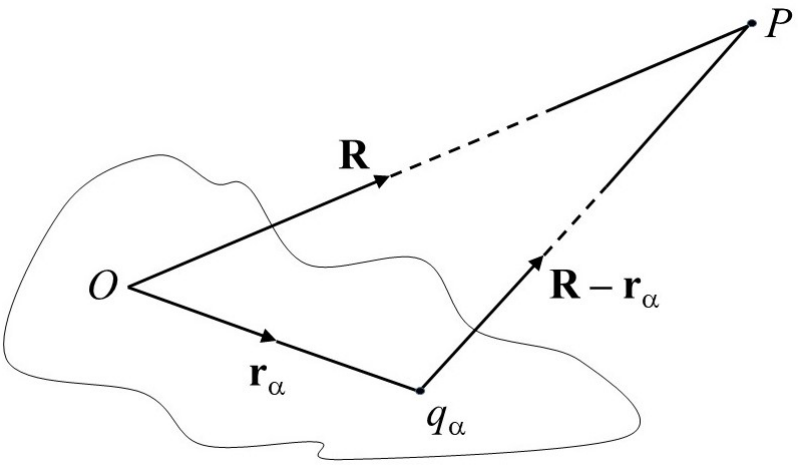

Figure 1.1: Coordinates and notation used for a discrete charge distribution.

Consider a distribution of N charges q_α in a vacuum ($\alpha = 1, 2, \cdots, N$), the charges having displacement vectors $\mathbf{r}_\alpha$ from the (arbitrary) origin O which is within, or close to, the distribution as indicated in Figure 1.1. The electrostatic potential ϕ which arises at an arbitrary point P with displacement vector $\mathbf{R}$ from O, where $R > r_\alpha$, is then

$$\phi(\mathbf{R}) = \frac{1}{4\pi\varepsilon_0} \sum_{\alpha=1}^{N} \frac{q_\alpha}{|\mathbf{R} - \mathbf{r}_\alpha|} \ . \tag{1.1}$$

The binomial theorem allows the denominator of this summation to be expanded,

yielding

$$\phi(\mathbf{R}) = \frac{1}{4\pi\varepsilon_0}\left[\frac{1}{R}\sum_\alpha q_\alpha + \frac{R_i}{R^3}\sum_\alpha q_\alpha\, r_{\alpha i} + \frac{3R_iR_j - R^2\delta_{ij}}{2R^5}\sum_\alpha q_\alpha\, r_{\alpha i}r_{\alpha j} + \cdots\right] . \tag{1.2}$$

Here, the Roman subscripts $i, j, \cdots$, denote tensor components, which can be equal to the Cartesian components 1, 2 or 3 of molecule-fixed axes $O(1, 2, 3)$. The Einstein summation convention is invoked, whereby a repeated Roman subscript denotes a summation over all three Cartesian components. δ_{ij} is the Kronecker delta tensor, with $\delta_{ij} = 1$ if $i = j$, $\delta_{ij} = 0$ if $i \neq j$. The electric moments of the distribution are:

the total charge

$$q = \sum_\alpha q_\alpha \ , \tag{1.3}$$

the electric dipole moment

$$\mu_i = \sum_\alpha q_\alpha\, r_{\alpha i} \ , \tag{1.4}$$

and the primitive (or traced) electric quadrupole moment

$$Q_{ij} = \sum_\alpha q_\alpha\, r_{\alpha i}r_{\alpha j} \ . \tag{1.5}$$

The higher-order moments (i.e. octopole, hexadecapole, $\cdots$) will not be considered in this work, since they make successively smaller contributions to the electrostatic potential, and we will be considering non-dipolar molecules which possess a permanent electric quadrupole moment as the leading moment. The electric quadrupole moment defined in equation (1.5) is the primitive (or traced) quadrupole moment. An alternative definition known as the traceless quadrupole moment is useful since

it describes the departure from spherical symmetry of the charge distribution: [29]

$$\Theta_{ij} = \frac{1}{2}\left(3Q_{ij} - Q_{kk}\delta_{ij}\right) = \frac{1}{2}\sum_{\alpha} q_{\alpha}\left(3r_{\alpha i}r_{\alpha j} - r_{\alpha}^{2}\delta_{ij}\right) \ . \tag{1.6}$$

Here $\Theta_{ii} = 0$, hence the name "traceless".

The electrostatic potential of the charge distribution can be written in terms of these moments of charge, becoming

$$\phi(\mathbf{R}) = \frac{1}{R}\,q + \frac{R_i}{R^3}\,\mu_i + \frac{3R_iR_j - R^2\delta_{ij}}{3R^5}\,\Theta_{ij} + \cdots \ . \tag{1.7}$$

In this expression, the terms for successively higher multipole moments make contributions which grow successively smaller by a factor of the order $\frac{1}{R}$. A consequence of this is that the leading non-zero moment will provide a reasonable description of the electrostatic potential ϕ at point P as long as the distance R is sufficiently large. Since the contribution to the expanded property arising from each of the multipole moments depends only on the displacement $\mathbf{R}$ of point P from O, the multipole moments are considered to be located at the origin O.

If an electrostatic field $\mathbf{E}$ is applied to the charge distribution, the distribution will experience a net force $\mathbf{F}$ given by

$$F_i = \sum_{\alpha} q_{\alpha}E_{\alpha i} = q(E_i)_0 + \mu_j(\nabla_j E_i)_0 + \frac{1}{3}\Theta_{jk}(\nabla_k\nabla_j E_i)_0 + \cdots \ . \tag{1.8}$$

Here, the field and its derivatives are determined at the origin O about which the Taylor expansion of the field has been taken. From equation (1.8), it can be shown that a dipolar charge distribution will experience a torque in a region of uniform field, or that a quadrupolar charge distribution will experience a torque in a region of uniform field gradient. Equation (1.8) can be used to determine the potential

energy U of the charge distribution in the presence of an applied electrostatic field $\mathbf{E}$ [31, 32]:

$$U = -\int_{r_1(\mathbf{E}=0)}^{r_2(\mathbf{E}=\mathbf{E})} F_i \, dr_i = q\phi - \int_0^{\mathbf{E}} \mu_i \, dE_i - \frac{1}{3}\int_0^{\mathbf{E}} \Theta_{ij} \, d(\nabla_j E_i) - \cdots \ . \tag{1.9}$$

For a rigid charge distribution, only the permanent multipole moments will contribute to equation (1.9), giving

$$U = q\phi - \mu_i^{(0)} E_i - \frac{1}{3}\Theta_{ij}^{(0)} \nabla_j E_i - \cdots \ . \tag{1.10}$$

Here, the permanent multipole moments are identified by a superscript $^{(0)}$.

For an axially symmetric charge distribution, each multipole moment is determined by a single scalar quantity, namely q, μ, Θ, $\cdots$; for example, the quadrupole moment Θ_{ij} has principal components $\Theta_{33} = \Theta$, $\Theta_{11} = \Theta_{22} = -\frac{1}{2}\Theta$.

The effect of a change of origin on a quadrupole moment can be established by moving O by $\mathbf{r}'$ to O'. The quadrupole moment Θ' relative to the new origin O' is

$$\Theta'_{ij} = \frac{1}{2}\sum_\alpha q_\alpha \left(3r'_{\alpha i} r'_{\alpha j} - (r'_\alpha)^2 \delta_{ij}\right) \tag{1.11}$$

which becomes

$$\Theta'_{ij} = \Theta_{ij} - \frac{3}{2}\mu_i r'_j - \frac{3}{2}\mu_j r'_i + \mu_k r'_k \delta_{ij} + \frac{1}{2} q \left\{3r'_i r'_j - (r')^2 \delta_{ij}\right\} \ . \tag{1.12}$$

The quadrupole moment is seen to be independent of the choice of origin provided both q and μ_i are zero. More generally, it is possible to show that only the leading non-zero electric multipole moment is independent of the choice of origin. For a dipolar molecule, the quadrupole moment *will* depend on the location of the ori-

gin. In this work, we will only consider non-dipolar molecules, since in the case of dipolar molecules the large contributions to $B_{\rm K}$ arising from the permanent dipole moments will most likely completely swamp the much smaller hyperpolarizability contributions.

1.5 The induced dipole moment

The total electric dipole moment of a molecule in the presence of both an oscillating light-wave field $\boldsymbol{\mathscr{E}}$ and static applied field $\mathbf{E}$ is [2, 5, 28, 33, 34]

$$\begin{aligned}\mu_i = &\mu_i^{(0)} + \alpha_{ij}(0;0)E_j + \alpha_{ij}(-\omega;\omega)\mathscr{E}_j + \tfrac{1}{2}\beta_{ijk}(0;0,0)E_jE_k + \beta_{ijk}(-\omega;\omega,0)\mathscr{E}_jE_k \\ &+ \tfrac{1}{6}\gamma_{ijkl}(0;0,0,0)E_jE_kE_l + \tfrac{1}{2}\gamma_{ijkl}(-\omega;\omega,0,0)\mathscr{E}_jE_kE_l + \cdots ,\end{aligned} \tag{1.13}$$

where all tensors are referred to the molecule-fixed axes $O(1,2,3)$. $\mu_i^{(0)}$ is the permanent dipole moment, while, respectively, $\alpha_{ij}(0;0)$ and $\alpha_{ij}(-\omega;\omega)$ are the static and dynamic dipole polarizabilities, $\beta_{ijk}(0;0,0)$ and $\beta_{ijk}(-\omega;\omega,0)$ are the static and dynamic first hyperpolarizabilities, and $\gamma_{ijkl}(0;0,0,0)$ and $\gamma_{ijkl}(-\omega;\omega,0,0)$ are the static and dynamic second hyperpolarizabilities. These molecular polarizabilities describe the distortion of the molecule by the external static and dynamic electric fields. The tensors $\beta_{ijk}(0;0,0)$ and $\gamma_{ijkl}(0;0,0,0)$ are symmetric in all indices, while $\beta_{ijk}(-\omega;\omega,0)$ is symmetric in ij, and $\gamma_{ijkl}(-\omega;\omega,0,0)$ is symmetric in ij and in kl. To simplify the notation, we write $\alpha_{ij}(0;0) = a_{ij}$, $\alpha_{ij}(-\omega;\omega) = \alpha_{ij}$, $\beta_{ijk}(0;0,0) = b_{ijk}$, $\beta_{ijk}(-\omega;\omega,0) = \beta_{ijk}$, $\gamma_{ijkl}(0;0,0,0) = g_{ijkl}$ and $\gamma_{ijkl}(-\omega;\omega,0,0) = \gamma_{ijkl}$. This permits equation (1.13) to be written as

$$\mu_i = \mu_i^{(0)} + a_{ij}E_j + \alpha_{ij}\mathscr{E}_j + \tfrac{1}{2}b_{ijk}E_jE_k + \beta_{ijk}\mathscr{E}_jE_k + \tfrac{1}{6}g_{ijkl}E_jE_kE_l + \tfrac{1}{2}\gamma_{ijkl}\mathscr{E}_jE_kE_l + \cdots . \tag{1.14}$$

1.6 Concluding remarks

The multipole expansion has been very successful in relating various macroscopic electromagnetic phenomena in matter to the microscopic structure of individual molecules (for gases) or of unit cells (for crystals) [28, 31]. It allows the description of two interacting molecules to be simplified as long as the separation of the molecules is sufficiently large, allowing the individual molecules to be characterized by a series of moments of charge. Armed with the multipole expansion as well the expression for the total electric dipole moment (permanent and induced) in a molecule in the presence of both a uniform static applied electric field and a dynamic light-wave electric field, we are now equipped to relate the induced dc Kerr-effect birefringence to these microscopic polarizabilities and multipole moments.

Chapter 2

The Theory of the Kerr Effect

2.1 The Kerr effect in an ideal gas

The electric-field-induced birefringence, or dc Kerr effect, is the anisotropy in the refractive index, $(n_x - n_y)$, which is observed when linearly-polarized light propagates through a fluid along the z-direction of space-fixed axes $O(x, y, z)$, z being perpendicular to a uniform applied electric field E_x. The molecular Kerr constant ${}_{\mathrm{m}}K$ proposed by Otterbein is then defined as [35]

$$ {}_{\mathrm{m}}K = \frac{18nV_{\mathrm{m}}}{3(n^2+2)^2(\varepsilon_{\mathrm{r}}+2)^2} \lim_{E_x \to 0} \left[\frac{n_x - n_y}{E_x^2} \right], \tag{2.1} $$

where n and ε_{r} are respectively the refractive index and relative permittivity of the medium in the absence of the field, and V_{m} is the molar volume. The theory of the Kerr effect must relate the macroscopic observable $(n_x - n_y)$ to the molecular property tensors of the individual molecules in the fluid. This has been achieved for an ideal gas by Buckingham and Pople [5], with minor subsequent refinements by Buckingham [36], and this theory is now reviewed.

Consider a neutral molecule in the presence of an external electrostatic field **E**. The orientation and position of the molecule is given by the variable σ. For all but

the lightest of molecules at typical experimental temperatures (of between 300 K to 500 K) the rotational energy levels are sufficiently close together that the orientation may be considered to vary continuously, and hence be treated classically rather than quantum mechanically.

The electric field $\mathbf{E}$ can be written in tensor notation as E_α. (In this work, Greek tensor subscripts will pertain to the laboratory frame, while Roman tensor subscripts will pertain to molecule-fixed axes.) A typical Kerr-effect apparatus comprises a gas cell which is a conducting metal cylinder down the length of which run two parallel-plate electrodes which are separated by a small distance, and which are equidistant from the cylinder's axis. The cylinder and one of the electrodes are earthed, while the other electrode is held at a potential relative to them, such that the axis experiences a high uniform electric field. The space-fixed laboratory frame $O(x, y, z)$ is fixed in the Kerr cell such that z is along the axis of the cylinder and in the direction of propagation of the light beam (which is parallel to, and centred on, the cell's axis), while the applied uniform electric field lies in the $x-$direction.

For a dilute gas, the oscillating electric dipole moment μ_i induced in a molecule arises due to the polarizing action of the oscillating electric field $\mathscr{E}_i$ of the light wave. The refractive index is primarily determined by this oscillating dipole, the optical-frequency polarizability tensor α_{ij} being modified by the uniform applied electric field as per equation (1.14), so that

$$\mu_i = \alpha_{ij}\mathscr{E}_j + \beta_{ijk}\mathscr{E}_j E_k + \tfrac{1}{2}\gamma_{ijkl}\mathscr{E}_j E_k E_l + \cdots . \tag{2.2}$$

The differential polarizability π_{ij} is defined as [5, 28]

$$\pi_{ij} = \frac{\partial \mu_i}{\partial \mathscr{E}_j} = \alpha_{ij} + \beta_{ijk}E_k + \tfrac{1}{2}\gamma_{ijkl}E_k E_l + \cdots . \tag{2.3}$$

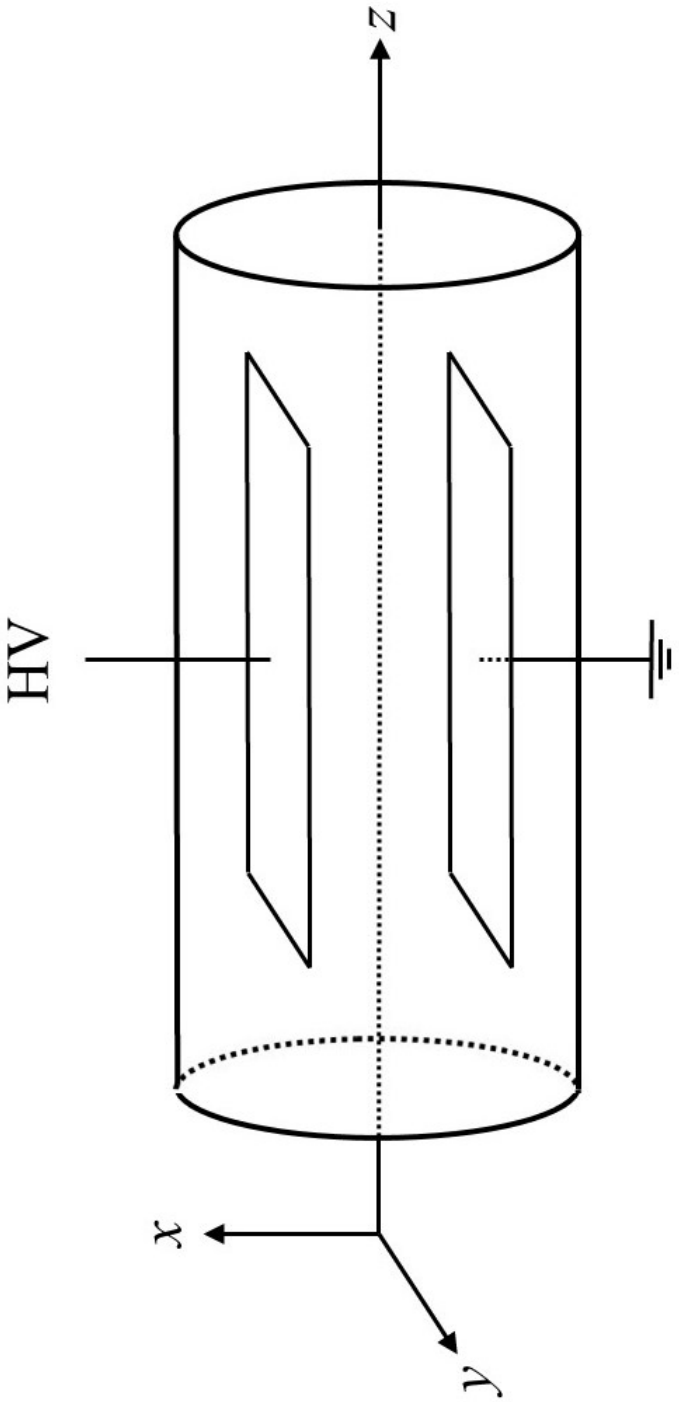

Figure 2.1: Schematic of the Kerr cell and laboratory reference frame $O(x,y,z)$.

The difference between the molecular polarizabilities in the directions parallel and perpendicular to E_x is $(\pi_{xx} - \pi_{yy})$, which, using the direction cosines a_i^α between the α space-fixed axes and i molecule-fixed axes, and for a particular molecular configuration σ, can be written

$$\pi(\sigma, \mathbf{E}) \;=\; \pi_{xx} \;-\; \pi_{yy} \;=\; \pi_{ij} \left(a_i^x a_j^x \;-\; a_i^y a_j^y \right). \tag{2.4}$$

The transformation of the electric field from the laboratory frame (*i.e.* space-fixed axes) into molecule-fixed axes is obtained using the direction cosine as follows:

$$E_i = a_\alpha^i E_\alpha \;. \tag{2.5}$$

Since the electric field E_α has as its only non-zero component E_x, E_i becomes $E_x\, a_x^i \;=\; E_x\, a_i^x$, so that equations (2.3) and (2.4) yield

$$\pi(\sigma, E) = \left(\alpha_{ij} + \beta_{ijk} E_x\, a_k^x + \tfrac{1}{2} \gamma_{ijkl} E_x^2\, a_k^x a_l^x + \cdots \right) \left(a_i^x a_j^x \;-\; a_i^y a_j^y \right). \tag{2.6}$$

The refractive index difference $(n_x - n_y)$ in the presence of E_x is obtained using the Lorenz-Lorentz equation which provides the link between the microscopic molecular property α (the polarizability) and the macrosopic observable n. For a gas in the absence of an applied field, in the electric dipole approximation, the Lorenz-Lorentz equation is

$$\frac{n^2 \;-\; 1}{n^2 \;+\; 2} \;=\; \frac{4\pi N_{\mathrm{A}}}{3(4\pi\varepsilon_0) V_{\mathrm{m}}} \; \langle \alpha \rangle, \tag{2.7}$$

where N_{A} is Avogadro's number, ε_0 is the permittivity of free space, V_{m} is the molar volume of the gas sample, and $\alpha = \frac{1}{3}\alpha_{\alpha\alpha}$ is the mean polarizability. The angular brackets denote an isotropic average, since the molecule is tumbling freely in space.

For light polarized in the x direction of the applied field E_x, equation (2.7) becomes

$$\frac{n_x^2 - 1}{n_x^2 + 2} = \frac{4\pi N_{\mathrm{A}}}{3(4\pi\varepsilon_0)V_{\mathrm{m}}}\,\overline{\pi_{xx}}, \tag{2.8}$$

while for light polarized perpendicular to E_x it becomes

$$\frac{n_y^2 - 1}{n_y^2 + 2} = \frac{4\pi N_{\mathrm{A}}}{3(4\pi\varepsilon_0)V_{\mathrm{m}}}\,\overline{\pi_{yy}}. \tag{2.9}$$

The overbar in $\overline{\pi}$ denotes the orientational average of π over all configurations in the presence of the biasing influence of the applied electric field. A little algebra yields

$$\frac{n_x^2 - 1}{n_x^2 + 2} - \frac{n_y^2 - 1}{n_y^2 + 2} = \frac{3\,(n_x + n_y)\,(n_x - n_y)}{(n_x^2 + 2)\left(n_y^2 + 2\right)}, \tag{2.10}$$

and since for gases $n \approx 1$, equation (2.10) is simplified by seting $(n_x + n_y) \approx 2n$ and $(n_x^2 + 2)\left(n_y^2 + 2\right) \approx (n^2 + 2)^2$, so that

$$\frac{n_x^2 - 1}{n_x^2 + 2} - \frac{n_y^2 - 1}{n_y^2 + 2} \approx \frac{6n}{(n^2 + 2)^2}\,(n_x - n_y)\,. \tag{2.11}$$

Equations (2.8), (2.9) and (2.11) yield

$$n_x - n_y \approx \frac{(n^2 + 2)^2}{6n} \cdot \frac{4\pi N_{\mathrm{A}}}{3(4\pi\varepsilon_0)V_{\mathrm{m}}}\,\overline{\pi}\,. \tag{2.12}$$

For an ideal gas in the limit of infinite dilution, with $n \to 1$, this reduces to

$$n_x - n_y = \frac{2\pi N_{\mathrm{A}}}{(4\pi\varepsilon_0)V_{\mathrm{m}}}\overline{\pi}, \tag{2.13}$$

It is fair to assume that the rapidly oscillating field of the incident light wave is sufficiently weak that it does not affect the orientation of the molecule, that the orientational variable σ is continuous, and that a Boltzmann-type weighting factor can be used to determine the orientational average required [5, 36]. $\overline{\pi}$ can then be

written as

$$\overline{\pi} = \frac{\int \pi(\sigma, E) e^{-U(\sigma,E)/kT} d\sigma}{\int e^{-U(\sigma,E)/kT} d\sigma} \ . \tag{2.14}$$

Here, $U(\sigma, E)$ is the energy of the molecule, which from equation (1.9) is given by

$$U(\sigma, E) = -\int_0^E \mu_i \ dE_i. \tag{2.15}$$

Using equation (1.14) in equation (2.15), and neglecting the terms in $\boldsymbol{\mathscr{E}}$ since $\boldsymbol{\mathscr{E}}$ is assumed not to orient a molecule,

$$\begin{aligned} U(\sigma, E) &= U^{(0)} - \mu_i^{(0)} E_i - \frac{1}{2} a_{ij} E_i E_j - \frac{1}{6} b_{ijk} E_i E_j E_k - \frac{1}{24} g_{ijkl} E_i E_j E_k E_l - \cdots \\ &= U^{(0)} - \mu_i^{(0)} E_x \, a_i^x - \frac{1}{2} a_{ij} E_x^2 \, a_i^x a_j^x - \frac{1}{6} b_{ijk} E_x^3 \, a_i^x a_j^x a_k^x - \frac{1}{24} g_{ijkl} E_x^4 \, a_i^x a_j^x a_k^x a_l^x - \cdots . \end{aligned} \tag{2.16}$$

The biased average $\overline{\pi}$ in equation (2.13) is converted into isotropic averages through a Taylor series expansion of $\overline{\pi}$ in powers of E,

$$\overline{\pi} = A + B \, E_x + C \, E_x^2 + \cdots , \tag{2.17}$$

where

$$A = \left(\overline{\pi} \right)_{E_x=0} , \quad B = \left(\frac{\partial \overline{\pi}}{\partial E_x} \right)_{E_x=0} \quad \text{and} \quad C = \frac{1}{2} \left(\frac{\partial^2 \overline{\pi}}{\partial E_x^2} \right)_{E_x=0} . \tag{2.18}$$

The isotropic average of a property $X(\sigma, E)$ with $E = 0$ is denoted as $\langle X \rangle$, and is

$$\langle X \rangle = \frac{\int X(\sigma, 0) e^{-U^{(0)}/kT} d\sigma}{\int e^{-U^{(0)}/kT} d\sigma}. \tag{2.19}$$

Setting $E_x = 0$ in equation (2.6) yields

$$A = \langle \pi \rangle = \alpha_{ij} \left\langle \left(a_i^x a_j^x \; - \; a_i^y a_j^y \right) \right\rangle = \alpha_{ij} \left(\left\langle a_i^x a_j^x \right\rangle \; - \; \left\langle a_i^y a_j^y \right\rangle \right) \; . \tag{2.20}$$

These second-rank isotropic averages have been shown to reduce to [30]

$$\left\langle a_i^x a_j^x \right\rangle = \left\langle a_i^y a_j^y \right\rangle = \tfrac{1}{3}\delta_{ij}, \tag{2.21}$$

so that $A = 0$.

To obtain an expression for B, the partial derivative of $\overline{\pi}$ which appears in equation (2.18) needs to be evaluated. This requires equation (2.14) and application of the product rule:

$$\begin{aligned} \left(\frac{\partial \overline{\pi}}{\partial E_x} \right) = & \frac{\int \frac{\partial \pi(\sigma, E_x)}{\partial E_x} e^{-U^{(\sigma, E_x)}/kT} d\sigma}{\int e^{-U^{(\sigma, E_x)}/kT} d\sigma} - \frac{1}{kT} \frac{\int \pi(\sigma, E_x) \frac{\partial U(\sigma, E_x)}{\partial E_x} e^{-U^{(\sigma, E_x)}/kT} d\sigma}{\int e^{-U^{(\sigma, E_x)}/kT} d\sigma} \\ & + \frac{1}{kT} \frac{\left(\int \pi(\sigma, E_x) e^{-U^{(\sigma, E_x)}/kT} d\sigma \right) \left(\int \frac{\partial U(\sigma, E_x)}{\partial E_x} e^{-U^{(\sigma, E_x)}/kT} d\sigma \right)}{\left(\int e^{-U^{(\sigma, E_x)}/kT} d\sigma \right)^2} \, . \end{aligned} \tag{2.22}$$

Hence,

$$B = \left\langle \frac{\partial \pi}{\partial E_x} \right\rangle - \frac{1}{kT} \left\langle \pi \frac{\partial U}{\partial E_x} \right\rangle + \frac{1}{kT} \langle \pi \rangle \left\langle \frac{\partial U}{\partial E_x} \right\rangle . \tag{2.23}$$

Since $A = \langle \pi \rangle = 0$, the expression for B reduces to

$$B = \left\langle \frac{\partial \pi}{\partial E_x} \right\rangle - \frac{1}{kT} \left\langle \pi \frac{\partial U}{\partial E_x} \right\rangle . \tag{2.24}$$

Equation (2.6) provides

$$\left(\frac{\partial \pi}{\partial E_x} \right)_{E_x = 0} = \beta_{ijk} \; a_k^x \left(a_i^x a_j^x - a_i^y a_j^y \right) , \tag{2.25}$$

so that

$$\left\langle \frac{\partial \pi}{\partial E_x} \right\rangle = \beta_{ijk} \Big\langle a_i^x a_j^x a_k^x - a_i^y a_j^y a_k^x \Big\rangle. \tag{2.26}$$

The only non-vanishing third-rank isotropic average is [30]

$$\left\langle a_i^x a_j^y a_k^z \right\rangle = \tfrac{1}{6} \varepsilon_{ijk}, \tag{2.27}$$

where ε_{ijk} is the Levi-Civita tensor, which is $+1$ or -1 if i, j, k is respectively an even or odd permutation of 1, 2, 3, or is zero if any two of the subscripts i, j, k are the same. Consequently, equation (2.26) is zero.

Similarly, equation (2.16) provides

$$\left(\frac{\partial U}{\partial E_x} \right)_{E_x=0} = -\mu_k^{(0)} a_k^x \tag{2.28}$$

so that

$$\left(\pi \frac{\partial U}{\partial E_x} \right)_{E_x=0} = -\alpha_{ij}\, \mu_k^{(0)} \left(a_i^x a_j^x a_k^x - a_i^y a_j^y a_k^x \right) \tag{2.29}$$

and

$$\left\langle \pi \frac{\partial U}{\partial E_x} \right\rangle = -\alpha_{ij}\, \mu_k^{(0)} \Big\langle a_i^x a_j^x a_k^x - a_i^y a_j^y a_k^x \Big\rangle = 0 \ . \tag{2.30}$$

Hence $B = 0$, and the leading non-vanishing term in the expansion of $\overline{\pi}$ is found to be in E_x^2.

The expression for C is obtained in an analagous procedure to that for B above. The double partial derivative of $\overline{\pi}$ which appears in equation (2.18) is evaluated by

taking $\partial/\partial E_x$ of $(\partial\overline{\pi}/\partial E_x)$ in equation (2.22), which yields [5]

$$C = \frac{1}{2}\left\langle \frac{\partial^2\pi}{\partial E_x^2} \right\rangle - \frac{1}{2kT}\left\langle 2\frac{\partial\pi}{\partial E_x}\frac{\partial U}{\partial E_x} + \pi\frac{\partial^2 U}{\partial E_x^2} \right\rangle + \frac{1}{2k^2T^2}\left\langle \pi\left(\frac{\partial U}{\partial E_x}\right)^2 \right\rangle . \tag{2.31}$$

Equation (2.31) is evaluated in a similar manner to equation (2.24) for B, using equations (2.6) and (2.16) together with the standard results for fourth-rank isotropic averages [5, 30, 37]

$$\left\langle a_i^x a_j^x a_k^x a_l^x \right\rangle = \tfrac{1}{15}\left(\delta_{ij}\delta_{kl} + \delta_{ik}\delta_{jl} + \delta_{il}\delta_{jk}\right) \tag{2.32}$$

and

$$\left\langle a_i^x a_j^x a_k^y a_l^y \right\rangle = \tfrac{1}{30}\left(4\delta_{ij}\delta_{kl} - \delta_{ik}\delta_{jl} - \delta_{il}\delta_{jk}\right) \ . \tag{2.33}$$

The second partial derivatives of equations (2.6) and (2.16) are

$$\left(\frac{\partial^2\pi}{\partial E_x^2}\right)_{E_x=0} = \gamma_{ijkl}\left(a_i^x a_j^x - a_i^y a_j^y\right) a_k^x a_l^x \tag{2.34}$$

and

$$\left(\frac{\partial^2 U}{\partial E_x^2}\right)_{E_x=0} = -a_{ij}\, a_i^x a_j^x \ . \tag{2.35}$$

The terms in equation (2.31) evaluate to

$$\begin{aligned} \frac{1}{2}\left\langle \frac{\partial^2\pi}{\partial E_x^2} \right\rangle &= \frac{1}{2}\gamma_{ijkl}\left\langle a_i^x a_j^x a_k^x a_l^x - a_i^y a_j^y a_k^x a_l^x \right\rangle \\ &= \frac{1}{30}\left(3\gamma_{ijij} - \gamma_{iijj}\right) \ , \end{aligned} \tag{2.36}$$

$$-\frac{1}{2kT}\left\langle 2\frac{\partial\pi}{\partial E_x}\frac{\partial U}{\partial E_x}+\pi\frac{\partial^2 U}{\partial E_x^2}\right\rangle = \frac{1}{kT}\left(\beta_{ijk}\mu_l^{(0)}+\tfrac{1}{2}\alpha_{ij}a_{kl}\right)\left\langle a_i^x a_j^x a_k^x a_l^x - a_i^y a_j^y a_k^x a_l^x\right\rangle$$

$$= \frac{2}{30kT}\left(3\beta_{iji}\mu_j^{(0)}-\beta_{iij}\mu_j^{(0)}\right)+\frac{1}{30kT}\left(3\alpha_{ij}a_{ij}-\alpha_{ii}a_{jj}\right)\,, \tag{2.37}$$

and

$$\frac{1}{2k^2T^2}\left\langle \pi\left(\frac{\partial U}{\partial E_x}\right)^2\right\rangle = \frac{1}{30k^2T^2}\left(3\alpha_{ij}\mu_i^{(0)}\mu_j^{(0)}-\alpha_{ii}\mu_j^{(0)}\mu_j^{(0)}\right)\,, \tag{2.38}$$

so that equation (2.17) becomes

$$\overline{\pi} = \frac{E_x^2}{30}\Bigg\{\left(3\gamma_{ijij}-\gamma_{iijj}\right)+\frac{2}{kT}\left(3\beta_{iji}\mu_j^{(0)}-\beta_{iij}\mu_j^{(0)}\right) + \frac{1}{kT}\left(3\alpha_{ij}a_{ij}-\alpha_{ii}a_{jj}\right)+\frac{1}{k^2T^2}\left(3\alpha_{ij}\mu_i^{(0)}\mu_j^{(0)}-\alpha_{ii}\mu_j^{(0)}\mu_j^{(0)}\right)\Bigg\}. \tag{2.39}$$

Equation (2.39) can then be substituted into equation (2.13), giving

$$n_x - n_y = \frac{2\pi N_\mathrm{A}}{(4\pi\varepsilon_0)V_\mathrm{m}}\overline{\pi}$$

$$= \frac{N_\mathrm{A}E_x^2}{60\varepsilon_0 V_\mathrm{m}}\Bigg\{\left(3\gamma_{ijij}-\gamma_{iijj}\right)+\frac{2}{kT}\left(3\beta_{iji}\mu_j^{(0)}-\beta_{iij}\mu_j^{(0)}\right) + \frac{1}{kT}\left(3\alpha_{ij}a_{ij}-\alpha_{ii}a_{jj}\right)+\frac{1}{k^2T^2}\left(3\alpha_{ij}\mu_i^{(0)}\mu_j^{(0)}-\alpha_{ii}\mu_j^{(0)}\mu_j^{(0)}\right)\Bigg\}. \tag{2.40}$$

Equation (2.40) is an expression for the birefringence induced in the gas by the uniform applied electric field expressed in terms of the microscopic molecular properties of an individual molecule. In the limit of infinite dilution, Otterbein's definition of

the molar Kerr constant ${}_{\mathrm{m}}K$ given in equation (2.1) becomes

$$ {}_{\mathrm{m}}K \;=\; \frac{2V_{\mathrm{m}}}{27} \lim_{E_x \to 0} \left[\frac{n_x \;-\; n_y}{E_x^2} \right] . \tag{2.41} $$

Substituting equation (2.40) into equation (2.41) gives an expression for the molar Kerr constant in the limit of infinite dilution as

$$ {}_{\mathrm{m}}K = \frac{N_{\mathrm{A}}}{810\varepsilon_0} \Bigg\{ \left(3\gamma_{ijij} - \gamma_{iijj}\right) + \frac{2}{kT} \left(3\beta_{iji}\mu_j^{(0)} - \beta_{iij}\mu_j^{(0)}\right) $$

$$ + \frac{1}{kT}\left(3\alpha_{ij}a_{ij} - \alpha_{ii}a_{jj}\right) + \frac{1}{k^2T^2} \left(3\alpha_{ij}\mu_i^{(0)}\mu_j^{(0)} - \alpha_{ii}\mu_j^{(0)}\mu_j^{(0)}\right) \Bigg\} . \tag{2.42} $$

This equation was initially derived by Buckingham and Pople [5, 36], and is a generalization of the Langevin-Born equation to include the effects of high field strengths on the polarizability.

In the Kerr experiment, a monochromatic beam of linearly-polarized laser light travels along the $z-$axis, which is chosen to coincide with the axis of the of the gas cell. Parallel electrodes establish the uniform electric field in the x direction. The laser beam enters the cell polarized at 45° to the xz plane, where it can be resolved into two components with orthogonal electric vectors $\mathscr{E}_x$ and $\mathscr{E}_y$ which will experience different refractive indices n_x and n_y as they travel through the birefringent medium. The beam emerges from the cell elliptically polarized, the two components now having a relative phase difference δ of

$$ \delta = \frac{2\pi l}{\lambda} \left(n_x - n_y\right) \;\; , \tag{2.43} $$

where l is the pathlength of the medium, and λ is the wavelength of the light. The azimuth of this elliptically-polarized beam remains 45° to the xz plane, so that if it

passes through a quarter-wave plate with fast axis set at an azimuth of 45°, the light will emerge linearly polarized but rotated from the initial 45° plane of polarization by an angle $\delta/2$ radians. The optical retardation δ is the observable property in the experiment, and from equation (2.43) it yields $(n_x - n_y)$, which together with knowledge of the refractive index and relative permittivity of the gas, its temperature and density, and the strength of the applied electric field, allows for the calculation of ${}_{\mathrm{m}}K$ via equation (2.40).

2.2 Interacting non-dipolar molecules

For higher gas densities, the approach adopted by Buckingham and Pople for the treatment of intermolecular interaction effects via a virial expansion is followed [38]. This approach is now briefly reviewed:

A range of electromagnetic properties of gases are found to be proportional to the number density of the constituent molecules. For ideal gases, this proportionality will be exact since there are no interactions between the molecules, so that each molecule can be considered to be an independent system. For real gases, where intermolecular interactions occur, the electromagnetic properties display a non-linear dependence on the number density of the molecules.

In 1956, Buckingham and Pople accounted for these intermolecular interaction effects through the use of a virial-type expansion [38]. If Q is a measurable molecular-optic property of a real gas, Q can be expressed as a virial expansion in inverse

powers of the molar volume V_{m}:

$$Q = A_Q + \frac{B_Q}{V_{\mathrm{m}}} + \frac{C_Q}{V_{\mathrm{m}}^2} + \cdots \ . \tag{2.44}$$

Here, the first virial coefficient A_Q is the ideal gas contribution to Q, B_Q is the second virial coefficient accounting for the contribution to Q from interacting pairs of molecules, while the third virial coefficient C_Q gives the contribution arising from interacting triplets. The virial coefficients are functions only of the temperature, or in the case of molecular-optical phenomena, of temperature and the wavelength of the light [38].

For a mole of ideal-gas molecules, the N_{A} mean contributions $\overline{q}$ of the individual isolated molecules sum to Q:

$$Q = A_Q = N_{\mathrm{A}}\,\overline{q}\ . \tag{2.45}$$

At higher gas densities, a representative molecule 1 will, on occasion, be interacting with a neighbouring molecule 2. If the relative intermolecular configuration is described by τ, then their contribution to Q at any given instant will be $q_{12}(\tau)$. Treating molecule 1 as half of an interacting pair, its contribution to Q at a given instant is $\frac{1}{2}q_{12}(\tau)$. Neglecting triplet and higher-order interactions, Q becomes

$$Q = N_{\mathrm{A}}\left\{\overline{q} + \int_{\tau}\left[\tfrac{1}{2}q_{12}(\tau) - \overline{q}\right]P(\tau)\,d\tau\right\}\ , \tag{2.46}$$

where $P(\tau)\,d\tau$ is the probability that molecule 1 has a neighbour in the range $(\tau, \tau + d\tau)$. The relationship between the intermolecular potential energy $U_{12}(\tau)$ and the probability function is given by

$$P(\tau) = \frac{N_{\mathrm{A}}}{\Omega V_{\mathrm{m}}} e^{-U_{12}(\tau)/kT}\ , \tag{2.47}$$

where $\Omega = V_{\rm m}^{-1} \int_\tau d\tau$. From equation (2.44),

$$B_Q = \lim_{V_{\rm m}\to\infty} \Big(Q - A_Q\Big) V_{\rm m} \ , \tag{2.48}$$

which combined with equations (2.45) to (2.47) gives

$$B_Q = \frac{N_{\rm A}^2}{\Omega} \int_\tau \Big[\tfrac{1}{2} q_{12}(\tau) - \overline{q}\Big] e^{-U_{12}(\tau)/kT} d\tau \ . \tag{2.49}$$

This general expression for B_Q can be applied to whichever molecular-optical property Q is under consideration. In this thesis, it will be applied to the second Kerr-effect virial coefficient $B_{\rm K}$ for interacting pairs of non-dipolar molecules.

Recall from equation (2.13) that in the limit of infinite dilution, the refractive index difference $n_x - n_y$ of a gas in the presence of a uniform applied electric field is

$$n_x - n_y = \frac{2\pi N_{\rm A}}{(4\pi\varepsilon_0) V_{\rm m}} \overline{\pi} \tag{2.50}$$

where $\overline{\pi}$ is the average over all configurations σ of the quantity $\pi_{ij}\left(a_i^x a_j^x - a_i^y a_j^y\right)$ of a representative isolated molecule in the presence of the biasing influence of the applied field.

For higher gas densities, the contribution of a representative molecule 1 to $n_x - n_y$ is not always given by equation (2.50), there now being times when molecule 1 has to be treated as half of an interacting pair. When molecule 1 is in the presence of a neighbouring molecule 2, their relative configuration being specified by τ, then the instantaneous contribution of molecule 1 to the induced birefringence is

$$\frac{1}{2}\left\{ \frac{2\pi N_{\rm A}}{(4\pi\varepsilon_0) V_{\rm m}} \pi^{(12)}(\tau, E) \right\} \tag{2.51}$$

where

$$\pi^{(12)}(\tau, E) = \pi^{(12)} = \pi_{ij}^{(12)} \left(a_i^x a_j^x - a_i^y a_j^y \right) \ . \tag{2.52}$$

$\pi_{ij}^{(12)}$ is the differential polarizability of the interacting pair, and an expression for $\pi_{ij}^{(12)}$ will need to be derived. Obtaining the biased orientational average $\overline{\pi^{(12)}(\tau, E)}$ requires that the molecular pair is allowed to rotate as a rigid whole (in the fixed configuration τ) in the presence of the biasing influence of the field E_α. This biased average is then converted into isotropic averages via a Taylor expansion in powers of E. An analysis similar to that of an isolated molecule provided in equations (2.17) to (2.40) gives the leading term as

$$\overline{\pi^{(12)}(\tau, E)} = \frac{1}{2} \left(\frac{\partial^2 \overline{\pi^{(12)}(\tau, E)}}{\partial E_x^2} \right)_{E_x=0} E_x^2 \tag{2.53}$$

where

$$\frac{1}{2} \left(\frac{\partial^2 \overline{\pi^{(12)}(\tau, E)}}{\partial E_x^2} \right)_{E_x=0} = \frac{1}{2} \left\langle \frac{\partial^2 \pi^{(12)}}{\partial E_x^2} \right\rangle - \frac{1}{2kT} \left\langle 2 \frac{\partial \pi^{(12)}}{\partial E_x} \frac{\partial U^{(12)}}{\partial E_x} + \pi^{(12)} \frac{\partial^2 U^{(12)}}{\partial E_x^2} \right\rangle$$

$$+ \frac{1}{2k^2T^2} \left\langle \pi^{(12)} \left(\frac{\partial U^{(12)}}{\partial E_x} \right)^2 \right\rangle . \tag{2.54}$$

In equation (2.54), $U^{(12)} = U^{(12)}(\tau, 0)$ is the potential energy of the interacting pair of molecules in the absence of the applied field. The quantities inside the angular brackets are initially referred to the molecule-fixed axes $O(1, 2, 3)$. The tensor product in $O(1, 2, 3)$ is fixed for a given interaction configuration τ. As the pair rotates as a rigid whole in the laboratory frame $O(x, y, z)$, the average projection of the pair properties, referred to $O(1, 2, 3)$, is averaged into $O(x, y, z)$ over all orientations. Averaging over the pair-interaction parameters τ can then be performed.

The density dependence of the molar Kerr constant ${}_{\rm m}K$ can be expressed by the virial expansion

$$ {}_{\rm m}K = A_{\rm K} + \frac{B_{\rm K}}{V_{\rm m}} + \frac{C_{\rm K}}{V_{\rm m}^2} + \cdots \ , \tag{2.55} $$

where $A_{\rm K}$, $B_{\rm K}$ and $C_{\rm K}$ are the first, second and third Kerr-effect virial coefficients, respectively. From equation (2.1), the molar Kerr constant ${}_{\rm m}K$ in the limit of infinite dilution is

$$ \begin{aligned} A_{\rm K} = \lim_{V_{\rm m}\to\infty} ({}_{\rm m}K) &= \lim_{V_{\rm m}\to\infty} \left\{ \frac{18n\,(n_x - n_y)\,V_{\rm m}}{3(n^2+2)^2(\varepsilon_r+2)^2\ E_x^2} \right\}_{E_x\to 0} \\ &= \frac{2\pi N_{\rm A}}{27(4\pi\varepsilon_0)} \left(\frac{\partial^2 \overline{\pi}}{\partial E_x^2} \right)_{E_x=0} \ . \end{aligned} \tag{2.56} $$

This expression can be extrapolated to higher densities, giving

$$ {}_{\rm m}K = A_{\rm K} + \int_\tau \frac{2\pi N_{\rm A}}{27(4\pi\varepsilon_0)} \left\{ \frac{1}{2} \left(\frac{\partial^2 \overline{\pi^{(12)}(\tau, E)}}{\partial E_x^2} \right)_{E_x=0} - \left(\frac{\partial^2 \overline{\pi}}{\partial E_x^2} \right)_{E_x=0} \right\} P(\tau) d\tau \ , \tag{2.57} $$

where $P(\tau)d\tau$ is the probability of molecule 1 having a neighbour in the range $(\tau, \tau + d\tau)$, $P(\tau)$ being given by equation (2.47). Comparing equation (2.57) with equation (2.55), $B_{\rm K}$ is seen to be

$$ B_{\rm K} = \frac{2\pi N_{\rm A}^2}{27\Omega(4\pi\varepsilon_0)} \int_\tau \left\{ \frac{1}{2} \left(\frac{\partial^2 \overline{\pi^{(12)}(\tau, E)}}{\partial E_x^2} \right)_{E_x=0} - \left(\frac{\partial^2 \overline{\pi}}{\partial E_x^2} \right)_{E_x=0} \right\} e^{-U_{12}(\tau)/kT} d\tau \ . \tag{2.58} $$

The relative configuration τ of two molecules of general symmetry may be expressed by seven parameters: the separation R of the two molecular centres, the Euler angles α_1, β_1 and γ_1 used to define the direction cosines a_i^α between the laboratory frame $O(x, y, z)$ (referred to by $\alpha, \beta, \gamma\ \cdots$) and the molecule-fixed axes $O(1, 2, 3)$

of molecule 1 (referred to by $i, j, k \ \cdots$), and the Euler angles α_2, β_2 and γ_2 defining the direction cosines $a_{i'}^{\alpha}$ between the laboratory frame and the molecule-fixed axes $O(1', 2', 3')$ of molecule 2 (referred to by $i', j', k' \ \cdots$). These parameters are fully described by Couling and Graham [9, 39], who also evaluate the normalization constant $\Omega = (8\pi^2)^2$. The explicit expressions for the direction cosine tensors are

$$a_i^{\alpha} = \begin{bmatrix} \cos\gamma_1 & \sin\gamma_1 & 0 \\ -\sin\gamma_1 & \cos\gamma_1 & 0 \\ 0 & 0 & 1 \end{bmatrix} \begin{bmatrix} \cos\beta_1 & 0 & -\sin\beta_1 \\ 0 & 1 & 0 \\ \sin\beta_1 & 0 & \cos\beta_1 \end{bmatrix} \begin{bmatrix} \cos\alpha_1 & \sin\alpha_1 & 0 \\ -\sin\alpha_1 & \cos\alpha_1 & 0 \\ 0 & 0 & 1 \end{bmatrix}$$

$$= \begin{bmatrix} \cos\alpha_1\cos\beta_1\cos\gamma_1 - \sin\alpha_1\sin\gamma_1 & \sin\alpha_1\cos\beta_1\cos\gamma_1 + \cos\alpha_1\sin\gamma_1 & -\sin\beta_1\cos\gamma_1 \\ -\cos\alpha_1\cos\beta_1\sin\gamma_1 - \sin\alpha_1\cos\gamma_1 & -\sin\alpha_1\cos\beta_1\sin\gamma_1 + \cos\alpha_1\cos\gamma_1 & \sin\beta_1\sin\gamma_1 \\ \cos\alpha_1\sin\beta_1 & \sin\alpha_1\sin\beta_1 & \cos\beta_1 \end{bmatrix}, \tag{2.59}$$

$$a_{i'}^{\alpha} = \begin{bmatrix} \cos\alpha_2\cos\beta_2\cos\gamma_2 - \sin\alpha_2\sin\gamma_2 & \sin\alpha_2\cos\beta_2\cos\gamma_2 + \cos\alpha_2\sin\gamma_2 & -\sin\beta_2\cos\gamma_2 \\ -\cos\alpha_2\cos\beta_2\sin\gamma_2 - \sin\alpha_2\cos\gamma_2 & -\sin\alpha_2\cos\beta_2\sin\gamma_2 + \cos\alpha_2\cos\gamma_2 & \sin\beta_2\sin\gamma_2 \\ \cos\alpha_2\sin\beta_2 & \sin\alpha_2\sin\beta_2 & \cos\beta_2 \end{bmatrix}. \tag{2.60}$$

Equation (2.58) becomes

$$B_{\mathrm{K}} = \frac{N_{\mathrm{A}}^2}{216\pi^2(4\pi\varepsilon_0)} \int_{R=0}^{\infty} \int_{\alpha_1=0}^{2\pi} \int_{\beta_1=0}^{\pi} \int_{\gamma_1=0}^{2\pi} \int_{\alpha_2=0}^{2\pi} \int_{\beta_2=0}^{\pi} \int_{\gamma_2=0}^{2\pi}$$

$$\times \left\{ \frac{1}{2} \left(\frac{\partial^2 \overline{\pi^{(12)}(\tau, E)}}{\partial E_x^2} \right)_{E_x=0} - \left(\frac{\partial^2 \bar{\pi}}{\partial E_x^2} \right)_{E_x=0} \right\} e^{-U_{12}(\tau)/kT} \tag{2.61}$$

$$\times R^2 \sin\beta_1 \sin\beta_2 \, dR \, d\alpha_1 \, d\beta_1 \, d\gamma_1 \, d\alpha_2 \, d\beta_2 \, d\gamma_2 \ .$$

In order to evaluate B_{K} by integrating over the pair interaction coordinates in equation (2.61), the intermolecular potential $U_{12}(\tau)$ is required. The expression $\frac{1}{2}\left(\partial^2\overline{\pi^{(12)}(\tau,E)}/\partial E_x^2\right)_{E_x=0}$ also needs to be evaluated, requiring the differential polarizability $\pi_{iw}^{(12)}$ for interacting pairs of molecules:

$$\pi_{iw}^{(12)} = \frac{\partial \mu_i^{(12)}}{\partial \mathscr{E}_w} \tag{2.62}$$

where $\mu_i^{(12)}(\mathscr{E}_w)$ is the total oscillating dipole moment induced on the interacting pair by the incident light-wave field $\mathscr{E}_w$.

To proceed, the classical long-range DID model is assumed to hold true: *i.e.* the molecules are assumed to always retain their separate identities. Although this will hold true in the long-range limit, at very short ranges the charge distributions of the molecules begin to overlap, a situation which can only be definitively described by high-level *ab initio* quantum-mechanical calculations. Such calculations require electron correlation effects to be taken into account, and require large basis sets with diffuse basis functions, rendering them extremely demanding and computationally intensive even for interacting atoms, but especially so for interacting molecules. For interaction-induced polarizabilities, the electron overlap contributions to the apparent polarizability (*i.e.* the polarizability in the presence of a neighbouring molecule) has been estimated to be $-8\times$DID for He, but only $-0.6\times$DID for H_2 and N_2 [13]. Indeed, treating diatomic and small polyatomic molecules as if they retain their separate identities even in the region of overlap has provided a useful model of molecular interactions for Rayleigh light-scattering [39–42] and the Kerr effect [8–11], where agreement between measured and calculated second virial coefficients can be achieved to within 10% or better, providing a measure of justification for the simplifying assumption. If this also holds true for the interaction-induced hyperpolarizabilities of molecules, then equation (2.62), even if it includes second

hyperpolarizability contributions in the induced dipole, can be written as

$$\pi_{iw}^{(12)} = \frac{\partial(\mu_i^{(1)} + \mu_i^{(2)})}{\partial \mathscr{E}_w} \ . \tag{2.63}$$

Substituting this into equation (2.52) gives the difference between the differential polarizabilities of an interacting pair in a specific configuration τ in the presence of the applied field as

$$\begin{aligned} \pi^{(12)}(\tau, E) &= \pi_{iw}^{(12)}(a_i^x a_w^x - a_i^y a_w^y) \\ &= \left(\frac{\partial \mu_i^{(1)}}{\partial \mathscr{E}_w} + \frac{\partial \mu_i^{(2)}}{\partial \mathscr{E}_w} \right) (a_i^x a_w^x - a_i^y a_w^y) \\ &= \left(\pi_{iw}^{(1)} + \pi_{iw}^{(2)} \right) (a_i^x a_w^x - a_i^y a_w^y) \\ &= \pi^{(1)}(\tau, E) + \pi^{(2)}(\tau, E) \ . \end{aligned} \tag{2.64}$$

Similarly, the potential of the interacting pair of molecules in the presence of the static applied field is defined to be [31]

$$U^{(12)}(\tau, E) = \ U^{(12)}(\tau, 0) - \int_0^E \mu_i^{(12)}(\tau, E)\, dE_i \ , \tag{2.65}$$

where $\mu_i^{(12)}$ is the total dipole moment of the pair in the presence of $\mathbf{E}$ which, using the above arguments, can be written as

$$\mu_i^{(12)} = \mu_i^{(1)} + \mu_i^{(2)}. \tag{2.66}$$

Here $\mu_i^{(\mathrm{p})}$ is the total dipole of molecule p in the presence of E_i and molecule q. For interacting pairs of non-dipolar molecules, the total static dipole and quadrupole

moments induced in molecule p are

$$\mu_i^{(\mathrm{p})} = a_{ij}^{(\mathrm{p})}\left(E_j + F_j^{(\mathrm{p})}\right) + \tfrac{1}{6}g_{ijkl}^{(\mathrm{p})}\left(E_j + F_j^{(\mathrm{p})}\right)\left(E_k + F_k^{(\mathrm{p})}\right)\left(E_l + F_l^{(\mathrm{p})}\right), \qquad (2.67)$$

$$\Theta_{ij}^{(\mathrm{p})} = \Theta_{0ij}^{(\mathrm{p})} + C_{ijkl}^{(\mathrm{p})}F_{kl}^{(\mathrm{p})}, \qquad (2.68)$$

where $\Theta_{0ij}^{(\mathrm{p})}$ is the permanent molecular electric quadrupole moment of molecule p, and where $F_j^{(\mathrm{p})}$ and $F_{jk}^{(\mathrm{p})}$ are the static field and field gradient arising at molecule p due to both the induced dipole and the permanent and induced quadrupole moments of molecule q. The field-gradient-induced C-tensor contribution will henceforth be assumed to be negligible, so that $\Theta_{ij}^{(\mathrm{p})}$ will be described solely by the leading contribution arising from the permanent quadrupole moment of the molecule. $F_j^{(\mathrm{p})}$ is given by

$$F_j^{(\mathrm{p})} = T_{jk}^{(\mathrm{p})}\mu_k^{(\mathrm{q})} - \tfrac{1}{3}T_{jkl}^{(\mathrm{p})}\Theta_{kl}^{(\mathrm{q})}. \qquad (2.69)$$

Here, it must be borne in mind that [28]

$$\mathbf{T}^{(1)} = (-1)^{(n)}\mathbf{T}^{(2)}, \qquad (2.70)$$

where n is the order of the $T-$tensor. Successive substitutions of $F_j^{(\mathrm{p})}$, $\mu_j^{(\mathrm{p})}$ and $\Theta_{jk}^{(\mathrm{p})}$ into equation (2.67) yields the interaction-induced contributions to the total static dipole, $\mu_i^{(\mathrm{p})}$, of molecule p:

$$\begin{aligned}\mu_i^{(\mathrm{p})} = \tfrac{1}{3}\Big(&-a_{ij}^{(\mathrm{p})}T_{jkv}\Theta_{0kv}^{(\mathrm{q})} + a_{ij}^{(\mathrm{p})}T_{jk}a_{kl}^{(\mathrm{q})}T_{lmv}\Theta_{0mv}^{(\mathrm{p})} - a_{ij}^{(\mathrm{p})}T_{jk}a_{kl}^{(\mathrm{q})}T_{lm}a_{mn}^{(\mathrm{p})}T_{npv}\Theta_{0pv}^{(\mathrm{q})} \\ &+ a_{ij}^{(\mathrm{p})}T_{jk}a_{kl}^{(\mathrm{q})}T_{lm}a_{mn}^{(\mathrm{p})}T_{np}a_{pq}^{(\mathrm{q})}T_{qrv}\Theta_{0rv}^{(\mathrm{p})} + \cdots\Big) \\ +\Big(&a_{iv}^{(\mathrm{p})} + a_{ij}^{(\mathrm{p})}T_{jk}a_{kv}^{(\mathrm{q})} + a_{ij}^{(\mathrm{p})}T_{jk}a_{kl}^{(\mathrm{q})}T_{lm}a_{mv}^{(\mathrm{p})} + a_{ij}^{(\mathrm{p})}T_{jk}a_{kl}^{(\mathrm{q})}T_{lm}a_{mn}^{(\mathrm{p})}T_{np}a_{pv}^{(\mathrm{q})} \\ &+ a_{ij}^{(\mathrm{p})}T_{jk}a_{kl}^{(\mathrm{q})}T_{lm}a_{mn}^{(\mathrm{p})}T_{np}a_{pq}^{(\mathrm{q})}T_{qr}a_{rv}^{(\mathrm{p})} + \cdots\Big)E_v + \mathrm{O}\big(E^2\big) + \cdots .\end{aligned} \tag{2.71}$$

Hence, using equations (2.71) and (2.66), equation (2.65) becomes

$$U^{(12)}(\tau, E) = U^{(12)}(\tau, 0) + U^{(1)}(\tau, E) + U^{(2)}(\tau, E) \tag{2.72}$$

where

$$\begin{aligned}U^{(\mathrm{p})}(\tau, E) = -\tfrac{1}{3}\Big(&-a_{ij}^{(\mathrm{p})}T_{jkv}\Theta_{0kv}^{(\mathrm{q})} + a_{ij}^{(\mathrm{p})}T_{jk}a_{kl}^{(\mathrm{q})}T_{lmv}\Theta_{0mv}^{(\mathrm{p})} - a_{ij}^{(\mathrm{p})}T_{jk}a_{kl}^{(\mathrm{q})}T_{lm}a_{mn}^{(\mathrm{p})}T_{npv}\Theta_{0pv}^{(\mathrm{q})} \\ &+ a_{ij}^{(\mathrm{p})}T_{jk}a_{kl}^{(\mathrm{q})}T_{lm}a_{mn}^{(\mathrm{p})}T_{np}a_{pq}^{(\mathrm{q})}T_{qrv}\Theta_{0rv}^{(\mathrm{p})} + \cdots\Big)E_x\, a_i^x \\ -\tfrac{1}{2}\Big(&a_{iv}^{(\mathrm{p})} + a_{ij}^{(\mathrm{p})}T_{jk}a_{kv}^{(\mathrm{q})} + a_{ij}^{(\mathrm{p})}T_{jk}a_{kl}^{(\mathrm{q})}T_{lm}a_{mv}^{(\mathrm{p})} + a_{ij}^{(\mathrm{p})}T_{jk}a_{kl}^{(\mathrm{q})}T_{lm}a_{mn}^{(\mathrm{p})}T_{np}a_{pv}^{(\mathrm{q})} \\ &+ a_{ij}^{(\mathrm{p})}T_{jk}a_{kl}^{(\mathrm{q})}T_{lm}a_{mn}^{(\mathrm{p})}T_{np}a_{pq}^{(\mathrm{q})}T_{qr}a_{rv}^{(\mathrm{p})} + \cdots\Big)E_x^2\, a_i^x a_v^x \\ &- \mathrm{O}\big(E^3\big) - \cdots .\end{aligned} \tag{2.73}$$

Returning to the oscillating dipole moment of molecule p, $\mu_i^{(\mathrm{p})}(\mathscr{E}_j)$, this is induced not exclusively by the oscillating light-wave field $\mathscr{E}_j$, but also partly by the field $\mathscr{F}_j^{(\mathrm{p})}$

which arises at molecule p due to the oscillating moments on molecule q, so that

$$\mu_i^{(\mathrm{p})}\left(\mathscr{E}_j\right) = \left(\alpha_{ij}^{(\mathrm{p})} + \tfrac{1}{2}\gamma_{ijkl}^{(\mathrm{p})}\left(E_k + F_k^{(\mathrm{p})}\right)\left(E_l + F_l^{(\mathrm{p})}\right) + \cdots\right)\left(\mathscr{E}_j + \mathscr{F}_j^{(\mathrm{p})}\right) \ . \quad (2.74)$$

With the aid of the second-rank $T-$tensor [28], $\mathscr{F}_j^{(1)}$ has the form

$$\mathscr{F}_j^{(\mathrm{p})} = T_{jm}^{(\mathrm{p})}\mu_m^{(\mathrm{q})} \quad (2.75)$$

where

$$\mu_m^{(\mathrm{q})}\left(\mathscr{E}_n\right) = \left(\alpha_{mn}^{(\mathrm{q})} + \tfrac{1}{2}\gamma_{mnab}^{(\mathrm{q})}\left(E_a + F_a^{(\mathrm{q})}\right)\left(E_b + F_b^{(\mathrm{q})}\right) + \cdots\right)\left(\mathscr{E}_n + \mathscr{F}_n^{(\mathrm{q})}\right) \ , \quad (2.76)$$

where, in turn,

$$\mathscr{F}_n^{(\mathrm{q})} = T_{np}^{(\mathrm{q})}\mu_p^{(\mathrm{p})} \ . \quad (2.77)$$

If equations (2.76) and (2.77) are substituted into equation (2.75), followed by successive substitutions of $\mathscr{F}_j^{(\mathrm{p})}$ and $\mathscr{F}_n^{(\mathrm{q})}$, a series of terms contributing to the net field $\mathscr{F}_j^{(\mathrm{p})}$ in equation (2.75) is obtained, which, when substituted into equation (2.74), yields the required expression for the total oscillating dipole moment induced on molecule p by the light-wave field in the presence of the neighbouring molecule q:

$$
\begin{aligned}
\mu_i^{(\mathrm{p})}(\mathscr{E}_w) = \Big(&\alpha_{iw}^{(\mathrm{p})} + \alpha_{ij}^{(\mathrm{p})}T_{jk}\alpha_{kw}^{(\mathrm{q})} + \alpha_{ij}^{(\mathrm{p})}T_{jk}\alpha_{kl}^{(\mathrm{q})}T_{lm}\alpha_{mw}^{(\mathrm{p})} + \alpha_{ij}^{(\mathrm{p})}T_{jk}\alpha_{kl}^{(\mathrm{q})}T_{lm}\alpha_{mn}^{(\mathrm{p})}T_{np}\alpha_{pw}^{(\mathrm{q})} \\
&+ \alpha_{ij}^{(\mathrm{p})}T_{jk}\alpha_{kl}^{(\mathrm{q})}T_{lm}\alpha_{mn}^{(\mathrm{p})}T_{np}\alpha_{pq}^{(\mathrm{q})}T_{qr}\alpha_{rw}^{(\mathrm{p})} \\
&+ \alpha_{ij}^{(\mathrm{p})}T_{jk}\alpha_{kl}^{(\mathrm{q})}T_{lm}\alpha_{mn}^{(\mathrm{p})}T_{np}\alpha_{pq}^{(\mathrm{q})}T_{qr}\alpha_{rs}^{(\mathrm{p})}T_{st}\alpha_{tw}^{(\mathrm{q})} + \cdots\Big)\mathscr{E}_w \\
+ \tfrac{1}{2}\Big(&\gamma_{iwab}^{(\mathrm{p})} + \gamma_{ijab}^{(\mathrm{p})}T_{jk}\alpha_{kw}^{(\mathrm{q})} + \alpha_{ij}^{(\mathrm{p})}T_{jk}\gamma_{kwab}^{(\mathrm{q})} + 2\gamma_{iwaj}^{(\mathrm{p})}T_{jk}a_{kb}^{(\mathrm{q})} + \gamma_{ijab}^{(\mathrm{p})}T_{jk}\alpha_{kl}^{(\mathrm{q})}T_{lm}\alpha_{mw}^{(\mathrm{p})} \\
&+ \alpha_{ij}^{(\mathrm{p})}T_{jk}\gamma_{klab}^{(\mathrm{q})}T_{lm}\alpha_{mw}^{(\mathrm{p})} + \alpha_{ij}^{(\mathrm{p})}T_{jk}\alpha_{kl}^{(\mathrm{q})}T_{lm}\gamma_{mwab}^{(\mathrm{p})} + \gamma_{iwjl}^{(\mathrm{p})}T_{jk}a_{ka}^{(\mathrm{q})}T_{lm}a_{mb}^{(\mathrm{q})} \\
&+ 2\gamma_{iwaj}^{(\mathrm{p})}T_{jk}a_{kl}^{(\mathrm{q})}T_{lm}a_{mb}^{(\mathrm{p})} + 2\gamma_{ijal}^{(\mathrm{p})}T_{jk}\alpha_{kw}^{(\mathrm{q})}T_{lm}a_{mb}^{(\mathrm{q})} + 2\alpha_{ij}^{(\mathrm{p})}T_{jk}\gamma_{kwal}^{(\mathrm{q})}T_{lm}a_{mb}^{(\mathrm{p})} \\
&+ \gamma_{ijab}^{(\mathrm{p})}T_{jk}\alpha_{kl}^{(\mathrm{q})}T_{lm}\alpha_{mn}^{(\mathrm{p})}T_{np}\alpha_{pw}^{(\mathrm{q})} + \alpha_{ij}^{(\mathrm{p})}T_{jk}\alpha_{kl}^{(\mathrm{q})}T_{lm}\alpha_{mn}^{(\mathrm{p})}T_{np}\gamma_{pwab}^{(\mathrm{q})} \\
&+ \alpha_{ij}^{(\mathrm{p})}T_{jk}\alpha_{kl}^{(\mathrm{q})}T_{lm}\gamma_{mnab}^{(\mathrm{p})}T_{np}\alpha_{pw}^{(\mathrm{q})} + \alpha_{ij}^{(\mathrm{p})}T_{jk}\gamma_{klab}^{(\mathrm{q})}T_{lm}\alpha_{mn}^{(\mathrm{p})}T_{np}\alpha_{pw}^{(\mathrm{q})} \\
&+ 2\gamma_{iwaj}^{(\mathrm{p})}T_{jk}a_{kl}^{(\mathrm{q})}T_{lm}a_{mn}^{(\mathrm{p})}T_{np}a_{pb}^{(\mathrm{q})} + \gamma_{iwjl}^{(\mathrm{p})}T_{jk}a_{ka}^{(\mathrm{q})}T_{lm}a_{mn}^{(\mathrm{q})}T_{np}a_{pb}^{(\mathrm{p})} \\
&+ \gamma_{ijln}^{(\mathrm{p})}T_{jk}\alpha_{kw}^{(\mathrm{q})}T_{lm}a_{ma}^{(\mathrm{q})}T_{np}a_{pb}^{(\mathrm{q})} + 2\alpha_{ij}^{(\mathrm{p})}T_{jk}\gamma_{kwln}^{(\mathrm{q})}T_{lm}a_{ma}^{(\mathrm{p})}T_{np}a_{pb}^{(\mathrm{p})} \\
&+ 2\gamma_{ijan}^{(\mathrm{p})}T_{jk}\alpha_{kl}^{(\mathrm{q})}T_{lm}\alpha_{mw}^{(\mathrm{p})}T_{np}a_{pb}^{(\mathrm{q})} + 2\alpha_{ij}^{(\mathrm{p})}T_{jk}\gamma_{klan}^{(\mathrm{q})}T_{lm}\alpha_{mw}^{(\mathrm{p})}T_{np}a_{pb}^{(\mathrm{p})} \\
&+ 2\alpha_{ij}^{(\mathrm{p})}T_{jk}\alpha_{kl}^{(\mathrm{q})}T_{lm}\gamma_{mwan}^{(\mathrm{p})}T_{np}a_{pb}^{(\mathrm{q})} + 2\gamma_{ijan}^{(\mathrm{p})}T_{jk}\alpha_{kw}^{(\mathrm{q})}T_{np}a_{pq}^{(\mathrm{q})}T_{qr}a_{rb}^{(\mathrm{p})} \\
&+ 2\alpha_{ij}^{(\mathrm{p})}T_{jk}\gamma_{kwan}^{(\mathrm{q})}T_{np}a_{pq}^{(\mathrm{p})}T_{qr}a_{rb}^{(\mathrm{q})} + \cdots\Big)E_aE_b\mathscr{E}_w + \cdots\ .
\end{aligned}
\tag{2.78}
$$

Performing the operation $\frac{\partial}{\partial\mathscr{E}_w}$ on equation (2.78) yields the expression for the differential polarizability of molecule p in the presence of both the applied field and a neighbouring molecule q in a specific relative configuration τ:

$$
\begin{aligned}
\pi^{(\mathrm{p})}_{iw} = \Big(& \alpha^{(\mathrm{p})}_{iw} + \alpha^{(\mathrm{p})}_{ij} T_{jk} \alpha^{(\mathrm{q})}_{kw} + \alpha^{(\mathrm{p})}_{ij} T_{jk} \alpha^{(\mathrm{q})}_{kl} T_{lm} \alpha^{(\mathrm{p})}_{mw} + \alpha^{(\mathrm{p})}_{ij} T_{jk} \alpha^{(\mathrm{q})}_{kl} T_{lm} \alpha^{(\mathrm{p})}_{mn} T_{np} \alpha^{(\mathrm{q})}_{pw} \\
& + \alpha^{(\mathrm{p})}_{ij} T_{jk} \alpha^{(\mathrm{q})}_{kl} T_{lm} \alpha^{(\mathrm{p})}_{mn} T_{np} \alpha^{(\mathrm{q})}_{pq} T_{qr} \alpha^{(\mathrm{p})}_{rw} \\
& + \alpha^{(\mathrm{p})}_{ij} T_{jk} \alpha^{(\mathrm{q})}_{kl} T_{lm} \alpha^{(\mathrm{p})}_{mn} T_{np} \alpha^{(\mathrm{q})}_{pq} T_{qr} \alpha^{(\mathrm{p})}_{rs} T_{st} \alpha^{(\mathrm{q})}_{tw} + \cdots \Big) \\
+ \tfrac{1}{2} \Big(& \gamma^{(\mathrm{p})}_{iwab} + \gamma^{(\mathrm{p})}_{ijab} T_{jk} \alpha^{(\mathrm{q})}_{kw} + \alpha^{(\mathrm{p})}_{ij} T_{jk} \gamma^{(\mathrm{q})}_{kwab} + 2\gamma^{(\mathrm{p})}_{iwaj} T_{jk} a^{(\mathrm{q})}_{kb} + \gamma^{(\mathrm{p})}_{ijab} T_{jk} \alpha^{(\mathrm{q})}_{kl} T_{lm} \alpha^{(\mathrm{p})}_{mw} \\
& + \alpha^{(\mathrm{p})}_{ij} T_{jk} \gamma^{(\mathrm{q})}_{klab} T_{lm} \alpha^{(\mathrm{p})}_{mw} + \alpha^{(\mathrm{p})}_{ij} T_{jk} \alpha^{(\mathrm{q})}_{kl} T_{lm} \gamma^{(\mathrm{p})}_{mwab} + \gamma^{(\mathrm{p})}_{iwjl} T_{jk} a^{(\mathrm{q})}_{ka} T_{lm} a^{(\mathrm{q})}_{mb} \\
& + 2\gamma^{(\mathrm{p})}_{iwaj} T_{jk} a^{(\mathrm{q})}_{kl} T_{lm} a^{(\mathrm{p})}_{mb} + 2\gamma^{(\mathrm{p})}_{ijal} T_{jk} \alpha^{(\mathrm{q})}_{kw} T_{lm} a^{(\mathrm{q})}_{mb} + 2\alpha^{(\mathrm{p})}_{ij} T_{jk} \gamma^{(\mathrm{q})}_{kwal} T_{lm} a^{(\mathrm{p})}_{mb} \\
& + \gamma^{(\mathrm{p})}_{ijab} T_{jk} \alpha^{(\mathrm{q})}_{kl} T_{lm} \alpha^{(\mathrm{p})}_{mn} T_{np} \alpha^{(\mathrm{q})}_{pw} + \alpha^{(\mathrm{p})}_{ij} T_{jk} \alpha^{(\mathrm{q})}_{kl} T_{lm} \alpha^{(\mathrm{p})}_{mn} T_{np} \gamma^{(\mathrm{q})}_{pwab} \\
& + \alpha^{(\mathrm{p})}_{ij} T_{jk} \alpha^{(\mathrm{q})}_{kl} T_{lm} \gamma^{(\mathrm{p})}_{mnab} T_{np} \alpha^{(\mathrm{q})}_{pw} + \alpha^{(\mathrm{p})}_{ij} T_{jk} \gamma^{(\mathrm{q})}_{klab} T_{lm} \alpha^{(\mathrm{p})}_{mn} T_{np} \alpha^{(\mathrm{q})}_{pw} \\
& + 2\gamma^{(\mathrm{p})}_{iwaj} T_{jk} a^{(\mathrm{q})}_{kl} T_{lm} a^{(\mathrm{p})}_{mn} T_{np} a^{(\mathrm{q})}_{pb} + \gamma^{(\mathrm{p})}_{iwjl} T_{jk} a^{(\mathrm{q})}_{ka} T_{lm} a^{(\mathrm{q})}_{mn} T_{np} a^{(\mathrm{p})}_{pb} \\
& + \gamma^{(\mathrm{p})}_{ijln} T_{jk} \alpha^{(\mathrm{q})}_{kw} T_{lm} a^{(\mathrm{q})}_{ma} T_{np} a^{(\mathrm{q})}_{pb} + 2\alpha^{(\mathrm{p})}_{ij} T_{jk} \gamma^{(\mathrm{q})}_{kwln} T_{lm} a^{(\mathrm{p})}_{ma} T_{np} a^{(\mathrm{p})}_{pb} \\
& + 2\gamma^{(\mathrm{p})}_{ijan} T_{jk} \alpha^{(\mathrm{q})}_{kl} T_{lm} \alpha^{(\mathrm{p})}_{mw} T_{np} a^{(\mathrm{q})}_{pb} + 2\alpha^{(\mathrm{p})}_{ij} T_{jk} \gamma^{(\mathrm{q})}_{klan} T_{lm} \alpha^{(\mathrm{p})}_{mw} T_{np} a^{(\mathrm{p})}_{pb} \\
& + 2\alpha^{(\mathrm{p})}_{ij} T_{jk} \alpha^{(\mathrm{q})}_{kl} T_{lm} \gamma^{(\mathrm{p})}_{mwan} T_{np} a^{(\mathrm{q})}_{pb} + 2\gamma^{(\mathrm{p})}_{ijan} T_{jk} \alpha^{(\mathrm{q})}_{kw} T_{np} a^{(\mathrm{q})}_{pq} T_{qr} a^{(\mathrm{p})}_{rb} \\
& + 2\alpha^{(\mathrm{p})}_{ij} T_{jk} \gamma^{(\mathrm{q})}_{kwan} T_{np} a^{(\mathrm{p})}_{pq} T_{qr} a^{(\mathrm{q})}_{rb} + \cdots \Big) E_a E_b + \cdots \ .
\end{aligned}
\tag{2.79}
$$

Use of equation (2.79) in equation (2.64) yields $\pi^{(p)}(\tau, E)$ as

$$
\pi^{(p)}(\tau, E) = \pi^{(p)}_{iw} \left(a^x_i a^x_w - a^y_i a^y_w \right). \tag{2.80}
$$

The term $\frac{1}{2}\left(\partial^2\overline{\pi^{(12)}(\tau,E)}/\partial E_x^2\right)_{E_x=0}$ in the expression for B_{K} in equation (2.61) can now be evaluated. Using equation (2.64) in equation (2.54) yields

$$\frac{1}{2}\left\langle\frac{\partial^2\pi^{(12)}}{\partial E_x^2}\right\rangle=\frac{1}{2}\left\langle\frac{\partial^2\pi^{(1)}}{\partial E_x^2}\right\rangle+\frac{1}{2}\left\langle\frac{\partial^2\pi^{(2)}}{\partial E_x^2}\right\rangle, \tag{2.81}$$

and since molecules 1 and 2 are identical, the isotropic averages of their molecular properties must be the same, so that

$$\frac{1}{2}\left\langle\frac{\partial^2\pi^{(12)}}{\partial E_x^2}\right\rangle=\left\langle\frac{\partial^2\pi^{(1)}}{\partial E_x^2}\right\rangle. \tag{2.82}$$

Similar arguments, together with equation (2.72), yield

$$\begin{aligned}\frac{1}{2}\left(\frac{\partial^2\overline{\pi^{(12)}(\tau,E)}}{\partial E_x^2}\right)_{E_x=0}&=\left\langle\frac{\partial^2\pi^{(1)}}{\partial E_x^2}\right\rangle-\frac{2}{kT}\left\{\left\langle 2\frac{\partial\pi^{(1)}}{\partial E_x}\frac{\partial U^{(1)}}{\partial E_x}\right\rangle+\left\langle 2\frac{\partial\pi^{(1)}}{\partial E_x}\frac{\partial U^{(2)}}{\partial E_x}\right\rangle\right\}\\&\quad-\frac{1}{kT}\left\{\left\langle\pi^{(1)}\frac{\partial^2U^{(1)}}{\partial E_x^2}\right\rangle+\left\langle\pi^{(1)}\frac{\partial^2U^{(2)}}{\partial E_x^2}\right\rangle\right\}\\&\quad+\frac{1}{(kT)^2}\left\{\left\langle\pi^{(1)}\left(\frac{\partial U^{(1)}}{\partial E_x}\right)^2\right\rangle+\left\langle 2\pi^{(1)}\frac{\partial U^{(1)}}{\partial E_x}\frac{\partial U^{(2)}}{\partial E_x}\right\rangle\right.\\&\quad\left.+\left\langle\pi^{(1)}\left(\frac{\partial U^{(2)}}{\partial E_x}\right)^2\right\rangle\right\}.\end{aligned} \tag{2.83}$$

Substituting in the explicit expressions for $\pi^{(p)}(\tau,E)$ and $U^{(p)}(\tau,E)$ (provided by equations (2.79) – (2.80) and equation (2.73), respectively) with $E=0$, as well as their first and second derivatives with respect to the applied field where appropriate, the contributions to B_{K} in equation (2.61) are obtained as

$$\left\{\frac{1}{2}\left(\frac{\partial^2\overline{\pi^{(12)}(\tau,E)}}{\partial E_x^2}\right)_{E_x=0}-\left(\frac{\partial^2\overline{\pi})}{\partial E_x^2}\right)_{E_x=0}\right\}$$

$$\begin{aligned}&=\alpha_2+\alpha_3+\alpha_4+\alpha_5+\alpha_6+\alpha_7+\cdots+\Theta_2\alpha_3+\Theta_2\alpha_4+\Theta_2\alpha_5\\&+\Theta_2\alpha_6+\Theta_2\alpha_7+\cdots+\gamma_1\alpha_1+\gamma_1\alpha_2+\gamma_1\alpha_3+\cdots\ ,\end{aligned}\tag{2.84}$$

where

$$\alpha_2=\frac{1}{kT}\left\{\alpha_{ab}^{(1)}a_{pq}^{(2)}\right\}\left\langle a_a^x a_b^x a_p^x a_q^x-a_a^y a_b^y a_p^x a_q^x\right\rangle,\tag{2.85}$$

$$\begin{aligned}\alpha_3=\frac{1}{kT}\Big\{&\alpha_{ad}^{(1)}a_{pq}^{(1)}T_{qr}a_{rs}^{(2)}+\alpha_{ad}^{(1)}a_{pq}^{(2)}T_{qr}a_{rs}^{(1)}+\alpha_{ab}^{(1)}T_{bc}\alpha_{cd}^{(2)}a_{ps}^{(1)}\\&+\alpha_{ab}^{(1)}T_{bc}\alpha_{cd}^{(2)}a_{ps}^{(2)}\Big\}\times\left\langle a_a^x a_d^x a_p^x a_s^x-a_a^y a_d^y a_p^x a_s^x\right\rangle,\end{aligned}\tag{2.86}$$

$$\begin{aligned}\alpha_4=\frac{1}{kT}\Big\{&\alpha_{af}^{(1)}a_{pq}^{(1)}T_{qr}a_{rs}^{(2)}T_{st}a_{tu}^{(1)}+\alpha_{af}^{(1)}a_{pq}^{(2)}T_{qr}a_{rs}^{(1)}T_{st}a_{tu}^{(2)}+\alpha_{ab}^{(1)}T_{bc}\alpha_{cf}^{(2)}a_{pq}^{(1)}T_{qr}a_{ru}^{(2)}\\&+\alpha_{ab}^{(1)}T_{bc}\alpha_{cf}^{(2)}a_{pq}^{(2)}T_{qr}a_{ru}^{(1)}+\alpha_{ab}^{(1)}T_{bc}\alpha_{cd}^{(2)}T_{de}\alpha_{ef}^{(1)}a_{pu}^{(1)}+\alpha_{ab}^{(1)}T_{bc}\alpha_{cd}^{(2)}T_{de}\alpha_{ef}^{(1)}a_{pu}^{(2)}\Big\}\\&\times\left\langle a_a^x a_f^x a_p^x a_u^x-a_a^y a_f^y a_p^x a_u^x\right\rangle,\end{aligned}\tag{2.87}$$

$$\begin{aligned}\alpha_5 = \frac{1}{kT}\Big\{ & \alpha^{(1)}_{ah} a^{(1)}_{pq} T_{qr} a^{(2)}_{rs} T_{st} a^{(1)}_{tu} T_{uv} a^{(2)}_{vw} + \alpha^{(1)}_{ah} a^{(2)}_{pq} T_{qr} a^{(1)}_{rs} T_{st} a^{(2)}_{tu} T_{uv} a^{(1)}_{vw} \\ & + \alpha^{(1)}_{ab} T_{bc} \alpha^{(2)}_{ch} a^{(1)}_{pq} T_{qr} a^{(2)}_{rs} T_{st} a^{(1)}_{tw} + \alpha^{(1)}_{ab} T_{bc} \alpha^{(2)}_{ch} a^{(2)}_{pq} T_{qr} a^{(1)}_{rs} T_{st} a^{(2)}_{tw} \\ & + \alpha^{(1)}_{ab} T_{bc} \alpha^{(2)}_{cd} T_{de} \alpha^{(1)}_{eh} a^{(1)}_{pq} T_{qr} a^{(2)}_{rw} + \alpha^{(1)}_{ab} T_{bc} \alpha^{(2)}_{cd} T_{de} \alpha^{(1)}_{eh} a^{(2)}_{pq} T_{qr} a^{(1)}_{rw} \\ & + \alpha^{(1)}_{ab} T_{bc} \alpha^{(2)}_{cd} T_{de} \alpha^{(1)}_{ef} T_{fg} \alpha^{(2)}_{gh} a^{(1)}_{pw} + \alpha^{(1)}_{ab} T_{bc} \alpha^{(2)}_{cd} T_{de} \alpha^{(1)}_{ef} T_{fg} \alpha^{(2)}_{gh} a^{(2)}_{pw} \Big\} \\ & \times \Big\langle a^x_a a^x_h a^x_p a^x_w - a^y_a a^y_h a^x_p a^x_w \Big\rangle,\end{aligned} \tag{2.88}$$

$$\begin{aligned}\alpha_6 = \frac{1}{kT}\Big\{ & \alpha^{(1)}_{\alpha\omega} a^{(1)}_{ij} T_{jk} a^{(2)}_{kl} T_{lm} a^{(1)}_{mn} T_{np} a^{(2)}_{pq} T_{qr} a^{(1)}_{rv} + \alpha^{(1)}_{\alpha\beta} T_{\beta\gamma} \alpha^{(2)}_{\gamma\delta} T_{\delta\epsilon} \alpha^{(1)}_{\epsilon\eta} T_{\eta\theta} \alpha^{(2)}_{\theta\mu} T_{\mu\nu} \alpha^{(1)}_{\nu\omega} a^{(1)}_{iv} \\ & + \alpha^{(1)}_{\alpha\beta} T_{\beta\gamma} \alpha^{(2)}_{\gamma\omega} a^{(1)}_{ij} T_{jk} a^{(2)}_{kl} T_{lm} a^{(1)}_{mn} T_{np} a^{(2)}_{pv} + \alpha^{(1)}_{\alpha\beta} T_{\beta\gamma} \alpha^{(2)}_{\gamma\delta} T_{\delta\epsilon} \alpha^{(1)}_{\epsilon\eta} T_{\eta\theta} \alpha^{(2)}_{\theta\omega} a^{(1)}_{ij} T_{jk} a^{(2)}_{kv} \\ & + \alpha^{(1)}_{\alpha\beta} T_{\beta\gamma} \alpha^{(2)}_{\gamma\delta} T_{\delta\epsilon} \alpha^{(1)}_{\epsilon\omega} a^{(1)}_{ij} T_{jk} a^{(2)}_{kl} T_{lm} a^{(1)}_{mv} + \alpha^{(1)}_{\alpha\omega} a^{(2)}_{ij} T_{jk} a^{(1)}_{kl} T_{lm} a^{(2)}_{mn} T_{np} a^{(1)}_{pq} T_{qr} a^{(2)}_{rv} \\ & + \alpha^{(1)}_{\alpha\beta} T_{\beta\gamma} \alpha^{(2)}_{\gamma\delta} T_{\delta\epsilon} \alpha^{(1)}_{\epsilon\eta} T_{\eta\theta} \alpha^{(2)}_{\theta\mu} T_{\mu\nu} \alpha^{(1)}_{\nu\omega} a^{(2)}_{iv} + \alpha^{(1)}_{\alpha\beta} T_{\beta\gamma} \alpha^{(2)}_{\gamma\omega} a^{(2)}_{ij} T_{jk} a^{(1)}_{kl} T_{lm} a^{(2)}_{mn} T_{np} a^{(1)}_{pv} \\ & + \alpha^{(1)}_{\alpha\beta} T_{\beta\gamma} \alpha^{(2)}_{\gamma\delta} T_{\delta\epsilon} \alpha^{(1)}_{\epsilon\eta} T_{\eta\theta} \alpha^{(2)}_{\theta\omega} a^{(2)}_{ij} T_{jk} a^{(1)}_{kv} + \alpha^{(1)}_{\alpha\beta} T_{\beta\gamma} \alpha^{(2)}_{\gamma\delta} T_{\delta\epsilon} \alpha^{(1)}_{\epsilon\omega} a^{(2)}_{ij} T_{jk} a^{(1)}_{kl} T_{lm} a^{(2)}_{mv} \Big\} \\ & \times \Big\langle a^x_\alpha a^x_\omega a^x_i a^x_v - a^y_\alpha a^y_\omega a^x_i a^x_v \Big\rangle,\end{aligned} \tag{2.89}$$

$$\alpha_7 = \frac{1}{kT}\Big\{\alpha^{(1)}_{\alpha\omega}a^{(1)}_{ij}T_{jk}a^{(2)}_{kl}T_{lm}a^{(1)}_{mn}T_{np}a^{(2)}_{pq}T_{qr}a^{(1)}_{rs}T_{st}a^{(2)}_{tv}$$

$$+\alpha^{(1)}_{\alpha\beta}T_{\beta\gamma}\alpha^{(2)}_{\gamma\delta}T_{\delta\epsilon}\alpha^{(1)}_{\epsilon\eta}T_{\eta\theta}\alpha^{(2)}_{\theta\mu}T_{\mu\nu}\alpha^{(1)}_{\nu\phi}T_{\phi\lambda}\alpha^{(2)}_{\lambda\omega}a^{(1)}_{iv} + \alpha^{(1)}_{\alpha\beta}T_{\beta\gamma}\alpha^{(2)}_{\gamma\delta}a^{(1)}_{ij}T_{jk}a^{(2)}_{kl}T_{lm}a^{(1)}_{mn}T_{np}a^{(2)}_{pq}T_{qr}a^{(1)}_{rv}$$

$$+\alpha^{(1)}_{\alpha\beta}T_{\beta\gamma}\alpha^{(2)}_{\gamma\delta}T_{\delta\epsilon}\alpha^{(1)}_{\epsilon\eta}T_{\eta\theta}\alpha^{(2)}_{\theta\mu}T_{\mu\nu}\alpha^{(1)}_{\nu\phi}a^{(1)}_{ij}T_{jk}a^{(2)}_{kv} + \alpha^{(1)}_{\alpha\beta}T_{\beta\gamma}\alpha^{(2)}_{\gamma\delta}T_{\delta\epsilon}\alpha^{(1)}_{\epsilon\eta}a^{(1)}_{ij}T_{jk}a^{(2)}_{kl}T_{lm}a^{(1)}_{mn}T_{np}a^{(2)}_{pv}$$

$$+\alpha^{(1)}_{\alpha\beta}T_{\beta\gamma}\alpha^{(2)}_{\gamma\delta}T_{\delta\epsilon}\alpha^{(1)}_{\epsilon\eta}T_{\eta\theta}\alpha^{(2)}_{\theta\mu}a^{(1)}_{ij}T_{jk}a^{(2)}_{kl}T_{lm}a^{(1)}_{mv} + \alpha^{(1)}_{\alpha\omega}a^{(2)}_{ij}T_{jk}a^{(1)}_{kl}T_{lm}a^{(2)}_{mn}T_{np}a^{(1)}_{pq}T_{qr}a^{(2)}_{rs}T_{st}a^{(1)}_{tv}$$

$$+\alpha^{(1)}_{\alpha\beta}T_{\beta\gamma}\alpha^{(2)}_{\gamma\delta}T_{\delta\epsilon}\alpha^{(1)}_{\epsilon\eta}T_{\eta\theta}\alpha^{(2)}_{\theta\mu}T_{\mu\nu}\alpha^{(1)}_{\nu\phi}T_{\phi\lambda}\alpha^{(2)}_{\lambda\omega}a^{(2)}_{iv} + \alpha^{(1)}_{\alpha\beta}T_{\beta\gamma}\alpha^{(2)}_{\gamma\delta}a^{(2)}_{ij}T_{jk}a^{(1)}_{kl}T_{lm}a^{(2)}_{mn}T_{np}a^{(1)}_{pq}T_{qr}a^{(2)}_{rv}$$

$$+\alpha^{(1)}_{\alpha\beta}T_{\beta\gamma}\alpha^{(2)}_{\gamma\delta}T_{\delta\epsilon}\alpha^{(1)}_{\epsilon\eta}T_{\eta\theta}\alpha^{(2)}_{\theta\mu}T_{\mu\nu}\alpha^{(1)}_{\nu\phi}a^{(2)}_{ij}T_{jk}a^{(1)}_{kv} + \alpha^{(1)}_{\alpha\beta}T_{\beta\gamma}\alpha^{(2)}_{\gamma\delta}T_{\delta\epsilon}\alpha^{(1)}_{\epsilon\eta}a^{(2)}_{ij}T_{jk}a^{(1)}_{kl}T_{lm}a^{(2)}_{mn}T_{np}a^{(1)}_{pv}$$

$$+\alpha^{(1)}_{\alpha\beta}T_{\beta\gamma}\alpha^{(2)}_{\gamma\delta}T_{\delta\epsilon}\alpha^{(1)}_{\epsilon\eta}T_{\eta\theta}\alpha^{(2)}_{\theta\mu}a^{(2)}_{ij}T_{jk}a^{(1)}_{kl}T_{lm}a^{(2)}_{mv}\Big\} \times \Big\langle a^x_\alpha a^x_\omega a^x_i a^x_v - a^y_\alpha a^y_\omega a^y_i a^x_v\Big\rangle, \tag{2.90}$$

$$\theta_2\alpha_3 = \frac{1}{(3kT)^2}\Big\{\alpha^{(1)}_{\alpha\tau}a^{(1)}_{ij}T_{jkv}\theta^{(2)}_{0kv}a^{(1)}_{ab}T_{bch}\theta^{(2)}_{0ch} + \alpha^{(1)}_{\alpha\tau}a^{(2)}_{ij}T_{jkv}\theta^{(1)}_{0kv}a^{(2)}_{ab}T_{bch}\theta^{(1)}_{0ch}$$

$$+2\alpha^{(1)}_{\alpha\tau}a^{(1)}_{ij}T_{jkv}\theta^{(2)}_{0kv}a^{(2)}_{ab}T_{bch}\theta^{(1)}_{0ch}\Big\} \times \Big\langle a^x_\alpha a^x_\tau a^x_a a^x_i - a^y_\alpha a^y_\tau a^x_a a^x_i\Big\rangle, \tag{2.91}$$

$$\theta_2\alpha_4 = \frac{1}{3\,(kT)^2}\Big\{\alpha^{(1)}_{\alpha\beta}T_{\beta\gamma}\alpha^{(2)}_{\gamma\omega}a^{(1)}_{ij}T_{jkv}\theta^{(2)}_{0kv}a^{(1)}_{ab}T_{abc}\theta^{(2)}_{0ct} - \alpha^{(1)}_{\alpha\omega}a^{(1)}_{ij}T_{jkv}\theta^{(2)}_{0kv}a^{(1)}_{ab}T_{bc}a^{(2)}_{cd}T_{det}\theta^{(1)}_{0et}$$

$$-\alpha^{(1)}_{\alpha\omega}a^{(1)}_{ij}T_{jk}a^{(2)}_{kl}T_{lmv}\theta^{(1)}_{0mv}a^{(1)}_{ab}T_{bct}\theta^{(2)}_{0ct} + \alpha^{(1)}_{\alpha\beta}T_{\beta\gamma}\alpha^{(2)}_{\gamma\omega}a^{(2)}_{ij}T_{jkv}\theta^{(1)}_{0kv}a^{(2)}_{ab}T_{abc}\theta^{(1)}_{0ct}$$

$$-\alpha^{(1)}_{\alpha\omega}a^{(2)}_{ij}T_{jkv}\theta^{(1)}_{0kv}a^{(2)}_{ab}T_{bc}a^{(1)}_{cd}T_{det}\theta^{(2)}_{0et} - \alpha^{(1)}_{\alpha\omega}a^{(2)}_{ij}T_{jk}a^{(1)}_{kl}T_{lmv}\theta^{(2)}_{0mv}a^{(2)}_{ab}T_{bct}\theta^{(1)}_{0ct}$$

$$-2\alpha^{(1)}_{\alpha\beta}T_{\beta\gamma}\alpha^{(2)}_{\gamma\omega}a^{(1)}_{ij}T_{jkv}\theta^{(2)}_{0kv}a^{(2)}_{ab}T_{abc}\theta^{(1)}_{0ct} + 2\alpha^{(1)}_{\alpha\omega}a^{(1)}_{ij}T_{jkv}\theta^{(2)}_{0kv}a^{(2)}_{ab}T_{bc}a^{(1)}_{cd}T_{det}\theta^{(2)}_{0et}$$

$$+2\alpha^{(1)}_{\alpha\omega}a^{(1)}_{ij}T_{jk}a^{(2)}_{kl}T_{lmv}\theta^{(1)}_{0mv}a^{(2)}_{ab}T_{bct}\theta^{(1)}_{0ct}\Big\} \times \Big\langle a^x_\alpha a^x_\omega a^x_i a^x_a - a^y_\alpha a^y_\omega a^x_i a^x_a\Big\rangle, \tag{2.92}$$

$$
\begin{aligned}
\theta_2\alpha_5 \;=\; & \frac{1}{3\,(kT)^2}\Big\{\alpha^{(1)}_{\alpha\omega}a^{(1)}_{ij}T_{jk}a^{(2)}_{kl}T_{lmv}\theta^{(1)}_{0mv}a^{(1)}_{ab}T_{bc}a^{(2)}_{cd}T_{det}\theta^{(1)}_{0et} \\
& + \alpha^{(1)}_{\alpha\omega}a^{(1)}_{ij}T_{jkv}\theta^{(2)}_{0kv}a^{(1)}_{ab}T_{bc}a^{(2)}_{cd}T_{de}a^{(1)}_{ef}T_{fgt}\theta^{(2)}_{0gt} + \alpha^{(1)}_{\alpha\omega}a^{(1)}_{ij}T_{jk}a^{(2)}_{kl}T_{lm}a^{(1)}_{mn}T_{npv}\theta^{(2)}_{0pv}a^{(1)}_{ab}T_{bct}\theta^{(2)}_{0ct} \\
& - \alpha^{(1)}_{\alpha\beta}T_{\beta\gamma}\alpha^{(2)}_{\gamma\omega}a^{(1)}_{ij}T_{jkv}\theta^{(2)}_{0kv}a^{(1)}_{ab}T_{bc}a^{(2)}_{cd}T_{det}\theta^{(1)}_{0et} - \alpha^{(1)}_{\alpha\beta}T_{\beta\gamma}\alpha^{(2)}_{\gamma\omega}a^{(1)}_{ij}T_{jk}a^{(2)}_{kl}T_{lmv}\theta^{(1)}_{0mv}a^{(1)}_{ab}T_{bct}\theta^{(2)}_{0ct} \\
& + \alpha^{(1)}_{\alpha\beta}T_{\beta\gamma}\alpha^{(2)}_{\gamma\delta}T_{\delta\epsilon}\alpha^{(1)}_{\epsilon\omega}a^{(1)}_{ij}T_{jkv}\theta^{(2)}_{0kv}a^{(1)}_{ab}T_{bct}\theta^{(2)}_{0ct} + \alpha^{(1)}_{\alpha\omega}a^{(2)}_{ij}T_{jk}a^{(1)}_{kl}T_{lmv}\theta^{(2)}_{0mv}a^{(2)}_{ab}T_{bc}a^{(1)}_{cd}T_{det}\theta^{(2)}_{0et} \\
& + \alpha^{(1)}_{\alpha\omega}a^{(2)}_{ij}T_{jkv}\theta^{(1)}_{0kv}a^{(2)}_{ab}T_{bc}a^{(1)}_{cd}T_{de}a^{(2)}_{ef}T_{fgt}\theta^{(1)}_{0gt} + \alpha^{(1)}_{\alpha\omega}a^{(2)}_{ij}T_{jk}a^{(1)}_{kl}T_{lm}a^{(2)}_{mn}T_{npv}\theta^{(1)}_{0pv}a^{(2)}_{ab}T_{bct}\theta^{(1)}_{0ct} \\
& - \alpha^{(1)}_{\alpha\beta}T_{\beta\gamma}\alpha^{(2)}_{\gamma\omega}a^{(2)}_{ij}T_{jkv}\theta^{(1)}_{0kv}a^{(2)}_{ab}T_{bc}a^{(1)}_{cd}T_{det}\theta^{(2)}_{0et} - \alpha^{(1)}_{\alpha\beta}T_{\beta\gamma}\alpha^{(2)}_{\gamma\omega}a^{(2)}_{ij}T_{jk}a^{(1)}_{kl}T_{lmv}\theta^{(2)}_{0mv}a^{(2)}_{ab}T_{bct}\theta^{(1)}_{0ct} \\
& + \alpha^{(1)}_{\alpha\beta}T_{\beta\gamma}\alpha^{(2)}_{\gamma\delta}T_{\delta\epsilon}\alpha^{(1)}_{\epsilon\omega}a^{(2)}_{ij}T_{jkv}\theta^{(1)}_{0kv}a^{(2)}_{ab}T_{bct}\theta^{(1)}_{0ct} + \alpha^{(1)}_{\alpha\omega}a^{(1)}_{ij}T_{jk}a^{(2)}_{kl}T_{lmv}\theta^{(1)}_{0mv}a^{(2)}_{ab}T_{bc}a^{(1)}_{cd}T_{det}\theta^{(2)}_{0et} \\
& + \alpha^{(1)}_{\alpha\omega}a^{(1)}_{ij}T_{jkv}\theta^{(2)}_{0kv}a^{(2)}_{ab}T_{bc}a^{(1)}_{cd}T_{de}a^{(2)}_{ef}T_{fgt}\theta^{(1)}_{0gt} + \alpha^{(1)}_{\alpha\omega}a^{(1)}_{ij}T_{jk}a^{(2)}_{kl}T_{lm}a^{(1)}_{mn}T_{npv}\theta^{(1)}_{0pv}a^{(1)}_{ab}T_{bct}\theta^{(2)}_{0ct} \\
& - \alpha^{(1)}_{\alpha\beta}T_{\beta\gamma}\alpha^{(2)}_{\gamma\omega}a^{(1)}_{ij}T_{jkv}\theta^{(2)}_{0kv}a^{(2)}_{ab}T_{bc}a^{(1)}_{cd}T_{det}\theta^{(2)}_{0et} - \alpha^{(1)}_{\alpha\beta}T_{\beta\gamma}\alpha^{(2)}_{\gamma\omega}a^{(1)}_{ij}T_{jk}a^{(2)}_{kl}T_{lmv}\theta^{(1)}_{0mv}a^{(2)}_{ab}T_{bct}\theta^{(1)}_{0ct} \\
& + \alpha^{(1)}_{\alpha\beta}T_{\beta\gamma}\alpha^{(2)}_{\gamma\delta}T_{\delta\epsilon}\alpha^{(1)}_{\epsilon\omega}a^{(1)}_{ij}T_{jkv}\theta^{(2)}_{0kv}a^{(2)}_{ab}T_{bct}\theta^{(1)}_{0ct}\Big\} \times \Big\langle a^x_\alpha a^x_\omega a^x_i a^x_a - a^y_\alpha a^y_\omega a^x_i a^x_a\Big\rangle,
\end{aligned}
\tag{2.93}
$$

$$\theta_2\alpha_6 = \frac{1}{3\,(kT)^2}\Big\{ - \alpha^{(1)}_{\alpha\omega} a^{(1)}_{ij} T_{jkv} \theta^{(2)}_{0kv} a^{(1)}_{ab} T_{bc} a^{(2)}_{cd} T_{de} a^{(1)}_{ef} T_{fg} a^{(2)}_{gh} T_{hst} \theta^{(1)}_{0st}$$

$$- \alpha^{(1)}_{\alpha\omega} a^{(1)}_{ij} T_{jk} a^{(2)}_{kl} T_{lm} a^{(1)}_{mn} T_{np} a^{(2)}_{pq} T_{qrv} \theta^{(1)}_{0rv} a^{(1)}_{ab} T_{bct} \theta^{(2)}_{0ct} - \alpha^{(1)}_{\alpha\omega} a^{(1)}_{ij} T_{jk} a^{(2)}_{kl} T_{lmv} \theta^{(1)}_{0mv} a^{(1)}_{ab} T_{bc} a^{(2)}_{cd} T_{de} a^{(1)}_{ef} T_{fgt} \theta^{(2)}_{0gt}$$

$$- \alpha^{(1)}_{\alpha\omega} a^{(1)}_{ij} T_{jk} a^{(2)}_{kl} T_{lm} a^{(1)}_{mn} T_{npv} \theta^{(2)}_{0pv} a^{(1)}_{ab} T_{bc} a^{(2)}_{cd} T_{det} \theta^{(1)}_{0et} + \alpha^{(1)}_{\alpha\beta} T_{\beta\gamma} \alpha^{(2)}_{\gamma\omega} a^{(1)}_{ij} T_{jk} a^{(2)}_{kl} T_{lmv} \theta^{(1)}_{0mv} a^{(1)}_{ab} T_{bc} a^{(2)}_{cd} T_{det} \theta^{(1)}_{0et}$$

$$+ \alpha^{(1)}_{\alpha\beta} T_{\beta\gamma} \alpha^{(2)}_{\gamma\omega} a^{(1)}_{ij} T_{jkv} \theta^{(2)}_{0kv} a^{(1)}_{ab} T_{bc} a^{(2)}_{cd} T_{de} a^{(1)}_{ef} T_{fgt} \theta^{(2)}_{0gt} + \alpha^{(1)}_{\alpha\beta} T_{\beta\gamma} \alpha^{(2)}_{\gamma\omega} a^{(1)}_{ij} T_{jk} a^{(2)}_{kl} T_{lm} a^{(1)}_{mn} T_{npv} \theta^{(2)}_{0pv} a^{(1)}_{ab} T_{bct} \theta^{(2)}_{0ct}$$

$$- \alpha^{(1)}_{\alpha\beta} T_{\beta\gamma} \alpha^{(2)}_{\gamma\delta} T_{\delta\epsilon} \alpha^{(1)}_{\epsilon\omega} a^{(1)}_{ij} T_{jkv} \theta^{(2)}_{0kv} a^{(1)}_{ab} T_{bc} a^{(2)}_{cd} T_{det} \theta^{(1)}_{0et} - \alpha^{(1)}_{\alpha\beta} T_{\beta\gamma} \alpha^{(2)}_{\gamma\delta} T_{\delta\epsilon} \alpha^{(1)}_{\epsilon\omega} a^{(1)}_{ij} T_{jk} a^{(2)}_{kl} T_{lmv} \theta^{(1)}_{0mv} a^{(1)}_{ab} T_{bct} \theta^{(2)}_{0ct}$$

$$+ \alpha^{(1)}_{\alpha\beta} T_{\beta\gamma} \alpha^{(2)}_{\gamma\delta} T_{\delta\epsilon} \alpha^{(1)}_{\epsilon\eta} T_{\eta\theta} \alpha^{(2)}_{\theta\omega} a^{(1)}_{ij} T_{jkv} \theta^{(2)}_{0kv} a^{(1)}_{ab} T_{bct} \theta^{(2)}_{0ct} - \alpha^{(1)}_{\alpha\omega} a^{(2)}_{ij} T_{jkv} \theta^{(1)}_{0kv} a^{(2)}_{ab} T_{bc} a^{(1)}_{cd} T_{de} a^{(2)}_{ef} T_{fg} a^{(1)}_{gh} T_{hst} \theta^{(2)}_{0st}$$

$$- \alpha^{(1)}_{\alpha\omega} a^{(2)}_{ij} T_{jk} a^{(1)}_{kl} T_{lm} a^{(2)}_{mn} T_{np} a^{(1)}_{pq} T_{qrv} \theta^{(2)}_{0rv} a^{(2)}_{ab} T_{bct} \theta^{(1)}_{0ct} - \alpha^{(1)}_{\alpha\omega} a^{(2)}_{ij} T_{jk} a^{(1)}_{kl} T_{lmv} \theta^{(2)}_{0mv} a^{(2)}_{ab} T_{bc} a^{(1)}_{cd} T_{de} a^{(2)}_{ef} T_{fgt} \theta^{(1)}_{0gt}$$

$$- \alpha^{(1)}_{\alpha\omega} a^{(2)}_{ij} T_{jk} a^{(1)}_{kl} T_{lm} a^{(2)}_{mn} T_{npv} \theta^{(1)}_{0pv} a^{(2)}_{ab} T_{bc} a^{(1)}_{cd} T_{det} \theta^{(2)}_{0et} + \alpha^{(1)}_{\alpha\beta} T_{\beta\gamma} \alpha^{(2)}_{\gamma\omega} a^{(2)}_{ij} T_{jk} a^{(1)}_{kl} T_{lmv} \theta^{(2)}_{0mv} a^{(2)}_{ab} T_{bc} a^{(1)}_{cd} T_{det} \theta^{(2)}_{0et}$$

$$+ \alpha^{(1)}_{\alpha\beta} T_{\beta\gamma} \alpha^{(2)}_{\gamma\omega} a^{(2)}_{ij} T_{jkv} \theta^{(1)}_{0kv} a^{(2)}_{ab} T_{bc} a^{(1)}_{cd} T_{de} a^{(2)}_{ef} T_{fgt} \theta^{(1)}_{0gt} + \alpha^{(1)}_{\alpha\beta} T_{\beta\gamma} \alpha^{(2)}_{\gamma\omega} a^{(2)}_{ij} T_{jk} a^{(1)}_{kl} T_{lm} a^{(2)}_{mn} T_{npv} \theta^{(1)}_{0pv} a^{(2)}_{ab} T_{bct} \theta^{(1)}_{0ct}$$

$$- \alpha^{(1)}_{\alpha\beta} T_{\beta\gamma} \alpha^{(2)}_{\gamma\delta} T_{\delta\epsilon} \alpha^{(1)}_{\epsilon\omega} a^{(2)}_{ij} T_{jkv} \theta^{(1)}_{0kv} a^{(2)}_{ab} T_{bc} a^{(1)}_{cd} T_{det} \theta^{(2)}_{0et} - \alpha^{(1)}_{\alpha\beta} T_{\beta\gamma} \alpha^{(2)}_{\gamma\delta} T_{\delta\epsilon} \alpha^{(1)}_{\epsilon\omega} a^{(2)}_{ij} T_{jk} a^{(1)}_{kl} T_{lmv} \theta^{(2)}_{0mv} a^{(2)}_{ab} T_{bct} \theta^{(1)}_{0ct}$$

$$+ \alpha^{(1)}_{\alpha\beta} T_{\beta\gamma} \alpha^{(2)}_{\gamma\delta} T_{\delta\epsilon} \alpha^{(1)}_{\epsilon\eta} T_{\eta\theta} \alpha^{(2)}_{\theta\omega} a^{(2)}_{ij} T_{jkv} \theta^{(1)}_{0kv} a^{(2)}_{ab} T_{bct} \theta^{(1)}_{0ct} + 2\alpha^{(1)}_{\alpha\omega} a^{(1)}_{ij} T_{jkv} \theta^{(2)}_{0kv} a^{(2)}_{ab} T_{bc} a^{(1)}_{cd} T_{de} a^{(2)}_{ef} T_{fg} a^{(1)}_{gh} T_{hst} \theta^{(2)}_{0st}$$

$$+ 2\alpha^{(1)}_{\alpha\omega} a^{(1)}_{ij} T_{jk} a^{(2)}_{kl} T_{lm} a^{(1)}_{mn} T_{np} a^{(2)}_{pq} T_{qrv} \theta^{(1)}_{0rv} a^{(2)}_{ab} T_{bct} \theta^{(1)}_{0ct} + 2\alpha^{(1)}_{\alpha\omega} a^{(1)}_{ij} T_{jk} a^{(2)}_{kl} T_{lmv} \theta^{(1)}_{0mv} a^{(2)}_{ab} T_{bc} a^{(1)}_{cd} T_{de} a^{(2)}_{ef} T_{fgt} \theta^{(1)}_{0gt}$$

$$+ \alpha^{(1)}_{\alpha\omega} a^{(1)}_{ij} T_{jk} a^{(2)}_{kl} T_{lm} a^{(1)}_{mn} T_{npv} \theta^{(2)}_{0pv} a^{(2)}_{ab} T_{bc} a^{(1)}_{cd} T_{det} \theta^{(2)}_{0et} - 2\alpha^{(1)}_{\alpha\beta} T_{\beta\gamma} \alpha^{(2)}_{\gamma\omega} a^{(1)}_{ij} T_{jk} a^{(2)}_{kl} T_{lmv} \theta^{(1)}_{0mv} a^{(2)}_{ab} T_{bc} a^{(1)}_{cd} T_{det} \theta^{(2)}_{0et}$$

$$- 2\alpha^{(1)}_{\alpha\beta} T_{\beta\gamma} \alpha^{(2)}_{\gamma\omega} a^{(1)}_{ij} T_{jkv} \theta^{(2)}_{0kv} a^{(2)}_{ab} T_{bc} a^{(1)}_{cd} T_{de} a^{(2)}_{ef} T_{fgt} \theta^{(1)}_{0gt} - 2\alpha^{(1)}_{\alpha\beta} T_{\beta\gamma} \alpha^{(2)}_{\gamma\omega} a^{(1)}_{ij} T_{jk} a^{(2)}_{kl} T_{lm} a^{(1)}_{mn} T_{npv} \theta^{(2)}_{0pv} a^{(2)}_{ab} T_{bct} \theta^{(1)}_{0ct}$$

$$+ 2\alpha^{(1)}_{\alpha\beta} T_{\beta\gamma} \alpha^{(2)}_{\gamma\delta} T_{\delta\epsilon} \alpha^{(1)}_{\epsilon\omega} a^{(1)}_{ij} T_{jkv} \theta^{(2)}_{0kv} a^{(2)}_{ab} T_{bc} a^{(1)}_{cd} T_{det} \theta^{(2)}_{0et} + 2\alpha^{(1)}_{\alpha\beta} T_{\beta\gamma} \alpha^{(2)}_{\gamma\delta} T_{\delta\epsilon} \alpha^{(1)}_{\epsilon\omega} a^{(1)}_{ij} T_{jk} a^{(2)}_{kl} T_{lmv} \theta^{(1)}_{0mv} a^{(2)}_{ab} T_{bct} \theta^{(1)}_{0ct}$$

$$- 2\alpha^{(1)}_{\alpha\beta} T_{\beta\gamma} \alpha^{(2)}_{\gamma\delta} T_{\delta\epsilon} \alpha^{(1)}_{\epsilon\eta} T_{\eta\theta} \alpha^{(2)}_{\theta\omega} a^{(1)}_{ij} T_{jkv} \theta^{(2)}_{0kv} a^{(2)}_{ab} T_{bct} \theta^{(1)}_{0ct} \Big\} \times \Big\langle a^x_\alpha a^x_\omega a^x_i a^x_a - a^y_\alpha a^y_\omega a^x_i a^x_a \Big\rangle, \tag{2.94}$$

$$
\begin{aligned}
\theta_2\alpha_7 \;=\; & \frac{1}{3\,(kT)^2}\Big\{\alpha^{(1)}_{\alpha\omega}a^{(1)}_{ij}T_{jk}a^{(2)}_{kl}T_{lm}a^{(1)}_{mn}T_{npv}\theta^{(2)}_{0pv}a^{(1)}_{ab}T_{bc}a^{(2)}_{cd}T_{de}a^{(1)}_{ef}T_{fgu}\theta^{(2)}_{0gu} \\
& + \alpha^{(1)}_{\alpha\omega}a^{(1)}_{ij}T_{jk}a^{(2)}_{kl}T_{lmv}\theta^{(1)}_{0mv}a^{(1)}_{ab}T_{bc}a^{(2)}_{cd}T_{de}a^{(1)}_{ef}T_{fg}a^{(2)}_{gh}T_{hsu}\theta^{(1)}_{0su} + \alpha^{(1)}_{\alpha\omega}a^{(1)}_{ij}T_{jk}a^{(2)}_{kl}T_{lm}a^{(1)}_{mn}T_{np}a^{(2)}_{pq}T_{qrv}\theta^{(1)}_{0rv}a^{(1)}_{ab}T_{bc}a^{(2)}_{cd}T_{deu}\theta^{(1)}_{0eu} \\
& + \alpha^{(1)}_{\alpha\omega}a^{(1)}_{ij}T_{jkv}\theta^{(2)}_{0kv}a^{(1)}_{ab}T_{bc}a^{(2)}_{cd}T_{de}a^{(1)}_{ef}T_{fg}a^{(2)}_{gh}T_{hw}a^{(1)}_{wy}T_{yzu}\theta^{(2)}_{0zu} + \alpha^{(1)}_{\alpha\omega}a^{(1)}_{ij}T_{jk}a^{(2)}_{kl}T_{lm}a^{(1)}_{mn}T_{np}a^{(2)}_{pq}T_{qr}a^{(1)}_{rs}T_{stv}\theta^{(2)}_{0tv}a^{(1)}_{ab}T_{bcu}\theta^{(2)}_{0cu} \\
& - \alpha^{(1)}_{\alpha\beta}T_{\beta\gamma}\alpha^{(2)}_{\gamma\omega}a^{(1)}_{ij}T_{jkv}\theta^{(2)}_{0kv}a^{(1)}_{ab}T_{bc}a^{(2)}_{cd}T_{de}a^{(1)}_{ef}T_{fg}a^{(2)}_{gh}T_{hsu}\theta^{(1)}_{0su} - \alpha^{(1)}_{\alpha\beta}T_{\beta\gamma}\alpha^{(2)}_{\gamma\omega}a^{(1)}_{ij}T_{jk}a^{(2)}_{kl}T_{lm}a^{(1)}_{mn}T_{np}a^{(2)}_{pq}T_{qrv}\theta^{(1)}_{0rv}a^{(1)}_{ab}T_{bcu}\theta^{(2)}_{0cu} \\
& - \alpha^{(1)}_{\alpha\beta}T_{\beta\gamma}\alpha^{(2)}_{\gamma\omega}a^{(1)}_{ij}T_{jk}a^{(2)}_{kl}T_{lmv}\theta^{(1)}_{0mv}a^{(1)}_{ab}T_{bc}a^{(2)}_{cd}T_{de}a^{(1)}_{ef}T_{fgu}\theta^{(2)}_{0gu} - \alpha^{(1)}_{\alpha\beta}T_{\beta\gamma}\alpha^{(2)}_{\gamma\omega}a^{(1)}_{ij}T_{jk}a^{(2)}_{kl}T_{lm}a^{(1)}_{mn}T_{npv}\theta^{(2)}_{0pv}a^{(1)}_{ab}T_{bc}a^{(2)}_{cd}T_{deu}\theta^{(1)}_{0eu} \\
& + \alpha^{(1)}_{\alpha\beta}T_{\beta\gamma}\alpha^{(2)}_{\gamma\delta}T_{\delta\epsilon}\alpha^{(1)}_{\epsilon\omega}a^{(1)}_{ij}T_{jk}a^{(2)}_{kl}T_{lmv}\theta^{(1)}_{0mv}a^{(1)}_{ab}T_{bc}a^{(2)}_{cd}T_{deu}\theta^{(1)}_{0eu} + \alpha^{(1)}_{\alpha\beta}T_{\beta\gamma}\alpha^{(2)}_{\gamma\delta}T_{\delta\epsilon}\alpha^{(1)}_{\epsilon\omega}a^{(1)}_{ij}T_{jkv}\theta^{(2)}_{0kv}a^{(1)}_{ab}T_{bc}a^{(2)}_{cd}T_{de}a^{(1)}_{ef}T_{fgu}\theta^{(2)}_{0gu} \\
& + \alpha^{(1)}_{\alpha\beta}T_{\beta\gamma}\alpha^{(2)}_{\gamma\delta}T_{\delta\epsilon}\alpha^{(1)}_{\epsilon\omega}a^{(1)}_{ij}T_{jk}a^{(2)}_{kl}T_{lm}a^{(1)}_{mn}T_{npv}\theta^{(2)}_{0pv}a^{(1)}_{ab}T_{bcu}\theta^{(2)}_{0cu} - \alpha^{(1)}_{\alpha\beta}T_{\beta\gamma}\alpha^{(2)}_{\gamma\delta}T_{\delta\epsilon}\alpha^{(1)}_{\epsilon\eta}T_{\eta\theta}\alpha^{(2)}_{\theta\omega}a^{(1)}_{ij}T_{jkv}\theta^{(2)}_{0kv}a^{(1)}_{ab}T_{bc}a^{(2)}_{cd}T_{deu}\theta^{(1)}_{0eu} \\
& - \alpha^{(1)}_{\alpha\beta}T_{\beta\gamma}\alpha^{(2)}_{\gamma\delta}T_{\delta\epsilon}\alpha^{(1)}_{\epsilon\eta}T_{\eta\theta}\alpha^{(2)}_{\theta\omega}a^{(1)}_{ij}T_{jk}a^{(2)}_{kl}T_{lmv}\theta^{(1)}_{0mv}a^{(1)}_{ab}T_{bcu}\theta^{(2)}_{0cu} + \alpha^{(1)}_{\alpha\beta}T_{\beta\gamma}\alpha^{(2)}_{\gamma\delta}T_{\delta\epsilon}\alpha^{(1)}_{\epsilon\eta}T_{\eta\theta}\alpha^{(2)}_{\theta\kappa}T_{\kappa\lambda}\alpha^{(1)}_{\lambda\omega}a^{(1)}_{ij}T_{jkv}\theta^{(2)}_{0kv}a^{(1)}_{ab}T_{bcu}\theta^{(2)}_{0cu} \\
& + \alpha^{(1)}_{\alpha\omega}a^{(2)}_{ij}T_{jk}a^{(1)}_{kl}T_{lm}a^{(2)}_{mn}T_{npv}\theta^{(1)}_{0pv}a^{(2)}_{ab}T_{bc}a^{(1)}_{cd}T_{de}a^{(2)}_{ef}T_{fgu}\theta^{(1)}_{0gu} + \alpha^{(1)}_{\alpha\omega}a^{(2)}_{ij}T_{jk}a^{(1)}_{kl}T_{lmv}\theta^{(2)}_{0mv}a^{(2)}_{ab}T_{bc}a^{(1)}_{cd}T_{de}a^{(2)}_{ef}T_{fg}a^{(1)}_{gh}T_{hsu}\theta^{(2)}_{0su} \\
& + \alpha^{(1)}_{\alpha\omega}a^{(2)}_{ij}T_{jk}a^{(1)}_{kl}T_{lm}a^{(2)}_{mn}T_{np}a^{(1)}_{pq}T_{qrv}\theta^{(2)}_{0rv}a^{(2)}_{ab}T_{bc}a^{(1)}_{cd}T_{deu}\theta^{(2)}_{0eu} + \alpha^{(1)}_{\alpha\omega}a^{(2)}_{ij}T_{jkv}\theta^{(1)}_{0kv}a^{(2)}_{ab}T_{bc}a^{(1)}_{cd}T_{de}a^{(2)}_{ef}T_{fg}a^{(1)}_{gh}T_{hw}a^{(2)}_{wy}T_{yzu}\theta^{(1)}_{0zu} \\
& + \alpha^{(1)}_{\alpha\omega}a^{(2)}_{ij}T_{jk}a^{(1)}_{kl}T_{lm}a^{(2)}_{mn}T_{np}a^{(1)}_{pq}T_{qr}a^{(2)}_{rs}T_{stv}\theta^{(1)}_{0tv}a^{(2)}_{ab}T_{bcu}\theta^{(1)}_{0cu} - \alpha^{(1)}_{\alpha\beta}T_{\beta\gamma}\alpha^{(2)}_{\gamma\omega}a^{(2)}_{ij}T_{jkv}\theta^{(1)}_{0kv}a^{(2)}_{ab}T_{bc}a^{(1)}_{cd}T_{de}a^{(2)}_{ef}T_{fg}a^{(1)}_{gh}T_{hsu}\theta^{(2)}_{0su} \\
& - \alpha^{(1)}_{\alpha\beta}T_{\beta\gamma}\alpha^{(2)}_{\gamma\omega}a^{(2)}_{ij}T_{jk}a^{(1)}_{kl}T_{lm}a^{(2)}_{mn}T_{np}a^{(1)}_{pq}T_{qrv}\theta^{(2)}_{0rv}a^{(2)}_{ab}T_{bcu}\theta^{(1)}_{0cu} - \alpha^{(1)}_{\alpha\beta}T_{\beta\gamma}\alpha^{(2)}_{\gamma\omega}a^{(2)}_{ij}T_{jk}a^{(1)}_{kl}T_{lmv}\theta^{(2)}_{0mv}a^{(2)}_{ab}T_{bc}a^{(1)}_{cd}T_{de}a^{(2)}_{ef}T_{fgu}\theta^{(1)}_{0gu} \\
& - \alpha^{(1)}_{\alpha\beta}T_{\beta\gamma}\alpha^{(2)}_{\gamma\omega}a^{(2)}_{ij}T_{jk}a^{(1)}_{kl}T_{lm}a^{(2)}_{mn}T_{npv}\theta^{(1)}_{0pv}a^{(2)}_{ab}T_{bc}a^{(1)}_{cd}T_{deu}\theta^{(2)}_{0eu} + \alpha^{(1)}_{\alpha\beta}T_{\beta\gamma}\alpha^{(2)}_{\gamma\delta}T_{\delta\epsilon}\alpha^{(1)}_{\epsilon\omega}a^{(2)}_{ij}T_{jk}a^{(1)}_{kl}T_{lmv}\theta^{(2)}_{0mv}a^{(2)}_{ab}T_{bc}a^{(1)}_{cd}T_{deu}\theta^{(2)}_{0eu} \\
& + \alpha^{(1)}_{\alpha\beta}T_{\beta\gamma}\alpha^{(2)}_{\gamma\delta}T_{\delta\epsilon}\alpha^{(1)}_{\epsilon\omega}a^{(2)}_{ij}T_{jkv}\theta^{(1)}_{0kv}a^{(2)}_{ab}T_{bc}a^{(1)}_{cd}T_{de}a^{(2)}_{ef}T_{fgu}\theta^{(1)}_{0gu} + \alpha^{(1)}_{\alpha\beta}T_{\beta\gamma}\alpha^{(2)}_{\gamma\delta}T_{\delta\epsilon}\alpha^{(1)}_{\epsilon\eta}T_{\eta\theta}\alpha^{(2)}_{\theta\omega}a^{(2)}_{ij}T_{jk}a^{(1)}_{kl}T_{lm}a^{(2)}_{mn}T_{npv}\theta^{(1)}_{0pv}a^{(2)}_{ab}T_{bcu}\theta^{(1)}_{0cu} \\
& - \alpha^{(1)}_{\alpha\beta}T_{\beta\gamma}\alpha^{(2)}_{\gamma\delta}T_{\delta\epsilon}\alpha^{(1)}_{\epsilon\eta}T_{\eta\theta}\alpha^{(2)}_{\theta\omega}a^{(2)}_{ij}T_{jkv}\theta^{(1)}_{0kv}a^{(2)}_{ab}T_{bc}a^{(1)}_{cd}T_{deu}\theta^{(2)}_{0eu} - \alpha^{(1)}_{\alpha\beta}T_{\beta\gamma}\alpha^{(2)}_{\gamma\delta}T_{\delta\epsilon}\alpha^{(1)}_{\epsilon\eta}T_{\eta\theta}\alpha^{(2)}_{\theta\omega}a^{(2)}_{ij}T_{jk}a^{(1)}_{kl}T_{lmv}\theta^{(2)}_{0mv}a^{(2)}_{ab}T_{bcu}\theta^{(1)}_{0cu} \\
& + \alpha^{(1)}_{\alpha\beta}T_{\beta\gamma}\alpha^{(2)}_{\gamma\delta}T_{\delta\epsilon}\alpha^{(1)}_{\epsilon\eta}T_{\eta\theta}\alpha^{(2)}_{\theta\kappa}T_{\kappa\lambda}\alpha^{(1)}_{\lambda\omega}a^{(2)}_{ij}T_{jkv}\theta^{(1)}_{0kv}a^{(2)}_{ab}T_{bcu}\theta^{(2)}_{0cu} - 2\alpha^{(1)}_{\alpha\omega}a^{(1)}_{ij}T_{jk}a^{(2)}_{kl}T_{lm}a^{(1)}_{mn}T_{npv}\theta^{(2)}_{0pv}a^{(2)}_{ab}T_{bc}a^{(1)}_{cd}T_{de}a^{(2)}_{ef}T_{fgu}\theta^{(1)}_{0gu} \\
& - 2\alpha^{(1)}_{\alpha\omega}a^{(1)}_{ij}T_{jk}a^{(2)}_{kl}T_{lmv}\theta^{(1)}_{0mv}a^{(2)}_{ab}T_{bc}a^{(1)}_{cd}T_{de}a^{(2)}_{ef}T_{fg}a^{(1)}_{gh}T_{hsu}\theta^{(2)}_{0su} - 2\alpha^{(1)}_{\alpha\omega}a^{(1)}_{ij}T_{jk}a^{(2)}_{kl}T_{lm}a^{(1)}_{mn}T_{np}a^{(2)}_{pq}T_{qrv}\theta^{(1)}_{0rv}a^{(2)}_{ab}T_{bc}a^{(1)}_{cd}T_{deu}\theta^{(2)}_{0eu} \\
& - 2\alpha^{(1)}_{\alpha\omega}a^{(1)}_{ij}T_{jkv}\theta^{(2)}_{0kv}a^{(2)}_{ab}T_{bc}a^{(1)}_{cd}T_{de}a^{(2)}_{ef}T_{fg}a^{(1)}_{gh}T_{hw}a^{(2)}_{wy}T_{yzu}\theta^{(1)}_{0zu} - 2\alpha^{(1)}_{\alpha\omega}a^{(1)}_{ij}T_{jk}a^{(2)}_{kl}T_{lm}a^{(1)}_{mn}T_{np}a^{(2)}_{pq}T_{qr}a^{(1)}_{rs}T_{stv}\theta^{(2)}_{0tv}a^{(2)}_{ab}T_{bcu}\theta^{(2)}_{0cu} \\
& + 2\alpha^{(1)}_{\alpha\beta}T_{\beta\gamma}\alpha^{(2)}_{\gamma\omega}a^{(1)}_{ij}T_{jkv}\theta^{(2)}_{0kv}a^{(2)}_{ab}T_{bc}a^{(1)}_{cd}T_{de}a^{(2)}_{ef}T_{fg}a^{(1)}_{gh}T_{hsu}\theta^{(2)}_{0su} + 2\alpha^{(1)}_{\alpha\beta}T_{\beta\gamma}\alpha^{(2)}_{\gamma\omega}a^{(1)}_{ij}T_{jk}a^{(2)}_{kl}T_{lm}a^{(1)}_{mn}T_{np}a^{(2)}_{pq}T_{qrv}\theta^{(1)}_{0rv}a^{(2)}_{ab}T_{bcu}\theta^{(1)}_{0cu} \\
& + 2\alpha^{(1)}_{\alpha\beta}T_{\beta\gamma}\alpha^{(2)}_{\gamma\omega}a^{(1)}_{ij}T_{jk}a^{(2)}_{kl}T_{lmv}\theta^{(1)}_{0mv}a^{(2)}_{ab}T_{bc}a^{(1)}_{cd}T_{de}a^{(2)}_{ef}T_{fgu}\theta^{(1)}_{0gu} + 2\alpha^{(1)}_{\alpha\beta}T_{\beta\gamma}\alpha^{(2)}_{\gamma\omega}a^{(1)}_{ij}T_{jk}a^{(2)}_{kl}T_{lm}a^{(1)}_{mn}T_{npv}\theta^{(2)}_{0pv}a^{(2)}_{ab}T_{bc}a^{(1)}_{cd}T_{deu}\theta^{(2)}_{0eu} \\
& - 2\alpha^{(1)}_{\alpha\beta}T_{\beta\gamma}\alpha^{(2)}_{\gamma\delta}T_{\delta\epsilon}\alpha^{(1)}_{\epsilon\omega}a^{(1)}_{ij}T_{jk}a^{(2)}_{kl}T_{lmv}\theta^{(1)}_{0mv}a^{(2)}_{ab}T_{bc}a^{(1)}_{cd}T_{deu}\theta^{(2)}_{0eu} - 2\alpha^{(1)}_{\alpha\beta}T_{\beta\gamma}\alpha^{(2)}_{\gamma\delta}T_{\delta\epsilon}\alpha^{(1)}_{\epsilon\omega}a^{(1)}_{ij}T_{jkv}\theta^{(2)}_{0kv}a^{(2)}_{ab}T_{bc}a^{(1)}_{cd}T_{de}a^{(2)}_{ef}T_{fgu}\theta^{(1)}_{0gu} \\
& - 2\alpha^{(1)}_{\alpha\beta}T_{\beta\gamma}\alpha^{(2)}_{\gamma\delta}T_{\delta\epsilon}\alpha^{(1)}_{\epsilon\omega}a^{(1)}_{ij}T_{jk}a^{(2)}_{kl}T_{lm}a^{(1)}_{mn}T_{npv}\theta^{(2)}_{0pv}a^{(2)}_{ab}T_{bcu}\theta^{(1)}_{0cu} + 2\alpha^{(1)}_{\alpha\beta}T_{\beta\gamma}\alpha^{(2)}_{\gamma\delta}T_{\delta\epsilon}\alpha^{(1)}_{\epsilon\eta}T_{\eta\theta}\alpha^{(2)}_{\theta\omega}a^{(1)}_{ij}T_{jkv}\theta^{(2)}_{0kv}a^{(2)}_{ab}T_{bc}a^{(1)}_{cd}T_{deu}\theta^{(2)}_{0eu} \\
& + 2\alpha^{(1)}_{\alpha\beta}T_{\beta\gamma}\alpha^{(2)}_{\gamma\delta}T_{\delta\epsilon}\alpha^{(1)}_{\epsilon\eta}T_{\eta\theta}\alpha^{(2)}_{\theta\omega}a^{(1)}_{ij}T_{jk}a^{(2)}_{kl}T_{lmv}\theta^{(1)}_{0mv}a^{(2)}_{ab}T_{bcu}\theta^{(1)}_{0cu} - 2\alpha^{(1)}_{\alpha\beta}T_{\beta\gamma}\alpha^{(2)}_{\gamma\delta}T_{\delta\epsilon}\alpha^{(1)}_{\epsilon\eta}T_{\eta\theta}\alpha^{(2)}_{\theta\kappa}T_{\kappa\lambda}\alpha^{(1)}_{\lambda\omega}a^{(1)}_{ij}T_{jkv}\theta^{(2)}_{0kv}a^{(2)}_{ab}T_{bcu}\theta^{(1)}_{0cu} \\
& - 2\alpha^{(1)}_{\alpha\beta}T_{\beta\gamma}\alpha^{(2)}_{\gamma\delta}T_{\delta\epsilon}\alpha^{(1)}_{\epsilon\eta}T_{\eta\theta}\alpha^{(2)}_{\theta\kappa}T_{\kappa\lambda}\alpha^{(1)}_{\lambda\omega}a^{(1)}_{ij}T_{jkv}\theta^{(2)}_{0kv}a^{(2)}_{ab}T_{bcu}\theta^{(1)}_{0cu}\Big\} \times \Big\langle a^x_\alpha a^x_\omega a^x_i a^x_a - a^y_\alpha a^y_\omega a^x_i a^x_a\Big\rangle,
\end{aligned}
\tag{2.95}
$$

$$\gamma_1\alpha_1 = \left\{\gamma^{(1)}_{ijab}T_{jk}\alpha^{(2)}_{kw} + \alpha^{(1)}_{ij}T_{jk}\gamma^{(2)}_{kwab} + 2\gamma^{(1)}_{iwaj}T_{jk}a^{(2)}_{kb}\right\}\left\langle a^x_i a^x_w a^x_a a^x_b - a^y_i a^y_w a^x_a a^x_b\right\rangle, \tag{2.96}$$

$$\begin{aligned}\gamma_1\alpha_2 = \Big\{&\gamma^{(1)}_{ijab}T_{jk}\alpha^{(2)}_{kl}T_{lm}\alpha^{(1)}_{mw} + \alpha^{(1)}_{ij}T_{jk}\gamma^{(2)}_{klab}T_{lm}\alpha^{(1)}_{mw} + \alpha^{(1)}_{ij}T_{jk}\alpha^{(2)}_{kl}T_{lm}\gamma^{(1)}_{mwab}\\ &+ \gamma^{(1)}_{iwjl}T_{jk}a^{(2)}_{ka}T_{lm}a^{(2)}_{mb} + 2\gamma^{(1)}_{iwaj}T_{jk}a^{(2)}_{kl}T_{lm}a^{(1)}_{mb} + 2\gamma^{(1)}_{ijal}T_{jk}\alpha^{(2)}_{kw}T_{lm}a^{(2)}_{mb}\\ &+ 2\alpha^{(1)}_{ij}T_{jk}\gamma^{(2)}_{kwal}T_{lm}a^{(1)}_{mb}\Big\}\left\langle a^x_i a^x_w a^x_a a^x_b - a^y_i a^y_w a^x_a a^x_b\right\rangle,\end{aligned} \tag{2.97}$$

$$\begin{aligned}\gamma_1\alpha_3 = \Big\{&\gamma^{(1)}_{ijab}T_{jk}\alpha^{(2)}_{kl}T_{lm}\alpha^{(1)}_{mn}T_{np}\alpha^{(2)}_{pw} + \alpha^{(1)}_{ij}T_{jk}\alpha^{(2)}_{kl}T_{lm}\alpha^{(1)}_{mn}T_{np}\gamma^{(2)}_{pwab}\\ &+ \alpha^{(1)}_{ij}T_{jk}\alpha^{(2)}_{kl}T_{lm}\gamma^{(1)}_{mnab}T_{np}\alpha^{(2)}_{pw} + \alpha^{(1)}_{ij}T_{jk}\gamma^{(2)}_{klab}T_{lm}\alpha^{(1)}_{mn}T_{np}\alpha^{(2)}_{pw}\\ &+ 2\gamma^{(1)}_{iwaj}T_{jk}a^{(2)}_{kl}T_{lm}a^{(1)}_{mn}T_{np}a^{(2)}_{pb} + 2\gamma^{(1)}_{iwjl}T_{jk}a^{(2)}_{ka}T_{lm}a^{(2)}_{mn}T_{np}a^{(1)}_{pb}\\ &+ \gamma^{(1)}_{ijln}T_{jk}\alpha^{(2)}_{kw}T_{lm}a^{(2)}_{ma}T_{np}a^{(2)}_{pb} + 2\alpha^{(1)}_{ij}T_{jk}\gamma^{(2)}_{kwln}T_{lm}a^{(1)}_{ma}T_{np}a^{(1)}_{pb}\\ &+ 2\gamma^{(1)}_{ijan}T_{jk}\alpha^{(2)}_{kl}T_{lm}\alpha^{(1)}_{mw}T_{np}a^{(2)}_{pb} + 2\alpha^{(1)}_{ij}T_{jk}\gamma^{(2)}_{klan}T_{lm}\alpha^{(1)}_{mw}T_{np}a^{(1)}_{pb}\\ &+ 2\alpha^{(1)}_{ij}T_{jk}\alpha^{(2)}_{kl}T_{lm}\gamma^{(1)}_{mwan}T_{np}a^{(2)}_{pb} + 2\gamma^{(1)}_{ijan}T_{jk}\alpha^{(2)}_{kw}T_{np}a^{(2)}_{pq}T_{qr}a^{(1)}_{rb}\\ &+ 2\alpha^{(1)}_{ij}T_{jk}\gamma^{(2)}_{kwan}T_{np}a^{(1)}_{pq}T_{qr}a^{(2)}_{rb}\Big\}\left\langle a^x_i a^x_w a^x_a a^x_b - a^y_i a^y_w a^x_a a^x_b\right\rangle.\end{aligned} \tag{2.98}$$

The isotropic averages in equations (2.85) to (2.98) are carried out using equations (2.32) and (2.33), which combine to give

$$\left\langle a^x_i a^x_j a^x_k a^x_l \;-\; a^y_i a^y_j a^x_k a^x_l\right\rangle \;=\; \tfrac{1}{30}\left(-2\delta_{ij}\delta_{kl} + 3\delta_{ik}\delta_{jl} + 3\delta_{il}\delta_{jk}\right)\;. \tag{2.99}$$

As an illustration of the procedure, the term for $\gamma_1\alpha_1$ is now evaluated explicitly:

$$\begin{aligned}
\gamma_1\alpha_1 &= \left\{\gamma^{(1)}_{ijab}T_{jk}\alpha^{(2)}_{kw} + \alpha^{(1)}_{ij}T_{jk}\gamma^{(2)}_{kwab} + 2\gamma^{(1)}_{iwaj}T_{jk}a^{(2)}_{kb}\right\}\left\langle a^x_i a^x_w a^x_a a^x_b - a^y_i a^y_w a^x_a a^x_b\right\rangle \\
&= \frac{1}{30}\left\{\gamma^{(1)}_{ijab}T_{jk}\alpha^{(2)}_{kw} + \alpha^{(1)}_{ij}T_{jk}\gamma^{(2)}_{kwab} + 2\gamma^{(1)}_{iwaj}T_{jk}a^{(2)}_{kb}\right\}\ (-2\delta_{iw}\delta_{ab} + 3\delta_{ia}\delta_{wb} + 3\delta_{ib}\delta_{wa}) \\
&= \frac{2}{30}\Big\{3\gamma^{(1)}_{ijiw}T_{jk}\alpha^{(2)}_{kw} - \gamma^{(1)}_{ijaa}T_{jk}\alpha^{(2)}_{ki} + 3\alpha^{(1)}_{ij}T_{jk}\gamma^{(2)}_{kwiw} - \alpha^{(1)}_{ij}T_{jk}\gamma^{(2)}_{kiaa} \\
&\qquad + 6\gamma^{(1)}_{iwji}T_{jk}a^{(2)}_{kw} - 2\gamma^{(1)}_{iiaj}T_{jk}a^{(2)}_{ka}\Big\}\ .
\end{aligned} \tag{2.100}$$

Note that the terms $\gamma_1\alpha_1$, $\gamma_1\alpha_2$ and $\gamma_1\alpha_3$ constitute the new work obtained by this project. The molecules treated in this project are N_2 and CO_2, which are axially-symmetric non-dipolar molecules belonging to the $D_{\infty h}$ symmetry point group, and C_2H_4, which is a planar non-dipolar molecule of D_{2h} symmetry. For the D_{2h} point group, the dynamic polarizability tensor $\alpha^{(1)}_{ij}$ has three independent components [28], namely

$$\alpha^{(1)}_{ij} = \alpha^{(2)}_{i'j'} = \begin{bmatrix} \alpha_{11} & 0 & 0 \\ 0 & \alpha_{22} & 0 \\ 0 & 0 & \alpha_{33} \end{bmatrix}\ . \tag{2.101}$$

The mean polarizability α is

$$\alpha = \tfrac{1}{3}\alpha_{ii} = \tfrac{1}{3}\left(\alpha_{11} + \alpha_{22} + \alpha_{33}\right)\ , \tag{2.102}$$

and the anisotropy in the polarizability $\Delta\alpha$ is defined as

$$\Delta\alpha = \tfrac{1}{\sqrt{2}}\left\{\left(\alpha_{11} - \alpha_{22}\right)^2 + \left(\alpha_{22} - \alpha_{33}\right)^2 + \left(\alpha_{33} - \alpha_{11}\right)^2\right\}^{1/2}\ . \tag{2.103}$$

$\alpha^{(2)}_{ij}$ is the dynamic polarizability tensor of molecule 2 expressed in the molecule-fixed axes of molecule 1, which is provided by

$$\alpha^{(2)}_{ij} = a^i_\alpha a^j_\beta a^\alpha_{i'} a^\beta_{j'} \alpha^{(2)}_{i'j'} \ . \tag{2.104}$$

The optical-frequency second hyperpolarizability for the dc Kerr-effect, namely $\gamma_{ijkl}(-\omega;\omega,0,0)$, is symmetric in the suffices ij and in the suffices kl. Standard group-theory techniques [43, 44] can be used to establish that for molecules of D_{2h} symmetry, $\gamma_{ijkl}(-\omega;\omega,0,0)$ has the 12 independent components

$$\begin{aligned}
&\gamma_{1111}\\
&\gamma_{2222}\\
&\gamma_{3333}\\
&\gamma_{1122}\\
&\gamma_{2211}\\
&\gamma_{1212} = \gamma_{2121} = \gamma_{1221} = \gamma_{2112}\\
&\gamma_{1133}\\
&\gamma_{3311}\\
&\gamma_{1313} = \gamma_{3131} = \gamma_{1331} = \gamma_{3113}\\
&\gamma_{2233}\\
&\gamma_{3322}\\
&\gamma_{2323} = \gamma_{3232} = \gamma_{2332} = \gamma_{3223} \ .
\end{aligned} \tag{2.105}$$

Consequently, for non-dipolar molecules of D_{2h} symmetry the tensors $\gamma^{(1)}_{ijkl}(-\omega;\omega,0,0)$ $= \gamma^{(2)}_{i'j'k'l'}(-\omega;\omega,0,0)$ have 21 non-zero components. The dynamic second hyperpolarizability tensor of molecule 2 expressed in the molecule-fixed axes of molecule

1 is given by

$$\gamma^{(2)}_{ijkl} = a^i_\alpha a^j_\beta a^k_\gamma a^l_\delta a^\alpha_{i'} a^\beta_{j'} a^\gamma_{k'} a^\delta_{l'} \gamma^{(2)}_{i'j'k'l'} \ . \tag{2.106}$$

For the Kerr effect, the measured second Kerr hyperpolarizability γ^{K} is defined by [2, 45]

$$\gamma^{\mathrm{K}} = \tfrac{3}{2}\Big(\gamma^{\mathrm{K}}_{\parallel}(-\omega;\omega,0,0) - \gamma^{\mathrm{K}}_{\perp}(-\omega;\omega,0,0)\Big) \ , \tag{2.107}$$

where $\gamma^{\mathrm{K}}_{\parallel}$ is the scalar component of γ_{ijkl} when the applied static electric field and the light wave field are parallel (i.e. the light-wave field is polarized in the $x-$direction of the laboratory frame), while $\gamma^{\mathrm{K}}_{\perp}$ is the scalar component when the light wave field is polarized perpendicular to the static field (i.e. in the $y-$direction). The measurable hyperpolarizability quantity γ^{K} thus contains the scalar components of γ_{ijkl} as given by

$$\gamma^{\mathrm{K}}_{\parallel} = \big\langle \gamma_{xxxx} \big\rangle = \gamma_{ijkl} \Big\langle a^x_i a^x_j a^x_k a^x_l \Big\rangle = \tfrac{1}{15}\big(\gamma_{iijj} + 2\gamma_{ijij}\big) \tag{2.108}$$

and

$$\gamma^{\mathrm{K}}_{\perp} = \big\langle \gamma_{yyxx} \big\rangle = \gamma_{ijkl} \Big\langle a^y_i a^y_j a^x_k a^x_l \Big\rangle = \tfrac{1}{15}\big(2\gamma_{iijj} - \gamma_{ijij}\big) \ . \tag{2.109}$$

Hence,

$$\gamma^{\mathrm{K}} = \tfrac{3}{2}\Big(\gamma^{\mathrm{K}}_{\parallel} - \gamma^{\mathrm{K}}_{\perp}\Big) = \tfrac{1}{10}\big(3\gamma_{ijij} - \gamma_{iijj}\big) \ . \tag{2.110}$$

For molecules of D_{2h} symmetry, the traceless electric quadrupole moment has two

independent components [28], and is given by

$$\Theta^{(1)}_{0ij} = \Theta^{(2)}_{0i'j'} = \begin{bmatrix} \Theta_{11} & 0 & 0 \\ 0 & \Theta_{22} & 0 \\ 0 & 0 & -\Theta_{11} - \Theta_{22} \end{bmatrix} . \tag{2.111}$$

Similarly,

$$\Theta^{(2)}_{0ij} = a^i_\alpha a^j_\beta a^\alpha_{i'} a^\beta_{j'} \Theta^{(2)}_{0i'j'} . \tag{2.112}$$

The second-rank $T-$tensor in space-fixed axes is [28]

$$T_{\alpha\beta} = \frac{1}{4\pi\varepsilon_0} \nabla_\alpha \nabla_\beta R^{-1} = \frac{1}{4\pi\varepsilon_0} \left(3R_\alpha R_\beta - R^2 \delta_{\alpha\beta}\right) R^{-5} . \tag{2.113}$$

In the molecule-fixed axes of molecule 1, $T_{ij} = a^i_\alpha a^j_\beta \, T_{\alpha\beta}$.

Similarly, the third-rank $T-$tensor in space-fixed axes is [28]

$$\begin{aligned} T_{\alpha\beta\gamma} &= \frac{1}{4\pi\varepsilon_0} \nabla_\alpha \nabla_\beta \nabla_\gamma R^{-1} \\ &= \frac{-3}{4\pi\varepsilon_0} \Big[5R_\alpha R_\beta R_\gamma - R^2 \big(R_\alpha \delta_{\beta\gamma} + R_\beta \delta_{\gamma\alpha} + R_\gamma \delta_{\alpha\beta} \big) \Big] R^{-7} . \end{aligned} \tag{2.114}$$

In the molecule-fixed axes of molecule 1, $T_{ijk} = a^i_\alpha a^j_\beta a^k_\gamma \, T_{\alpha\beta\gamma}$.

The tensor-manipulation package of the Macsyma algebraic manipulation program was used to evaluate the expressions for the terms in equations (2.85) to (2.98), and proved to be an invaluable aid especially for the more complex expressions. These final expressions are often extremely large, and so they are not presented here, but the Macsyma program translates them directly into Fortran code, hence minimizing the introduction of spurious typographical errors. The integration of the final

expressions over the pair-interaction coordinates as per equation (2.61) enumerates the contributions to B_{K} of each of the terms in equation (2.84).

The integral in equation (2.61) requires the intermolecular potential $U_{12}(\tau)$. As in previous work [9, 39], the classical potential

$$U_{12}(\tau) = U_{LJ} + U_{\Theta,\Theta} + U_{\Theta,\ \mathrm{ind}\ \mu} + U_{\mathrm{shape}} \tag{2.115}$$

is used, where U_{LJ} is the Lennard-Jones 6:12 potential, $U_{\Theta,\Theta}$ is the electrostatic quadrupole-quadrupole interaction energy of the two molecules, and $U_{\Theta,\ \mathrm{ind}\ \mu}$ is the quadrupole-induced dipole interaction energy. The angular dependence of short range repulsive forces for non-spherical molecules is accounted for by U_{shape}. Explicit expressions for each of these contributions to $U_{12}(\tau)$ for molecules of D_{2h} symmetry and higher have already been provided [9, 39]. In order to compute the induction energy $U_{\Theta,\ \mathrm{ind}\ \mu}$, the static molecular polarizability a_{ij} is required.

The integrals were evaluated by numerical integration using Gaussian quadrature. The ranges of the orientation angles were divided into 16 intervals each, while the intermolecular separation R was given the range of 0.1 to 3.0 nm divided into 64 intervals. An example of the Fortran programs used to compute the contributions to B_{K} is provided in Appendix A.1, this being the program to evaluate $\gamma_1\alpha_1$. All programs were run in double precision using the Salford F90 compiler on a personal computer with a dual-core processor. Run times were *ca.* 20 minutes per program.

Chapter 3 presents the results of the computations of B_{K} for the molecules N_2, CO_2 and C_2H_4, these molecules being chosen since there are experimentally measured B_{K} data reported in the literature, hence allowing for a critical comparison of experiment theory.

Chapter 3

Results

3.1 Nitrogen

The molecular data required to calculate B_{K} for the axially-symmetric homonuclear diatomic molecule N_2, which belongs to the $D_{\infty h}$ symmetry point group, are presented in Table 3.1. Optimized values for the Lennard-Jones force constants R_0 and ε/k and the shape parameter D have been obtained by fitting values of the second pressure virial coefficient $B(T)$, calculated using

$$B(T) = \frac{N_{\mathrm{A}}}{2\Omega} \int_{\tau} \left[1 - e^{-U_{12}(\tau)/kT}\right] d\tau \,, \tag{3.1}$$

to the available experimental data (as found in the tabulations of Dymond *et al.* [46]) over a range of temperature.

For axially-symmetric molecules, the two independent polarizability tensor components can be deduced from measured values of the mean polarizability $\alpha = \frac{1}{3}\alpha_{ii} = \frac{1}{3}\left(2\alpha_{\perp} + \alpha_{\parallel}\right)$ and the polarizability anisotropy $\Delta\alpha = \left(\alpha_{\parallel} - \alpha_{\perp}\right)$, where in equation (2.101), $\alpha_{11} = \alpha_{22} = \alpha_{\perp}$ and $\alpha_{33} = \alpha_{\parallel}$. This yields $\alpha_{\perp} = \alpha - \frac{1}{3}\Delta\alpha$ and $\alpha_{\parallel} = \alpha + \frac{2}{3}\Delta\alpha$.

Also, for axially-symmetric molecules, $\gamma_{ijkl}(-\omega;\omega,0,0)$ has six independent components, namely

$$\begin{aligned}
&\gamma_{1111} = \gamma_{2222} \\
&\gamma_{3333} \\
&\gamma_{1133} = \gamma_{2233} \\
&\gamma_{3311} = \gamma_{3322} \\
&\gamma_{1331} = \gamma_{3131} = \gamma_{3113} = \gamma_{1313} = \gamma_{2332} = \gamma_{3232} = \gamma_{2323} = \gamma_{3223} \\
&\gamma_{1122} = \gamma_{2211} = (\gamma_{1111} - 2\gamma_{1212}) \ .
\end{aligned} \tag{3.2}$$

Since $\gamma_{1122} = \gamma_{2211} = (\gamma_{1111} - 2\gamma_{1212})$, the following dependent components are also non-zero:

$$\gamma_{1212} = \tfrac{1}{2}\left(\gamma_{1111} - \gamma_{1122}\right) = \gamma_{2121} = \gamma_{1221} = \gamma_{2112} \ . \tag{3.3}$$

Hence, the tensors $\gamma^{(1)}_{ijkl}(-\omega;\omega,0,0) = \gamma^{(2)}_{i'j'k'l'}(-\omega;\omega,0,0)$ have a total of 21 non-zero components.

The traceless quadrupole moment has one independent component [28], given by

$$\Theta^{(1)}_{0ij} = \Theta^{(2)}_{0i'j'} = \begin{bmatrix} \Theta_{11} = -\frac{1}{2}\Theta_{33} & 0 & 0 \\ 0 & \Theta_{22} = -\frac{1}{2}\Theta_{33} & 0 \\ 0 & 0 & \Theta_{33} \end{bmatrix} . \tag{3.4}$$

All optical-frequency polarizabilities and second hyperpolarizabilities in this chapter are quoted for the helium-neon laser wavelength of $\lambda = 632.8$ nm, this being the wavelength used in almost all dc Kerr-effect experimental studies reported in the literature to date.

Hättig, Christiansen and Jørgensen have calculated the frequency-dependent second hyperpolarizability for N_2 using coupled cluster cubic response theory [47], computing the hyperpolarizability tensor components required for obtaining comparison with various experimentally measured properties, which are usually in terms of a scalar component of the tensor γ_{ijkl} [2, 34, 47]. Recall from equation (2.110) that for the Kerr effect, the measured second Kerr hyperpolarizability γ^{K} is [2, 45]

$$\gamma^{\mathrm{K}} = \tfrac{3}{2}\Big(\gamma_{\parallel}^{\mathrm{K}} - \gamma_{\perp}^{\mathrm{K}}\Big) = \tfrac{1}{10}\Big(3\gamma_{ijij}(-\omega;\omega,0,0) - \gamma_{iijj}(-\omega;\omega,0,0)\Big)\ . \qquad (3.5)$$

A CCSD wavefunction was utilized, with the triply-augmented correlation consistent polarized valence triple zeta (t-aug-cc-pVTZ) basis of Woon and Dunning [47, 48], and all calculations for the N_2 molecule were performed at its equilibrium bond length of $r_e = 1.098$ Å. This level of theory gives results of $\gamma_{ijkl}(-2\omega;\omega,\omega,0)$ which are in excellent agreement (2% at $\lambda = 632.8$ nm) with precise measured values of $\gamma_{\parallel}^{\mathrm{ESHG}}(-2\omega;\omega,\omega,0)$ deduced from electric-field-induced second-harmonic generation (ESHG) experiments [47, 49, 50], so that the calculated $\gamma_{ijkl}(-\omega;\omega,0,0)$ can be used used with confidence. While computations at the CC3 level of theory can further refine the $\gamma_{ijkl}(-2\omega;\omega,\omega,0)$ components, having been found to bring the agreement between experiment and theory for $\gamma_{\parallel}^{\mathrm{ESHG}}(-2\omega;\omega,\omega,0)$ for N_2 to 0.6% at $\lambda = 632.8$ nm [51], the computational cost rises significantly, and so evaluations of the $\gamma_{ijkl}(-\omega;\omega,0,0)$ components at the CC3 level of theory have not been implemented here.

We have installed the DALTON molecular electronic-structure program [52] on a DELL R720 PowerEdge 2.60 GHz workstation with 8-core CPU, and have reproduced the $\gamma_{ijkl}(-\omega;\omega,0,0)$ tensor-component calculations of Hättig *et al.* for a wavelength of 632.8 nm [47], proceeding to then also calculate the additionally-required γ_{1122} component for N_2. The results are reported in Table 3.1, together

with the $\gamma^{\mathrm{K}} = 0.0597 \times 10^{-60}\,\mathrm{C^4\,m^4\,J^{-3}}$ deduced using equation (3.5). The only measured γ^{K} for N_2 at $\lambda = 632.8$ nm is that obtained in 1970 by Buckingham *et al.* of $\gamma^{\mathrm{K}} = (0.09 \pm 0.01) \times 10^{-60}\,\mathrm{C^4\,m^4\,J^{-3}}$ [45]. Whenever comparing calculated and measured γ^{K} values for non-dipolar molecules, one needs to bear in mind the exceptionally demanding nature of measurement of the temperature-independent contribution to the molar Kerr constant in equation (2.42), as discussed in references [53, 54].

Tables 3.2 to 3.5 provide the relative magnitudes of the various contributions to B_{K} calculated over the temperature span 200 K to 500 K, which was chosen since the usual range of experimental temperature for Kerr-effect measurements in the literature is between these limits. In these tables, the contributions from the series in pure collision-induced polarizability (α_n), the quadrupole series ($\Theta_2\alpha_n$) and the series in the second-hyperpolarizability ($\gamma_1\alpha_n$) are each summed separately, yielding $\sum \alpha_n$, $\sum \Theta_2\alpha_n$ and $\sum \gamma_1\alpha_n$, respectively. This facilitates the comparison of their respective contributions to B_{K}. At $T = 200$ K, $\sum \alpha_n$ contributes 87.5% to B_{K}, while $\sum \Theta_2\alpha_n$ contributes 10.8% and $\sum \gamma_1\alpha_n$ only 1.7%. At $T = 500$ K, the picture is a little different, since the α_n series of terms has an inverse temperature dependence, while the $\Theta_2\alpha_n$ series has a T^{-2} dependence and the $\gamma_1\alpha_n$ series is temperature independent (see equation (2.83)). Consequently, at $T = 500$ K, $\sum \alpha_n$ contributes 91.2% to B_{K}, while the $\sum \Theta_2\alpha_n$ and $\sum \gamma_1\alpha_n$ contributions are now almost equivalent, being 4.6% and 4.2% respectively.

Table 3.1: The molecular properties of N_2 used in the calculation of B_K. All optical-frequency properties are for $\lambda = 632.8$ nm.

Property	Value	Reference
R_0 (nm)	0.368	[55]
ε/k (K)	91.50	[55]
D_1	0.112[a]	[56]
D_2	0.000	
$10^{40}\,\Theta_{11}(\mathrm{C\,m^2})$	$2.48_5 \pm 0.08$	[57]
$10^{40}\,\Theta_{22}(\mathrm{C\,m^2})$	$2.48_5 \pm 0.08$	
$10^{40}\,\Theta_{33}(\mathrm{C\,m^2})$	-4.97 ± 0.16	
$10^{40}\,\alpha(\mathrm{C^2\,m^2\,J^{-1}})$	1.967	[58]
$10^{40}\,\Delta\alpha(\mathrm{C^2\,m^2\,J^{-1}})$	0.784 ± 0.010	[57]
$10^{40}\,\alpha_{11}(\mathrm{C^2\,m^2\,J^{-1}})$	1.706 ± 0.010	[57]
$10^{40}\,\alpha_{22}(\mathrm{C^2\,m^2\,J^{-1}})$	1.706 ± 0.010	
$10^{40}\,\alpha_{33}(\mathrm{C^2\,m^2\,J^{-1}})$	2.490 ± 0.012	
$10^{40}\,a(\mathrm{C^2\,m^2\,J^{-1}})$	1.93532 ± 0.00017	[59, 60]
$10^{40}\,\Delta a(\mathrm{C^2\,m^2\,J^{-1}})$	0.757 ± 0.008	[61]
$10^{40}\,a_{11}(\mathrm{C^2\,m^2\,J^{-1}})$	1.683 ± 0.001	
$10^{40}\,a_{22}(\mathrm{C^2\,m^2\,J^{-1}})$	1.683 ± 0.001	
$10^{40}\,a_{33}(\mathrm{C^2\,m^2\,J^{-1}})$	2.440 ± 0.003	
$10^{60}\,\gamma_{1111}(\mathrm{C^4\,m^4\,J^{-3}})$	0.05147	[47]
$10^{60}\,\gamma_{3333}(\mathrm{C^4\,m^4\,J^{-3}})$	0.07796	
$10^{60}\,\gamma_{1133}(\mathrm{C^4\,m^4\,J^{-3}})$	0.02049	
$10^{60}\,\gamma_{3311}(\mathrm{C^4\,m^4\,J^{-3}})$	0.02066	
$10^{60}\,\gamma_{1331}(\mathrm{C^4\,m^4\,J^{-3}})$	0.02068	
$10^{60}\,\gamma_{1122}(\mathrm{C^4\,m^4\,J^{-3}})$	0.01711	this work
$10^{60}\,\gamma^{K}(\mathrm{C^4\,m^4\,J^{-3}})$	0.05965	this work

[a]Obtained by fitting to pressure virial coefficients reported in Ref. 46

Table 3.2: The relative magnitudes of the contributions to B_{K} for N_2 at $T = 200$ K

Contibuting Term	$10^{32} \times$ value ($\mathrm{C^2m^8J^{-2}mol^{-2}}$)	% contribution to B_{K}
α_2	0.0148	1.47
α_3	−0.2115	−20.96
α_4	1.0350	102.62
α_5	0.0396	3.93
α_6	0.0050	0.50
α_7	0.0003	0.03
$\Theta_2\alpha_3$	0.0770	7.64
$\Theta_2\alpha_4$	0.0245	2.43
$\Theta_2\alpha_5$	0.0063	0.62
$\Theta_2\alpha_6$	0.0007	0.07
$\Theta_2\alpha_7$	0.0001	0.01
$\gamma_1\alpha_1$	−0.0016	−0.16
$\gamma_1\alpha_2$	0.0177	1.76
$\gamma_1\alpha_3$	0.0006	0.06
$\sum_{n=2}^{7} \alpha_n$	0.8832	87.57
$\sum_{n=3}^{7} \Theta_2\alpha_n$	0.1086	10.77
$\sum_{n=1}^{3} \gamma_1\alpha_n$	0.0167	1.66
B_{K}	1.0085	

Table 3.3: The relative magnitudes of the contributions to B_{K} for N_2 at $T = 300$ K

Contibuting Term	$10^{32} \times$ value ($\mathrm{C^2m^8J^{-2}mol^{-2}}$)	% contribution to B_{K}
α_2	0.0062	0.96
α_3	−0.1108	−17.11
α_4	0.6584	101.65
α_5	0.0261	4.03
α_6	0.0035	0.54
α_7	0.0002	0.03
$\Theta_2\alpha_3$	0.0337	5.20
$\Theta_2\alpha_4$	0.0106	1.64
$\Theta_2\alpha_5$	0.0030	0.46
$\Theta_2\alpha_6$	0.0004	0.06
$\Theta_2\alpha_7$	0.0001	0.02
$\gamma_1\alpha_1$	−0.0012	−0.18
$\gamma_1\alpha_2$	0.0169	2.61
$\gamma_1\alpha_3$	0.0006	0.09
$\sum_{n=2}^{7} \alpha_n$	0.5836	90.10
$\sum_{n=3}^{7} \Theta_2\alpha_n$	0.0478	7.38
$\sum_{n=1}^{3} \gamma_1\alpha_n$	0.0163	2.52
B_{K}	0.6477	

Table 3.4: The relative magnitudes of the contributions to B_{K} for N_2 at $T = 400$ K

Contibuting Term	$10^{32} \times$ value ($\mathrm{C^2m^8J^{-2}mol^{-2}}$)	% contribution to B_{K}
α_2	0.0035	0.72
α_3	−0.0730	−14.93
α_4	0.4910	100.47
α_5	0.0202	4.13
α_6	0.0028	0.57
α_7	0.0002	0.04
$\Theta_2\alpha_3$	0.0194	3.97
$\Theta_2\alpha_4$	0.0062	1.27
$\Theta_2\alpha_5$	0.0019	0.39
$\Theta_2\alpha_6$	0.0002	0.04
$\Theta_2\alpha_7$	0.0000	0.00
$\gamma_1\alpha_1$	−0.0011	−0.23
$\gamma_1\alpha_2$	0.0168	3.44
$\gamma_1\alpha_3$	0.0006	0.12
$\sum_{n=2}^{7} \alpha_n$	0.4447	91.00
$\sum_{n=3}^{7} \Theta_2\alpha_n$	0.0277	5.67
$\sum_{n=1}^{3} \gamma_1\alpha_n$	0.0163	3.33
B_{K}	0.4887	

Table 3.5: The relative magnitudes of the contributions to B_{K} for N_2 at $T = 500$ K

Contibuting Term	$10^{32} \times$ value ($\mathrm{C^2m^8J^{-2}mol^{-2}}$)	% contribution to B_{K}
α_2	0.0022	0.55
α_3	−0.0532	−13.34
α_4	0.3953	99.15
α_5	0.0168	4.21
α_6	0.0024	0.60
α_7	0.0002	0.05
$\Theta_2\alpha_3$	0.0128	3.21
$\Theta_2\alpha_4$	0.0042	1.05
$\Theta_2\alpha_5$	0.0013	0.33
$\Theta_2\alpha_6$	0.0002	0.05
$\Theta_2\alpha_7$	0.0000	0.00
$\gamma_1\alpha_1$	−0.0010	−0.25
$\gamma_1\alpha_2$	0.0169	4.24
$\gamma_1\alpha_3$	0.0006	0.15
$\sum_{n=2}^{7} \alpha_n$	0.3637	91.22
$\sum_{n=3}^{7} \Theta_2\alpha_n$	0.0185	4.64
$\sum_{n=1}^{3} \gamma_1\alpha_n$	0.0165	4.14
B_{K}	0.3987	

Table 3.6: A summary of the calculated B_{K} values for N_2

T (K)	$10^{32}\, B_{\mathrm{K}}$ ($C^2m^8J^{-2}mol^{-2}$)
200	1.0085
250	0.7844
300	0.6477
350	0.5553
400	0.4887
450	0.4384
500	0.3987

Table 3.6 summarizes the calculated B_{K} temperature dependence, which is plotted together with the available measured B_{K} data for N_2 in Figure 3.1. Note that for the α_n series, the term in α_4 is dominant, contributing *ca.* 100% to B_{K} at all temperatures in the range 200 to 500 K, and the series then converges rapidly. For the $\Theta_2\alpha_n$ series, the leading $\Theta_2\alpha_3$ term is dominant, making a contribution to B_{K} of only 7.6% at 200 K, and 4.6% at 500 K, the series then converging rapidly. With the $\gamma_1\alpha_n$ series, the term in $\gamma_1\alpha_2$ makes the dominant contribution (1.8% at 200 K and 4.2% at 500 K). The series has converged sufficiently by $\gamma_1\alpha_3$ that higher-order terms need not be considered. The experimental data are of limited precision, the contributions arising from pair-interaction effects being small for non-dipolar molecules. There is considerable scatter in the measured B_{K} data, which have questionable accuracy.

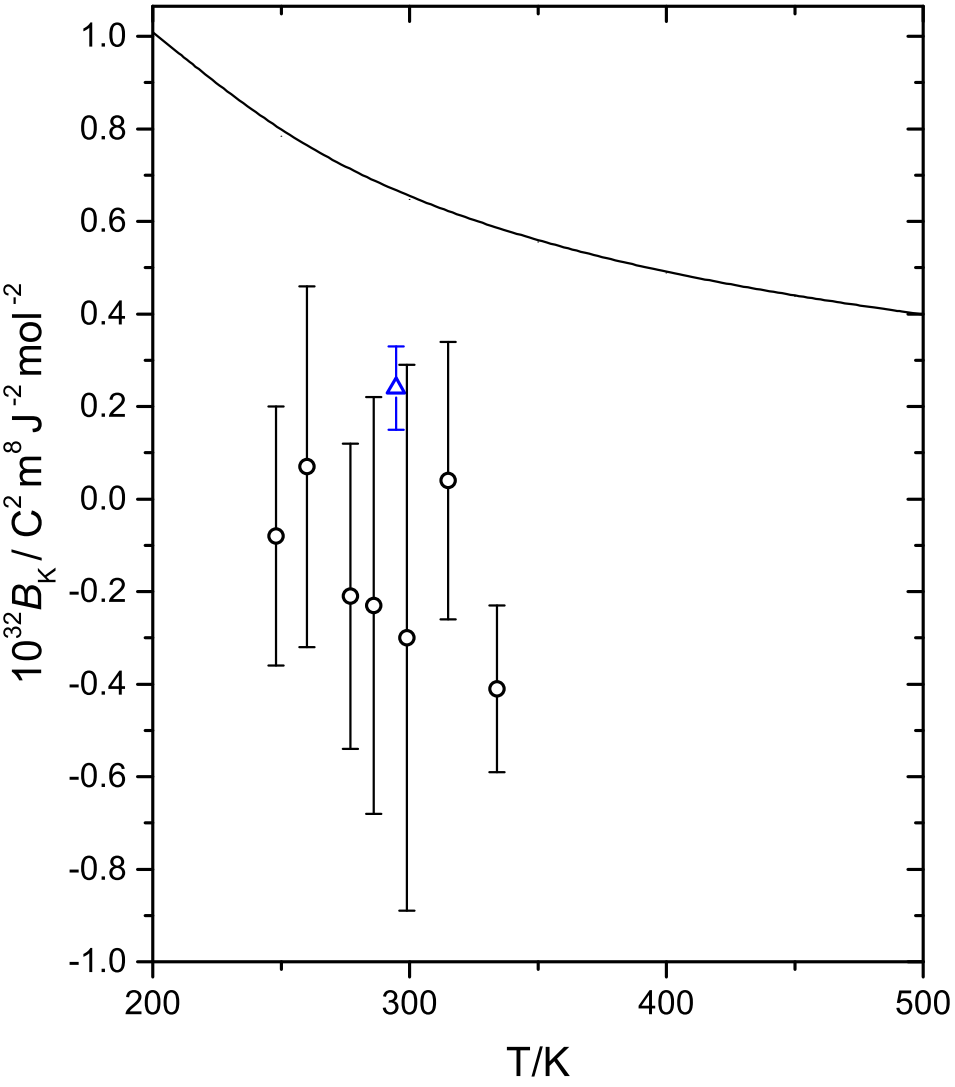

Figure 3.1: Temperature dependence of the measured and calculated B_{K} values of N_2. The solid line is our calculated curve, the circles are the measured values of Buckingham *et al.* [45] and the blue triangle is the single measured value of Read *et al.*, which is not directly comparable since it was measured at $\lambda = 590$ nm [62].

Recalling equation (2.55), namely

$$ {}_{\mathrm{m}}K = A_{\mathrm{K}} + \frac{B_{\mathrm{K}}}{V_{\mathrm{m}}} + \frac{C_{\mathrm{K}}}{V_{\mathrm{m}}^2} + \cdots \ , \tag{3.6} $$

it is now possible to calculate the $B_{\mathrm{K}}/V_{\mathrm{m}}$ pair-interaction contribution to ${}_{\mathrm{m}}K$. The molar volume is obtained by solving the equation

$$ V_{\mathrm{m}} = \frac{RT}{P}\left(1 + \frac{B(T)}{V_{\mathrm{m}}} + \frac{C(T)}{V_{\mathrm{m}}^2}\right) \ , \tag{3.7} $$

using the appropriate second and third pressure virial coefficients from the tabulations of Dymond *et al.* [46].

N_2 has a critical temperature and pressure of $T_{\mathrm{c}} = 126.2$ K and $P_{\mathrm{c}} = 3.390$ MPa, respectively. For temperatures and pressures exceeding T_{c} and P_{c}, the N_2 becomes a supercritical fluid, the phase behaviour of which becomes ambiguous, being neither a well-defined gas nor liquid. Under these conditions, the virial equation of state can become unreliable in calculating the the molar volume, and experimentally measured isotherms of the compressibility factor $Z = PV_{\mathrm{m}}/RT$ are used to obtain reliable values for V_{m}, such as the N_2 data of Nowak *et al.* [63], Klimeck *et al.* [64], Span and Wagner [65] and Mantilla *et al.* [66]. Depending on the temperature and pressure, the supercritical fluid can tend to behave more like a gas or more like a liquid.

The relative contribution made to ${}_{\mathrm{m}}K$ by interacting pairs of molecules in N_2 is now assessed over the temperature range 200 to 500 K and the pressure range 2 to 10 MPa. Typical Kerr-effect measurements in the literature have been performed for pressures up to around 1 MPa in the temperature range 250 to 500 K, though pressures up to 4 MPa are readily accessible to our existing Kerr-effect apparatus [67]. Pressures of 10 MPa could be reached, but would probably require significant modifications to the apparatus. Table 3.7 contains the N_2 inverse molar volumes (or

densities) $V_{\rm m}^{-1}$ for the temperatures 200, 300, 400 and 500 K at the pressures 2, 4 and 10 MPa. These $V_{\rm m}^{-1}$ data, combined with the $B_{\rm K}$ data in Table 3.6, yield the calculated $B_{\rm K}/V_{\rm m}$ estimates listed in Table 3.8. For comparative purposes, Table 3.8 also contains the $A_{\rm K}$ values interpolated from the Kerr-effect measurements of Buckingham *et al.* [45], together with their expected uncertainties. The only other measurement of the Kerr effect of gaseous N_2 is that of Read *et al.*, which yielded a value of $A_{\rm K} = (0.2843 \pm 0.0023) \times 10^{-27}\,{\rm C^2m^5J^{-2}mol^{-1}}$ at $\lambda = 590$ nm and $T = 294.8$ K [62].

Table 3.7: Densities (inverse molar volumes) for gaseous N_2 at relevant temperatures and pressures

T (K)	at $P = 2$ MPa, $V_{\rm m}^{-1}$ (mol m^{-3})	at $P = 4$ MPa, $V_{\rm m}^{-1}$ (mol m^{-3})	at $P = 10$ MPa, $V_{\rm m}^{-1}$ (mol m^{-3})
200	1255.6	2617.0	7152.7
300	804.1	1609.6	3989.0
400	598.0	1188.4	2906.2
500	477.3	946.7	2305.9

The smallest value for $B_{\rm K}/V_{\rm m}$ of $0.002 \times 10^{-27}\,{\rm C^2m^5J^{-2}mol^{-1}}$ (obtained at $P = 2$ MPa and $T = 500$ K) is 0.96% of $A_{\rm K}$, which is the same as the experimental uncertainty limits of Read *et al.* [62], and so lies at the presently available experimental limits of detection. Accumulating a large number of ${}_{\rm m}K$ measurements at this temperature and pressure could reduce the experimental uncertainty by up to an order of magnitude, rendering $B_{\rm K}$ contributions detectable even for the highest temperature and lowest pressure in Table 3.7. For the lower temperatures and higher pressures in the table, the $B_{\rm K}/V_{\rm m}$ contribution is generally sufficiently large that it should be measurable. This is borne out by the measurement

Table 3.8: Calculated B_K/V_m contributions to ${}_mK$ for N_2 at $\lambda = 632.8$ nm and the temperatures and pressures in Table 3.7, compared against the available measured A_K data.

T (K)	$10^{27}A_K^a$ ($C^2m^5J^{-2}mol^{-1}$)	at $P = 2$ MPa, $10^{27}B_K/V_m$ ($C^2m^5J^{-2}mol^{-1}$)	at $P = 4$ MPa, $10^{27}B_K/V_m$ ($C^2m^5J^{-2}mol^{-1}$)	at $P = 10$ MPa, $10^{27}B_K/V_m$ ($C^2m^5J^{-2}mol^{-1}$)
200	0.409 ± 0.021	0.013	0.026	0.072
300	0.298 ± 0.015^b	0.005	0.010	0.026
400	0.242 ± 0.012	0.003	0.006	0.014
500	0.209 ± 0.010	0.002	0.004	0.009

[a]These A_K values have been interpolated from the measured data in Ref. 45. The uncertainties are indicative of the experimental uncertainties in Ref. 45.

[b]To be compared with the $A_K = (0.2843 \pm 0.0023) \times 10^{-27}\,C^2m^5J^{-2}mol^{-1}$ obtained by Read *et al.* at $T = 294.8$ K and $\lambda = 590$ nm [62].

of $B_K = (0.24 \pm 0.09) \times 10^{-32}\,C^2m^8J^{-2}mol^{-2}$ attained by Read *et al.* [62] at a temperature of $T = 294.8$K and wavelength of $\lambda = 590$ nm.

Some general conclusions can be drawn from the foregoing analysis. It is clear that more accurate and precise experimental measurement of the Kerr effect of gaseous N_2 is required for a critical comparison of experiment and theory, which will require measurements at higher pressures, perhaps even up to 10 MPa. Furthermore, the collision-induced hyperpolarizability contribution to B_K is revealed to be small but non-negligible, particularly at higher temperatures, where at 500 K the contribution of 4% is almost as significant as that arising from the quadrupole series.

3.2 Carbon Dioxide

Table 3.9 contains the molecular data required for the calculation of B_{K} for the axially-symmetric CO_2 molecule. As for N_2, the $\gamma_{ijkl}(-\omega;\omega,0,0)$ tensor components were calculated using a CCSD wavefunction and a t-aug-cc-pVTZ basis set. The calculations for the CO_2 molecule were performed at the C−O equilibrium bond length of $r_{\mathrm{C-O}} = 1.161\ 226$ Å [68], and yield $\gamma^{\mathrm{K}} = 0.0823 \times 10^{-60}\,\mathrm{C^4\,m^4\,J^{-3}}$. This is to be compared with the measured γ^{K} for CO_2 obtained by Buckingham *et al.* of $\gamma^{\mathrm{K}} = (0.56 \pm 0.42) \times 10^{-60}\,\mathrm{C^4\,m^4\,J^{-3}}$ [45, 53], by Gentle *et al.* of $\gamma^{\mathrm{K}} = (0.125 \pm 0.032) \times 10^{-60}\,\mathrm{C^4\,m^4\,J^{-3}}$ [54], and by Tammer and Hüttner of $\gamma^{\mathrm{K}} = (0.040 \pm 0.026) \times 10^{-60}\,\mathrm{C^4\,m^4\,J^{-3}}$ [69].

Both the quadrupole moment of CO_2 and its polarizability anisotropy are three times larger in magnitude than those of N_2, suggesting that B_{K} for CO_2 should be considerably larger than that for N_2. This is borne out by the calculated data tabulated below, with tables 3.10 to 3.13 providing the relative magnitudes of the terms contributing to B_{K} calculated at intervals of temperature spanning $T = 200$ K to 500 K.

The quadrupole series of terms $\sum \Theta_2\alpha_n$ dominates B_{K} for lower temperatures (68.9% of B_{K} at 200 K), and even at $T = 500$ K this series contributes a substantial 45.7% to B_{K}. For the $\sum \Theta_2\alpha_n$ series, it is the leading $\Theta_2\alpha_3$ term which dominates, the series rapidly converging for higher-order quadrupole terms. Notice how, particularly at the lower temperatures, the $\sum \alpha_n$ series contribution is around an order of magnitude greater than for N_2, while the $\sum \Theta_2\alpha_n$ is around two orders of magnitude greater than for N_2. The collision-induced hyperpolarizability series of terms, $\sum \gamma_1\alpha_n$, is nearly four times larger than for N_2 at 200 K, but overall it makes a negligible 0.32% contribution to B_{K} at 200 K, and a small but non-negligible 1.5% contribution to B_{K} at 500 K.

Table 3.9: The molecular properties of CO_2 used in the calculation of B_K. All optical-frequency properties are for $\lambda = 632.8$ nm.

Property	Value	Reference
R_0 (nm)	0.400	[55]
ε/k (K)	190.0	[55]
D_1	0.250[a]	[70]
D_2	0.000	
$10^{40}\Theta_{11}(\mathrm{C\,m^2})$	$7.13_5 \pm 0.17$	[70, 71]
$10^{40}\Theta_{22}(\mathrm{C\,m^2})$	$7.13_5 \pm 0.17$	
$10^{40}\Theta_{33}(\mathrm{C\,m^2})$	-14.27 ± 0.33	
$10^{40}\alpha(\mathrm{C^2\,m^2\,J^{-1}})$	2.93141 ± 0.00021	[72]
$10^{40}\Delta\alpha(\mathrm{C^2\,m^2\,J^{-1}})$	2.356 ± 0.003	[70]
$10^{40}\alpha_{11}(\mathrm{C^2\,m^2\,J^{-1}})$	2.1461 ± 0.0012	
$10^{40}\alpha_{22}(\mathrm{C^2\,m^2\,J^{-1}})$	2.1461 ± 0.0012	
$10^{40}\alpha_{33}(\mathrm{C^2\,m^2\,J^{-1}})$	4.5021 ± 0.0012	
$10^{40}\alpha^{(0)}(\mathrm{C^2\,m^2\,J^{-1}})$	3.2402 ± 0.0004	[59, 60]
$10^{40}\Delta\alpha^{(0)}(\mathrm{C^2\,m^2\,J^{-1}})$	2.530 ± 0.009	[70, 73]
$10^{40}\alpha_{11}^{(0)}(\mathrm{C^2\,m^2\,J^{-1}})$	2.3969 ± 0.0034	
$10^{40}\alpha_{22}^{(0)}(\mathrm{C^2\,m^2\,J^{-1}})$	2.3969 ± 0.0034	
$10^{40}\alpha_{33}^{(0)}(\mathrm{C^2\,m^2\,J^{-1}})$	4.9269 ± 0.0064	
$10^{60}\gamma_{1111}(\mathrm{C^4\,m^4\,J^{-3}})$	0.07026	this work
$10^{60}\gamma_{3333}(\mathrm{C^4\,m^4\,J^{-3}})$	0.07907	
$10^{60}\gamma_{1133}(\mathrm{C^4\,m^4\,J^{-3}})$	0.03603	
$10^{60}\gamma_{3311}(\mathrm{C^4\,m^4\,J^{-3}})$	0.03674	
$10^{60}\gamma_{1331}(\mathrm{C^4\,m^4\,J^{-3}})$	0.03629	
$10^{60}\gamma_{1122}(\mathrm{C^4\,m^4\,J^{-3}})$	0.02343	
$10^{60}\,\gamma^{\mathrm{K}}(\mathrm{C^4\,m^4\,J^{-3}})$	0.08228	

[a]Obtained by fitting to pressure virial coefficients reported in Ref. 46

Table 3.10: The relative magnitudes of the contributions to B_{K} for CO_2 at $T = 200$ K

Contibuting Term	$10^{32} \times$ value ($\mathrm{C^2m^8J^{-2}mol^{-2}}$)	% contribution to B_{K}
α_2	3.039	15.57
α_3	−6.833	−35.01
α_4	9.407	48.20
α_5	0.334	1.71
α_6	0.066	0.34
α_7	0.003	0.02
$\Theta_2\alpha_3$	11.326	58.03
$\Theta_2\alpha_4$	1.624	8.32
$\Theta_2\alpha_5$	0.425	2.18
$\Theta_2\alpha_6$	0.054	0.28
$\Theta_2\alpha_7$	0.008	0.04
$\gamma_1\alpha_1$	−0.017	−0.09
$\gamma_1\alpha_2$	0.076	0.39
$\gamma_1\alpha_3$	0.003	0.02
$\sum_{n=2}^{7} \alpha_n$	6.016	30.83
$\sum_{n=3}^{7} \Theta_2\alpha_n$	13.437	68.85
$\sum_{n=1}^{3} \gamma_1\alpha_n$	0.062	0.32
B_{K}	19.515	

Table 3.11: The relative magnitudes of the contributions to B_{K} for CO_2 at $T = 300$ K

Contibuting Term	$10^{32} \times$ value ($\mathrm{C^2m^8J^{-2}mol^{-2}}$)	% contribution to B_{K}
α_2	0.919	12.74
α_3	−3.231	−44.78
α_4	4.921	68.20
α_5	0.171	2.37
α_6	0.035	0.48
α_7	0.002	0.03
$\Theta_2\alpha_3$	3.716	51.51
$\Theta_2\alpha_4$	0.470	6.51
$\Theta_2\alpha_5$	0.143	1.98
$\Theta_2\alpha_6$	0.018	0.25
$\Theta_2\alpha_7$	0.003	0.04
$\gamma_1\alpha_1$	−0.012	−0.17
$\gamma_1\alpha_2$	0.058	0.81
$\gamma_1\alpha_3$	0.002	0.03
$\sum_{n=2}^{7} \alpha_n$	2.817	39.04
$\sum_{n=3}^{7} \Theta_2\alpha_n$	4.350	60.29
$\sum_{n=1}^{3} \gamma_1\alpha_n$	0.048	0.67
B_{K}	7.215	

Table 3.12: The relative magnitudes of the contributions to B_{K} for CO_2 at $T = 400$ K

Contibuting Term	$10^{32} \times$ value ($\mathrm{C^2m^8J^{-2}mol^{-2}}$)	% contribution to B_{K}
α_2	0.445	10.68
α_3	−2.009	−48.19
α_4	3.362	80.64
α_5	0.118	2.83
α_6	0.025	0.60
α_7	0.001	0.02
$\Theta_2\alpha_3$	1.873	44.92
$\Theta_2\alpha_4$	0.222	5.33
$\Theta_2\alpha_5$	0.075	1.80
$\Theta_2\alpha_6$	0.010	0.24
$\Theta_2\alpha_7$	0.002	0.05
$\gamma_1\alpha_1$	−0.010	−0.24
$\gamma_1\alpha_2$	0.053	1.27
$\gamma_1\alpha_3$	0.002	0.05
$\sum_{n=2}^{7} \alpha_n$	1.942	46.58
$\sum_{n=3}^{7} \Theta_2\alpha_n$	2.182	52.34
$\sum_{n=1}^{3} \gamma_1\alpha_n$	0.045	1.08
B_{K}	4.169	

Table 3.13: The relative magnitudes of the contributions to B_{K} for CO_2 at $T = 500$ K

Contibuting Term	$10^{32} \times$ value ($\mathrm{C^2m^8J^{-2}mol^{-2}}$)	% contribution to B_{K}
α_2	0.265	9.10
α_3	−1.417	−48.69
α_4	2.575	88.49
α_5	0.092	3.16
α_6	0.020	0.69
α_7	0.001	0.03
$\Theta_2\alpha_3$	1.143	39.28
$\Theta_2\alpha_4$	0.132	4.54
$\Theta_2\alpha_5$	0.048	1.65
$\Theta_2\alpha_6$	0.006	0.21
$\Theta_2\alpha_7$	0.001	0.03
$\gamma_1\alpha_1$	−0.008	−0.28
$\gamma_1\alpha_2$	0.050	1.72
$\gamma_1\alpha_3$	0.002	0.07
$\sum_{n=2}^{7} \alpha_n$	1.536	52.78
$\sum_{n=3}^{7} \Theta_2\alpha_n$	1.330	45.71
$\sum_{n=1}^{3} \gamma_1\alpha_n$	0.044	1.51
B_{K}	2.910	

Table 3.14: A summary of the calculated B_{K} values for CO_2

T (K)	$10^{32}\,B_{\mathrm{K}}$ ($C^2m^8J^{-2}mol^{-2}$)
200	19.52
250	10.87
300	7.22
350	5.31
400	4.17
450	3.43
500	2.91

Table 3.14 summarizes the calculated B_{K} temperature dependence, which is plotted together with the available experimental B_{K} data for CO_2 in Figure 3.2.

The critical temperature and pressure of CO_2 are $T_{\mathrm{c}} = 304.1$ K and $P_{\mathrm{c}} = 7.4$ MPa, respectively. Reliable values for V_{m} of CO_2 have been determined as a function of pressure and temperature using experimentally-measured isotherms of the compressibility factor $Z = PV_{\mathrm{m}}/RT$, including the CO_2 data of Holste *et al.* [74], Duschek *et al.* [75], Mantilla *et al.* [76] and Gomez-Osorio *et al.* [77].

The relative contribution made to ${}_{\mathrm{m}}K$ by interacting pairs of molecules in CO_2 is now assessed over the temperature range 200 to 500 K and the pressure range 1.7 to 10 MPa. The Kerr-effect measurements in the literature for CO_2 have been performed for pressures up to around 1 MPa in the temperature range 200 to 500 K [45, 54, 69]. Table 3.15 contains the CO_2 inverse molar volumes V_{m}^{-1} for the tem-

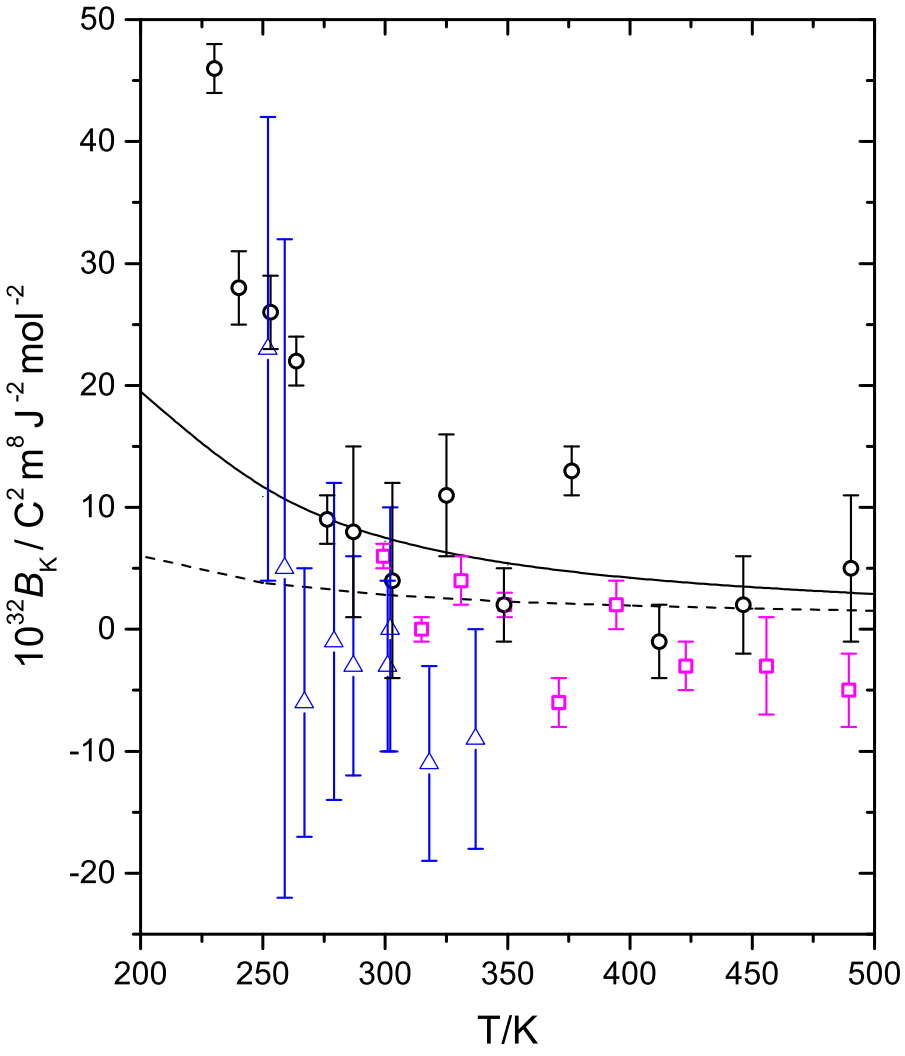

Figure 3.2: Temperature dependence of the measured and calculated B_K values of CO_2. The solid line is our calculated curve, the dashed line is the calculated curve for the pure collision-induced polarizability contributions, the blue triangles are the measured values of Buckingham *et al.* [45], the magenta squares are the measured data of Gentle *et al.* [54], while the black circles are the measured data of Tammer and Hüttner [69].

peratures 250, 300, 400 and 500 K at the pressures 1.7, 4 and 10 MPa. These V_m^{-1} data, combined with the B_K data in Table 3.14, yield the calculated B_K/V_m estimates listed in Table 3.16. For comparative purposes, Table 3.16 also contains the A_K values interpolated from the Kerr-effect measurements of Buckingham *et al.* [45], Gentle *et al.* [54] and Tammer and Hüttner [69], with their expected uncertainties.

Table 3.15: Densities (inverse molar volumes) for gaseous CO_2 at relevant temperatures and pressures

T (K)	at $P = 1.7$ MPa, V_m^{-1} (mol m^{-3})	at $P = 4$ MPa, V_m^{-1} (mol m^{-3})	at $P = 10$ MPa, V_m^{-1} (mol m^{-3})
200	–[a]	–	–
250	995.6[b]	–	–
300	747.6	2095.8	–
400	527.2	1293.2	3563.2
500	413.8	987.4	2526.2

[a]The dash – indicates temperatures and pressures for which the CO_2 is in the liquid or solid phase
[b]At $T = 250$ K, $P = 1.7$ MPa is just under the saturation vapour pressure of 1.784 MPa

The picture which emerges is that the theoretical B_K/V_m contributions for CO_2 are generally much greater than the uncertainty limits of the A_K measurements of Gentle *et al.* and of Tammer and Hüttner even for pressures of 1.7 MPa. This suggests that the measured B_K data should be more reliable than that obtained for N_2, where the B_K/V_m contributions at 2 MPa were smaller than the A_K measurement uncertainties by two to five times. However, the plot in Figure 3.2 reveals substantial scatter in the measured B_K data, confirming the considerable experimental challenge of reli-

Table 3.16: Calculated B_K/V_m contributions to ${}_mK$ for CO_2 at the temperatures and pressures in Table 3.15, compared against A_K

T (K)	$10^{27}A_K^a$ ($C^2m^8J^{-2}mol^{-2}$)	$10^{27}A_K^b$ ($C^2m^8J^{-2}mol^{-2}$)	$10^{27}A_K^c$ ($C^2m^8J^{-2}mol^{-2}$)	at $P = 1.7$ MPa, $10^{27}B_K/V_m$ ($C^2m^8J^{-2}mol^{-2}$)	at $P = 4$ MPa, $10^{27}B_K/V_m$ ($C^2m^8J^{-2}mol^{-2}$)	at $P = 10$ MPa, $10^{27}B_K/V_m$ ($C^2m^8J^{-2}mol^{-2}$)
200	3.88 ± 0.20	3.550 ± 0.003	3.674 ± 0.006	–	–	–
300	2.74 ± 0.14	2.402 ± 0.003	2.478 ± 0.006	0.054	0.151	–
400	2.17 ± 0.11	1.828 ± 0.004	1.881 ± 0.006	0.022	0.054	0.149
500	1.83 ± 0.09	1.483 ± 0.004	1.522 ± 0.006	0.012	0.029	0.074

[a]interpolated from the measured data of Buckingham *et al.* [45]
[b]interpolated from the measured data of Gentle *et al.* [54]
[c]interpolated from the measured data of Tammer and Hüttner [69]

ably measuring this property for non-dipolar species. The B_K/V_m data tabulated in Table 3.14 provides a useful guide to experimentalists, indicating the upper experimental pressures required if meaningful pair-interaction virial coefficients are to be extracted. Future experimental studies of CO_2 undertaken over pressures of up to 4 MPa would clearly assist in providing more precise and accurate B_K data.

The dashed line in the B_K versus T plot in Figure 3.2 provides the collision-induced polarizability contribution $\sum \alpha_n$ to our calculated B_K, while the solid line includes the quadrupole and (almost negligible) hyperpolarizability contributions. Comparing these two curves, it is clear that the QID contributions need to be included, particularly at lower temperatures where they become predominant. The long-range theory then provides a reasonable description of the pair-interaction contributions to the Kerr effect for CO_2. A definitive comparison of experiment and theory will require a more precise experimental determination of the temperature dependence of B_K for this molecule.

3.3 Ethene

Ethene is of D_{2h} symmetry, and it has been shown that approximating the molecule to be axially symmetric in molecular-tensor theories of electro-optical effects has resulted in considerable disagreement between calculated and measured second light-scattering virial coefficients B_ρ [56, 78] and second Kerr-effect virial coefficients B_K [79] of as much as 40%. When the full symmetry of the molecule is accounted for in describing the molecular properties, which necessitates a considerable development of the molecular-tensor theories, the calculated B_ρ is brought to within 3% of the measured value [39], and the measured and calculated B_K values over the experimental range of temperature (202 to 364 K) are brought into satisfactory agreement [12].

Bearing this caveat in mind, the contribution of γ_{ijkl} to B_K for C_2H_4 is now evaluated taking into account the full molecular symmetry. Table 3.17 contains the molecular data required for this calculation. The $\gamma_{ijkl}(-\omega;\omega,0,0)$ tensor components were calculated using a CCSD wavefunction and a t-aug-cc-pVTZ basis set. The calculations for the C_2H_4 molecule were performed at the equilibrium geometry of $r_{C-C} = 1.339$ Å, $r_{C-H} = 1.085$ Å and $\Theta_{HCH} = 117.83°$ [80], and yield $\gamma^K = 0.4509 \times 10^{-60}\,C^4\,m^4\,J^{-3}$. This is to be compared with the measured γ^K for C_2H_4 obtained by Buckingham *et al.* of $\gamma^K = (-0.04 \pm 0.25) \times 10^{-60}\,C^4\,m^4\,J^{-3}$ [45], and by Tammer and Hüttner of $\gamma^K = (0.562 \pm 0.028) \times 10^{-60}\,C^4\,m^4\,J^{-3}$ [79].

C_2H_4 has a larger polarizability than CO_2, while their quadrupole moments and polarizability anisotropies are comparable. The γ^K of C_2H_4 is more than five times that of CO_2, suggesting that the γ_{ijkl} contribution to B_K for C_2H_4 will be considerably larger than that for CO_2. This expectation is confirmed by the calculated data, which are tabulated below. Tables 3.18 to 3.21 provide the relative magnitudes of the terms contributing to B_K calculated at 100 K intervals spanning $T = 200$ K to 500 K, while Table 3.22 summarizes the calculated B_K temperature dependence.

Table 3.17: The molecular properties of C_2H_4 used in the calculation of B_K. All optical-frequency properties are for $\lambda = 632.8$ nm.

Property	Value	Reference
R_0 (nm)	0.4232	[39, 81]
ε/k (K)	190.0	[39, 81]
D_1	0.22965[a]	[39]
D_2	0.21383	
$10^{40}\Theta_{11}(\mathrm{C\,m^2})$	5.57 ± 0.63	[82]
$10^{40}\Theta_{22}(\mathrm{C\,m^2})$	-10.54 ± 0.63	
$10^{40}\Theta_{33}(\mathrm{C\,m^2})$	4.94 ± 0.33	
$10^{40}\alpha(\mathrm{C^2\,m^2\,J^{-1}})$	4.71 ± 0.03	[79]
$10^{40}\Delta\alpha(\mathrm{C^2\,m^2\,J^{-1}})$	1.92 ± 0.04	[79]
$10^{40}\alpha_{11}(\mathrm{C^2\,m^2\,J^{-1}})$	4.41 ± 0.04	[79]
$10^{40}\alpha_{22}(\mathrm{C^2\,m^2\,J^{-1}})$	3.79 ± 0.03	
$10^{40}\alpha_{33}(\mathrm{C^2\,m^2\,J^{-1}})$	5.94 ± 0.02	
$10^{40}a(\mathrm{C^2\,m^2\,J^{-1}})$	4.73 ± 0.03	[79]
$10^{40}\Delta a(\mathrm{C^2\,m^2\,J^{-1}})$	1.63 ± 0.05	[79]
$10^{40}a_{11}(\mathrm{C^2\,m^2\,J^{-1}})$	4.30 ± 0.04	[79]
$10^{40}a_{22}(\mathrm{C^2\,m^2\,J^{-1}})$	4.09 ± 0.03	
$10^{40}a_{33}(\mathrm{C^2\,m^2\,J^{-1}})$	5.81 ± 0.02	
$10^{60}\gamma_{1111}(\mathrm{C^4\,m^4\,J^{-3}})$	0.24754	this work
$10^{60}\gamma_{2222}(\mathrm{C^4\,m^4\,J^{-3}})$	0.66013	
$10^{60}\gamma_{3333}(\mathrm{C^4\,m^4\,J^{-3}})$	0.37591	
$10^{60}\gamma_{1122}(\mathrm{C^4\,m^4\,J^{-3}})$	0.14946	
$10^{60}\gamma_{2211}(\mathrm{C^4\,m^4\,J^{-3}})$	0.15790	
$10^{60}\gamma_{1212}(\mathrm{C^4\,m^4\,J^{-3}})$	0.15394	
$10^{60}\gamma_{1133}(\mathrm{C^4\,m^4\,J^{-3}})$	0.12833	
$10^{60}\gamma_{3311}(\mathrm{C^4\,m^4\,J^{-3}})$	0.13173	
$10^{60}\gamma_{1313}(\mathrm{C^4\,m^4\,J^{-3}})$	0.13056	
$10^{60}\gamma_{2233}(\mathrm{C^4\,m^4\,J^{-3}})$	0.19662	
$10^{60}\gamma_{3322}(\mathrm{C^4\,m^4\,J^{-3}})$	0.19884	
$10^{60}\gamma_{2323}(\mathrm{C^4\,m^4\,J^{-3}})$	0.19963	
$10^{60}\,\gamma^{\mathrm{K}}(\mathrm{C^4\,m^4\,J^{-3}})$	0.4509	

[a]Obtained by fitting to pressure virial coefficients reported in Ref. 46

Table 3.18: The relative magnitudes of the contributions to B_{K} for C_2H_4 at $T = 200$ K

Contibuting Term	$10^{32} \times$ value ($C^2m^8J^{-2}mol^{-2}$)	% contribution to B_{K}
α_2	23.249	35.93
α_3	−57.123	−88.28
α_4	60.747	93.88
α_5	3.491	5.40
α_6	2.054	3.17
α_7	0.197	0.30
$\Theta_2\alpha_3$	−4.997	−7.72
$\Theta_2\alpha_4$	20.495	31.67
$\Theta_2\alpha_5$	10.028	15.50
$\Theta_2\alpha_6$	4.176	6.45
$\Theta_2\alpha_7$	1.122	1.73
$\gamma_1\alpha_1$	−0.232	−0.36
$\gamma_1\alpha_2$	1.402	2.17
$\gamma_1\alpha_3$	0.101	0.16
$\sum_{n=2}^{7} \alpha_n$	32.615	50.40
$\sum_{n=3}^{7} \Theta_2\alpha_n$	30.824	47.63
$\sum_{n=1}^{3} \gamma_1\alpha_n$	1.271	1.96
B_{K}	64.710	

Table 3.19: The relative magnitudes of the contributions to B_{K} for C_2H_4 at T = 300 K

Contibuting Term	$10^{32} \times$ value ($\mathrm{C^2m^8J^{-2}mol^{-2}}$)	% contribution to B_{K}
α_2	2.826	14.48
α_3	−9.191	−47.09
α_4	20.710	106.11
α_5	1.256	6.44
α_6	0.377	1.93
α_7	0.034	0.17
$\Theta_2\alpha_3$	0.023	0.12
$\Theta_2\alpha_4$	1.752	8.98
$\Theta_2\alpha_5$	0.739	3.79
$\Theta_2\alpha_6$	0.250	1.28
$\Theta_2\alpha_7$	0.060	0.31
$\gamma_1\alpha_1$	−0.055	−0.28
$\gamma_1\alpha_2$	0.695	3.56
$\gamma_1\alpha_3$	0.042	0.22
$\sum_{n=2}^{7} \alpha_n$	16.012	82.04
$\sum_{n=3}^{7} \Theta_2\alpha_n$	2.824	14.47
$\sum_{n=1}^{3} \gamma_1\alpha_n$	0.682	3.49
B_{K}	19.518	

Table 3.20: The relative magnitudes of the contributions to B_{K} for C_2H_4 at $T = 400$ K

Contibuting Term	$10^{32} \times$ value ($C^2m^8J^{-2}mol^{-2}$)	% contribution to B_{K}
α_2	0.973	7.54
α_3	−3.940	−30.53
α_4	13.187	102.18
α_5	0.818	6.34
α_6	0.208	1.61
α_7	0.019	0.15
$\Theta_2\alpha_3$	0.120	0.93
$\Theta_2\alpha_4$	0.607	4.70
$\Theta_2\alpha_5$	0.240	1.86
$\Theta_2\alpha_6$	0.071	0.55
$\Theta_2\alpha_7$	0.015	0.12
$\gamma_1\alpha_1$	−0.032	−0.25
$\gamma_1\alpha_2$	0.585	4.54
$\gamma_1\alpha_3$	0.034	0.26
$\sum_{n=2}^{7} \alpha_n$	11.265	87.29
$\sum_{n=3}^{7} \Theta_2\alpha_n$	1.053	8.16
$\sum_{n=1}^{3} \gamma_1\alpha_n$	0.587	4.55
B_{K}	12.905	

Table 3.21: The relative magnitudes of the contributions to B_{K} for C_2H_4 at $T = 500$ K

Contibuting Term	$10^{32} \times$ value ($\mathrm{C^2m^8J^{-2}mol^{-2}}$)	% contribution to B_{K}
α_2	0.489	4.91
α_3	−2.309	−23.19
α_4	9.852	98.97
α_5	0.622	6.25
α_6	0.151	1.52
α_7	0.014	0.14
$\Theta_2\alpha_3$	0.094	0.94
$\Theta_2\alpha_4$	0.322	3.23
$\Theta_2\alpha_5$	0.126	1.27
$\Theta_2\alpha_6$	0.035	0.35
$\Theta_2\alpha_7$	0.007	0.07
$\gamma_1\alpha_1$	−0.023	−0.23
$\gamma_1\alpha_2$	0.543	5.46
$\gamma_1\alpha_3$	0.032	0.32
$\sum_{n=2}^{7} \alpha_n$	8.819	88.59
$\sum_{n=3}^{7} \Theta_2\alpha_n$	0.584	5.87
$\sum_{n=1}^{3} \gamma_1\alpha_n$	0.552	5.55
B_{K}	9.955	

Table 3.22: A summary of the calculated B_{K} values for C_2H_4

T (K)	$10^{32}\,B_{\mathrm{K}}$ ($C^2m^8J^{-2}mol^{-2}$)
200	64.71
250	28.47
300	19.52
350	15.39
400	12.91
450	11.21
500	9.96

The calculated B_{K} temperature dependence of C_2H_4 is plotted, together with the available experimental B_{K} data, in Figure 3.3.

The quadrupole series of terms $\sum \Theta_2\alpha_n$ makes a significant contribution to B_{K} of 47.6% at 200 K, but this contribution diminishes quite rapidly as the temperature increases, and is only 5.9% of B_{K} at 500 K. Conversely, the collision-induced polarizability contribution, $\sum \alpha_n$, rises from 50.4% at 200 K to 88.6% at 500 K. The collision-induced hyperpolarizability contributions, $\sum \gamma_1\alpha_n$, are a non-negligible 2.0% of B_{K} at 200 K, and this contribution steadily rises with increasing temperature, contributing a sizeable 5.5% at 500 K. All three series are seen to converge much more slowly than for N_2 or CO_2, which is presumably an artefact of the lower symmetry of the C_2H_4 molecule. This is the reason for having included terms up to α_7 and $\theta_2\alpha_7$, allowing for convergence of the series to be clearly established, and all contributions down to the *ca.* 1% level to be included.

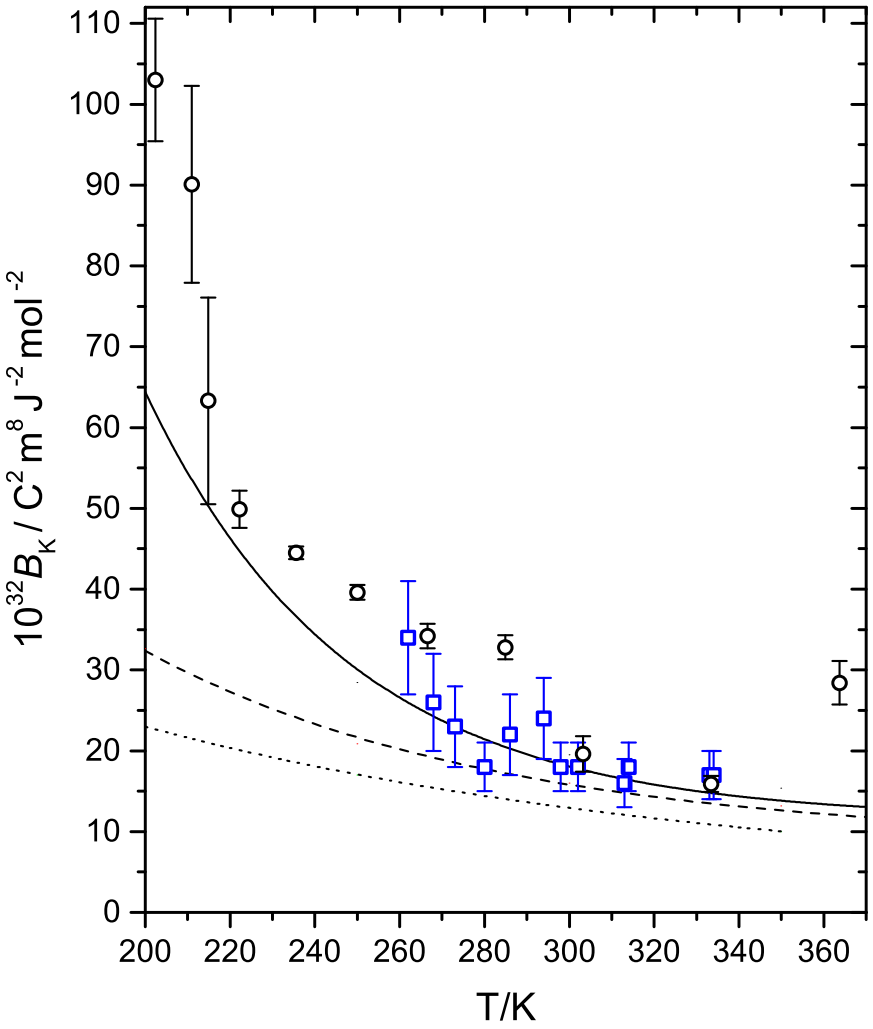

Figure 3.3: Temperature dependence of the measured and calculated B_{K} values of C_2H_4. The solid line is our calculated curve, the dashed line is our calculated curve for pure collision-induced polarizability contributions, and the dotted line is the calculated curve of Tammer and Hüttner [79] (approximating the molecule to be of axial symmetry and accounting only for collision-induced polarizability). The blue squares are the measured values of Buckingham *et al.* [45] and the black circles are the measured values of Tammer and Hüttner [79].

C_2H_4 has a critical temperature of T_c = 282.4 K and a critical pressure of P_c = 5.06 MPa. The molar volume of C_2H_4 has been accurately determined as a function of temperature and pressure through experimentally measured isotherms of the compressibility factor Z [83, 84]. Table 3.23 contains the C_2H_4 inverse molar volumes V_m^{-1} for the temperatures 250, 300, 400 and 500 K at the pressures 2, 4 and 10 MPa. These V_m^{-1} data, combined with the B_K data in Table 3.22, yield the calculated B_K/V_m estimates listed in Table 3.24. For comparative purposes, Table 3.24 also contains the A_K values interpolated from the experimental Kerr-effect data of Buckingham *et al.* [45] and Tammer and Hüttner [79].

Table 3.23: Densities (inverse molar volumes) for gaseous C_2H_4 at relevant temperatures and pressures

T (K)	at P = 2 MPa, V_m^{-1} (mol m^{-3})	at P = 4 MPa, V_m^{-1} (mol m^{-3})	at P = 10 MPa, V_m^{-1} (mol m^{-3})
200	–[a]	–	–
250	1268.8	–	–
300	911.1	2187.2	11511.2[b]
400	628.4	1315.3	3755.1
500	489.2	993.2	2565.7

[a]The dash – indicates temperatures and pressures for which the C_2H_4 is in the liquid phase
[b]For this temperature and pressure, the supercritical phase closely resembles the liquid phase, having a high density

What emerges is that the theoretical B_K/V_m contributions for C_2H_4 are even more significant than those for CO_2, the B_K for C_2H_4 being around three times larger than those of CO_2 over the 200 to 500 K temperature range. At a pressure of 2 MPa, the

Table 3.24: Calculated B_K/V_m contributions to ${}_mK$ for C_2H_4 at the temperatures and pressures in Table 3.23, compared against A_K

T (K)	$10^{27}A_K^a$ ($C^2m^8J^{-2}mol^{-2}$)	$10^{27}A_K^b$ ($C^2m^8J^{-2}mol^{-2}$)	at $P = 2$ MPa, $10^{27}B_K/V_m$ ($C^2m^8J^{-2}mol^{-2}$)	at $P = 4$ MPa, $10^{27}B_K/V_m$ ($C^2m^8J^{-2}mol^{-2}$)	at $P = 10$ MPa, $10^{27}B_K/V_m$ ($C^2m^8J^{-2}mol^{-2}$)
200	2.27 ± 0.12	2.312 ± 0.010	–	–	–
300	1.48 ± 0.08	1.707 ± 0.004	0.178	0.427	–
400	1.09 ± 0.06	1.404 ± 0.003	0.081	0.170	0.485
500	0.86 ± 0.05	1.223 ± 0.003	0.049	0.099	0.256

[a]interpolated from the measured data of Buckingham *et al.* [45]
[b]interpolated from the measured data of Tammer and Hüttner [69]

B_K/V_m contribution greatly exceeds the A_K measurement uncertainties of Tammer and Hüttner's data, which indicates that the measured B_K data should be the most reliable of the three molecules considered in this study. This is confirmed by the plot in Figure 3.3, where the measured B_K data points display a clear trend over the experimental temperature range of 202 to 364 K. These measured virial coefficients promise to provide the most stringent test of the molecular-tensor theory. Three theoretical curves are included in the plot, namely the solid line which represents our calculated B_K curve, the dashed line which is the calculated collision-induced polarizability contribution, and the dotted curve which was obtained by Tammer and Hüttner using isotropic DID theory [79]. The isotropic DID theory fails to take into account the full symmetry of the C_2H_4 molecule, and fails to model the temperature dependence of B_K. Taking into account the full symmetry of the molecule increases the calculated B_K value by 35% at 200 K, and more than 50% at 364 K, but the data still considerably underestimate the measured B_K. It is only upon inclusion of the QID terms that agreement between experiment and theory becomes satisfactory.

Of particular relevance to this project, the collision-induced hyperpolarizability contribution to B_{K} for C_2H_4 is revealed to be far from negligible, particularly at higher temperatures, where at 500 K the contribution of 5.5% is as significant as that arising from the quadrupole series.

3.4 Concluding Remarks

The existing long-range DID molecular-tensor theory accounting for intermolecular pair-interaction contributions to the Kerr effect in fluids has been extented to take into account contributions arising from the collision-induced hyperpolarizability for non-dipolar species. The second Kerr-effect virial coefficient B_{K} has been calculated over a range of temperature for the molecules N_2, CO_2 and C_2H_4. These molecules have been chosen since experimental measurements of ${}_{\mathrm{m}}K$ in the literature have provided measured data of B_{K}, and the molecular properties required in the computation of B_{K} are precisely known, or, in the case of the dynamic second hyperpolarizability tensor $\gamma_{ijkl}(-\omega;\omega,0,0)$, the properties have been calculated as part of this project.

The goal of this project was to ascertain whether the hyperpolarizability contributions to B_{K} are sufficiently small as to be safely disregarded. What emerges from the investigation is hyperpolarizability contributions to B_{K} over the temperature range $T = 200$ to 500 K of 0.3 to 1.5% for CO_2, 1.7 to 4.1% for N_2, and 2.0 to 5.5% for C_2H_4. These contributions are clearly non-negligible, and are too significant to be disregarded, particularly at the higher temperatures.

The extent to which short-range electron overlap effects will affect the collision-induced hyperpolarizability contributions for polyatomic molecules such as CO_2 and

C_2H_4 will only be revealed by full *ab initio* quantum mechanical calculations which employ large basis sets with diffuse basis functions, and which take into account the effects of electron correlation. Such calculations could prove to be computationally expensive, requiring considerable computational resources, but the findings of this project suggest that the hyperpolarizability contributions to B_{K} are sufficiently large to warrant the investigation.

This investigation has also provided, for the N_2, CO_2 and C_2H_4 molecules, useful tabulations which quantify the extent of pair-interaction contributions to A_{K} for a range of pressure and temperature. These tabulations can serve as a guide to experimentalists when undertaking future Kerr-effect investigations of these species. The tabulations indicate the range of pressures which should be investigated at each temperature if precise B_{K} values are to be extractable. Indeed, the theory can be used to construct such tabulations for any non-dipolar species provided the molecular properties used in the calculations are known to a sufficient degree of accuracy.

A useful extension to this work could be to evaluate the QID hyperpolarizability contributions, which might possibly also make a non-negligible contribution to B_{K}.

Appendix A

A.1 Fortran Program to calculate the $\gamma_1\alpha_1$ contribution to $B_{\mathbf{K}}$.

```
      PROGRAM KERR_G1A1

C PROGRAM TO CALCULATE TERM G1A1 FOR C2H4 USING GAUSSIAN INTEGRATION WITH
C 64 INTERVALS FOR THE RANGE, AND 16 INTERVALS FOR ALL ANGULAR VARIABLES
C (I.E. ALPHA1, BETA1, GAMMA1, ALPHA2, BETA2 AND GAMMA2).
C DOUBLE PRECISION IS USED THROUGHOUT.
C

C ----------------------
C SYSTEM INITIALIZATION:
C ----------------------

      IMPLICIT DOUBLE PRECISION (A-H,O-Z)
      COMMON COEF1,DCTC
      DIMENSION COEF2(64,2),COEF1(16,2),SEP(64),AL1(16),BE1(16),GA1(16)
     + ,AL2(16),BE2(16),GA2(16),DCTC(9,16,16,16),FI(16,16,16,16,16),D1(6
     + 4),E1(16,16,16,16,16),F1(16,16,16,16,16),SE3(64),SE4(64),SE5(64),
     + SE6(64),SE8(64),SE12(64),G1(16,16,16),DDP(16,16,16,16,16),DQP(16,
     + 16,16,16,16),DIDP(16,16,16,16,16)
      INTEGER X1,X2,X3,X4,X5,X6,X7


C
C MOLECULAR DATA FOR ethene (632.8 nm):
C

      SS1=0.000000
      SS2=0.000000
      SS3=0.000000
      SS4=0.000000
      SS5=0.000000
      SS6=0.000000
      SS7=0.000000
      DIP=0.000
```

```
       A11=4.41
       A22=3.79
       A33=5.94
       ALDYN=(A11+A22+A33)/3
       V11=4.30
       V22=4.09
       V33=5.81
       ALSTAT=(V11+V22+V33)/3
       Q1=5.57
       Q2=-10.54
       G1111=0.247535
       G2222=0.660134
       G3333=0.375913
       G1122=0.149460
       G2211=0.157903
       G1212=0.153936
       G1133=0.128332
       G3311=0.131727
       G1313=0.130563
       G2233=0.196620
       G3322=0.198837
       G2323=0.199626
       AMIN1=0.1000
       AMAX1=3.0000

C
C READ THE GAUSSIAN COEFFICIENTS FROM THE DATAFILE GAUSS64.DAT:
C
       OPEN(UNIT=10,FILE='GAUSS64.DAT')
         DO 10 ICTR1=1,64
           DO 20 ICTR2=1,2
             READ(10,1010,END=11)COEF2(ICTR1,ICTR2)
1010         FORMAT(F18.15)
20         CONTINUE
10       CONTINUE
11     CLOSE(UNIT=10)

C
C CALCULATE THE INTEGRATION POINTS FOR THE RANGE:
C
       SEP1=(AMAX1-AMIN1)/2
       SEP2=(AMAX1+AMIN1)/2
       DO 30 INDX=1,64
         SEP(INDX)=SEP1*COEF2(INDX,1)+SEP2
30     CONTINUE

C
C READ THE GAUSSIAN COEFFICIENTS FROM THE DATAFILE GAUSS16.DAT:
C
```

```
       OPEN(UNIT=11,FILE='GAUSS16.DAT')
         DO 100 ICTR1=1,16
           DO 110 ICTR2=1,2
             READ(11,6000,END=12)COEF1(ICTR1,ICTR2)
6000         FORMAT(F18.15)
110        CONTINUE
100      CONTINUE
12       CLOSE(UNIT=11)

C
C CALCULATE THE INTEGRATION POINTS FOR ALPHA1:
C
       AMIN=0.0
       AMAX=2.*3.14159265358979323846

       AL11=(AMAX-AMIN)/2.
       AL12=(AMAX+AMIN)/2.
       DO 120 INDX=1,16
         AL1(INDX)=AL11*COEF1(INDX,1)+AL12
120    CONTINUE

C
C CALCULATE THE INTEGRATION POINTS FOR BETA1:
C
       AMIN=0.0
       AMAX=3.14159265358979323846

       BE11=(AMAX-AMIN)/2.
       BE12=(AMAX+AMIN)/2.
       DO 121 INDX=1,16
         BE1(INDX)=BE11*COEF1(INDX,1)+BE12
121    CONTINUE

C
C CALCULATE THE INTEGRATION POINTS FOR GAMMA1:
C
       AMIN=0.0
       AMAX=2.*3.14159265358979323846

       GA11=(AMAX-AMIN)/2.
       GA12=(AMAX+AMIN)/2.
       DO 122 INDX=1,16
         GA1(INDX)=GA11*COEF1(INDX,1)+GA12
122    CONTINUE

C
C CALCULATE THE INTEGRATION POINTS FOR ALPHA2:
C
       AMIN=0.0
```

```
       AMAX=2.*3.14159265358979323846

       AL21=(AMAX-AMIN)/2.
       AL22=(AMAX+AMIN)/2.
       DO 123 INDX=1,16
         AL2(INDX)=AL21*COEF1(INDX,1)+AL22
123    CONTINUE

C
C CALCULATE THE INTEGRATION POINTS FOR BETA2:
C
       AMIN=0.0
       AMAX=3.14159265358979323846

       BE21=(AMAX-AMIN)/2.
       BE22=(AMAX+AMIN)/2.
       DO 124 INDX=1,16
         BE2(INDX)=BE21*COEF1(INDX,1)+BE22
124    CONTINUE

C
C CALCULATE THE INTEGRATION POINTS FOR GAMMA2:
C
       AMIN=0.0
       AMAX=2.*3.14159265358979323846

       GA21=(AMAX-AMIN)/2.
       GA22=(AMAX+AMIN)/2.
       DO 125 INDX=1,16
         GA2(INDX)=GA21*COEF1(INDX,1)+GA22
125    CONTINUE

C -------------
C MAIN PROGRAM:
C -------------

      OPEN(UNIT=4,FILE='kg1a1_450K')

C
C INPUT MOLECULAR PARAMETERS:
C

C       WRITE(6,470)
C470    FORMAT(1X,'INPUT THE TEMPERATURE (IN KELVIN)')
C       READ(5,471)TEMP
C471    FORMAT(F10.5)
       TEMP=450.0
       TEMPK=TEMP*1.380622E-23
```

```
C       WRITE(6,472)
C472    FORMAT(1X,'INPUT R(0) (IN nm)')
C       READ(5,473)R
C473    FORMAT(F10.5)
       R=0.4232

C       WRITE(6,474)
C474    FORMAT(1X,'E/K (IN K)')
C       READ(5,475)PARAM2
C475    FORMAT(F10.5)
       PARAM2=190.0

C       WRITE(6,476)
C476    FORMAT(1X,'SHAPE1 ')
C       READ(5,477)SHAPE1
C477    FORMAT(F10.5)
       SHAPE1=0.229650

C       WRITE(6,478)
C478    FORMAT(1X,'SHAPE2 ')
C       READ(5,479)SHAPE2
C479    FORMAT(F10.5)
       SHAPE2=0.213830

C
C CALCULATION OF THE LENNARD-JONES 6:12 POTENTIAL & STORAGE OF THE
C VALUES IN AN ARRAY:
C

       DO 61 X1=1,64

       D1(X1)=4.*PARAM2*1.380622E-23*((R/SEP(X1))**12-(R/SEP(X1))**6)
       SE12(X1)=SEP(X1)**12
       SE5(X1)=SEP(X1)**5
       SE8(X1)=SEP(X1)**8
       SE3(X1)=SEP(X1)**3
       SE4(X1)=SEP(X1)**4
       SE6(X1)=SEP(X1)**6

61     CONTINUE


C
C THE DIRECTION COSINE TENSOR COMPONENTS ARE STORED IN AN ARRAY:
C

       DO 66 X4=1,16
         DO 77 X3=1,16
           DO 88 X2=1,16
```

```
C
C DIRECTION COSINE TENSOR COMPONENTS:
C

       A1=COS(AL1(X2))*COS(BE1(X3))*COS(GA1(X4))-1.*SIN(AL1(X2))*SIN(GA1
     + (X4))
       A2=SIN(AL1(X2))*COS(BE1(X3))*COS(GA1(X4))+COS(AL1(X2))*SIN(GA1(X4
     + ))
       A3=-1.*SIN(BE1(X3))*COS(GA1(X4))
       A4=-1.*COS(AL1(X2))*COS(BE1(X3))*SIN(GA1(X4))-1.*SIN(AL1(X2))*COS
     + (GA1(X4))
       A5=-1.*SIN(AL1(X2))*COS(BE1(X3))*SIN(GA1(X4))+COS(AL1(X2))*COS(GA
     + 1(X4))
       A6=SIN(BE1(X3))*SIN(GA1(X4))
       A7=COS(AL1(X2))*SIN(BE1(X3))
       A8=SIN(AL1(X2))*SIN(BE1(X3))
       A9=COS(BE1(X3))

       DCTC(1,X2,X3,X4)=A1
       DCTC(2,X2,X3,X4)=A2
       DCTC(3,X2,X3,X4)=A3
       DCTC(4,X2,X3,X4)=A4
       DCTC(5,X2,X3,X4)=A5
       DCTC(6,X2,X3,X4)=A6
       DCTC(7,X2,X3,X4)=A7
       DCTC(8,X2,X3,X4)=A8
       DCTC(9,X2,X3,X4)=A9

88         CONTINUE
77       CONTINUE
66     CONTINUE


C
C THE MULTIPOLE INTERACTION ENERGIES ARE CALCULATED AND STORED
C IN ARRAYS:
C

       DO 939 X7=1,16
       WRITE(4,1000)X7
1000   FORMAT (1X, 'INDEX (IN RANGE 1 TO 16) IS CURRENTLY ',I2 )
       WRITE(6,1111)X7
1111   FORMAT (1X, 'Index (in range 1 to 16) is currently ',I2 )
         DO 40 X6=1,16

           DO 50 X5=1,16

C
```

```
C MOLECULE 2'S DIRECTION COSINE TENSOR COMPONENTS:
C

       B1=DCTC(1,X5,X6,X7)
       B2=DCTC(2,X5,X6,X7)
       B3=DCTC(3,X5,X6,X7)
       B4=DCTC(4,X5,X6,X7)
       B5=DCTC(5,X5,X6,X7)
       B6=DCTC(6,X5,X6,X7)
       B7=DCTC(7,X5,X6,X7)
       B8=DCTC(8,X5,X6,X7)
       B9=DCTC(9,X5,X6,X7)


             DO 60 X4=1,16
               DO 70 X3=1,16
                 DO 80 X2=1,16

C
C MOLECULE 1'S DIRECTION COSINE TENSOR COMPONENTS:
C

       A1=DCTC(1,X2,X3,X4)
       A2=DCTC(2,X2,X3,X4)
       A3=DCTC(3,X2,X3,X4)
       A4=DCTC(4,X2,X3,X4)
       A5=DCTC(5,X2,X3,X4)
       A6=DCTC(6,X2,X3,X4)
       A7=DCTC(7,X2,X3,X4)
       A8=DCTC(8,X2,X3,X4)
       A9=DCTC(9,X2,X3,X4)

C
C CALCULATION OF THE DIPOLE-DIPOLE POTENTIAL:
C
       DDP(X2,X3,X4,X5,X6)=8.98758E-24*DIP**2*(-2*A9*B9+A6*B6+A3*B3)

C
C CALCULATION OF THE DIPOLE-QUADRUPOLE POTENTIAL:
C
       DQP(X2,X3,X4,X5,X6)=8.98758E-25*DIP*(Q2*(-2*A9*B9**2+(2*A6*B6+2*A
     + 3*B3+2*A9**2-2*A8**2-A6**2+A5**2-A3**2+A2**2)*B9+2*A9*B8**2+(-2*A
     + 6*B5-2*A3*B2)*B8+A9*B6**2+(2*A5*A8-2*A6*A9)*B6-A9*B5**2+A9*B3**2+
     + (2*A2*A8-2*A3*A9)*B3-A9*B2**2)+Q1*(-2*A9*B9**2+(2*A6*B6+2*A3*B3+2
     + *A9**2-2*A7**2-A6**2+A4**2-A3**2+A1**2)*B9+2*A9*B7**2+(-2*A6*B4-2
     + *A3*B1)*B7+A9*B6**2+(2*A4*A7-2*A6*A9)*B6-A9*B4**2+A9*B3**2+(2*A1*
     + A7-2*A3*A9)*B3-A9*B1**2))

C
```

```
C CALCULATION OF THE DIPOLE-INDUCED DIPOLE POTENTIAL:
C
       DIDP(X2,X3,X4,X5,X6)=-0.50*ALSTAT*8.07765E-27*DIP**2*(3*B9**2
     + +3*A9**2-2)


C
C CALCULATION OF THE QUADRUPOLE-QUADRUPOLE POTENTIAL:
C
       quad1=-16.*(a6*a9-a5*a8)*(b6*b9-b5*b8)-16.*(a3*a9-a2*a8)*(b3*b9-b
     + 2*b8)+4.*(2.*a9**2-2.*a8**2-a6**2+a5**2-a3**2+a2**2)*(b9-b8)*(b9+
     + b8)+(-4.*a9**2+4.*a8**2+3.*a6**2-3.*a5**2+a3**2-a2**2)*(b6**2-b5*
     + *2)+4.*(a3*a6-a2*a5)*(b3*b6-b2*b5)+(-4.*a9**2+4.*a8**2+a6**2-a5**
     + 2+3.*a3**2-3.*a2**2)*(b3**2-b2**2)

       quad2=-16.*(a6*a9-a4*a7)*(b6*b9-b4*b7)-16.*(a3*a9-a1*a7)*(b3*b9-b
     + 1*b7)+4.*(2.*a9**2-2.*a7**2-a6**2+a4**2-a3**2+a1**2)*(b9-b7)*(b9+
     + b7)+(-4.*a9**2+4.*a7**2+3.*a6**2-3.*a4**2+a3**2-a1**2)*(b6**2-b4*
     + *2)+4.*(a3*a6-a1*a4)*(b3*b6-b1*b4)+(-4.*a9**2+4.*a7**2+a6**2-a4**
     + 2+3.*a3**2-3.*a1**2)*(b3**2-b1**2)

       quad3=4.*(4.*A9**2-2.*(A8**2+A7**2+A6**2+A3**2)+A5**2+A4**2+A2**2
     + +A1**2)*B9**2-16.*(2.*A6*A9-A5*A8-A4*A7)*B6*B9-16*(2.*A3*A9-A2*A8
     + -A1*A7)*B3*B9-4.*(2.*A9**2-2.*A7**2-A6**2+A4**2-A3**2+A1**2)*B8**
     + 2+16.*(A6*A9-A4*A7)*B5*B8+16.*(A3*A9-A1*A7)*B2*B8-4.*(2.*A9**2-2.
     + *A8**2-A6**2+A5**2-A3**2+A2**2)*B7**2+16.*(A6*A9-A5*A8)*B4*B7+16.
     + *(A3*A9-A2*A8)*B1*B7+(-8.*A9**2+4.*(A8**2+A7**2)+6.*A6**2-3.*(A5*
     + *2+A4**2)+2*A3**2-A2**2-A1**2)*B6**2+4.*(2.*A3*A6-A2*A5-A1*A4)*B3
     + *B6+(4.*A9**2-4.*A7**2-3.*A6**2+3.*A4**2-A3**2+A1**2)*B5**2-4.*(A
     + 3*A6-A1*A4)*B2*B5+(4.*A9**2-4.*A8**2-3.*A6**2+3.*A5**2-A3**2+A2**
     + 2)*B4**2-4.*(A3*A6-A2*A5)*B1*B4+(-8.*A9**2+4.*(A8**2+A7**2)+2.*A6
     + **2-A5**2-A4**2+6.*A3**2-3.*(A2**2+A1**2))*B3**2+(4.*A9**2-4.*A7*
     + *2-A6**2+A4**2-3.*A3**2+3.*A1**2)*B2**2+(4.*A9**2-4.*A8**2-A6**2+
     + A5**2-3.*A3**2+3.*A2**2)*B1**2

       E1(X2,X3,X4,X5,X6)=8.98758E-26*(1./3.)*(Q2**2*QUAD1+Q1**2*QUAD
     + 2+Q1*Q2*QUAD3)


C
C CALCULATION OF THE QUADRUPOLE-INDUCED DIPOLE POTENTIAL:
C

       QID1=Q2**2*(4.*A9**4+(-8.*A8**2+4.*A5**2+4.*A2**2)*A9**2+(-8.*A5*
     + A6-8.*A2*A3)*A8*A9+4.*A8**4+(4.*A6**2+4.*A3**2)*A8**2+A6**4+(-2.*
     + A5**2+2.*A3**2-2.*A2**2)*A6**2+A5**4+(2.*A2**2-2.*A3**2)*A5**2+A3
     + **4-2.*A2**2*A3**2+A2**4)+Q1**2*(4.*A9**4+(-8.*A7**2+4.*A4**2+4.*
     + A1**2)*A9**2+(-8.*A4*A6-8.*A1*A3)*A7*A9+4.*A7**4+(4.*A6**2+4.*A3*
     + *2)*A7**2+A6**4+(-2.*A4**2+2.*A3**2-2.*A1**2)*A6**2+A4**4+(2.*A1*
```

```
     + *2-2.*A3**2)*A4**2+A3**4-2.*A1**2*A3**2+A1**4)+Q1*Q2*(8.*A9**4+(-
     + 8.*A8**2-8.*A7**2+4.*A5**2+4.*A4**2+4.*A2**2+4.*A1**2)*A9**2+((-8
     + .*A5*A6-8.*A2*A3)*A8+(-8.*A4*A6-8.*A1*A3)*A7)*A9+(8.*A7**2+4.*A6*
     + *2-4.*A4**2+4.*A3**2-4.*A1**2)*A8**2+(8.*A4*A5+8.*A1*A2)*A7*A8+(4
     + .*A6**2-4.*A5**2+4.*A3**2-4.*A2**2)*A7**2+2.*A6**4+(-2.*A5**2-2.*
     + A4**2+4.*A3**2-2.*A2**2-2.*A1**2)*A6**2+(2.*A4**2-2.*A3**2+2.*A1*
     + *2)*A5**2+(2.*A2**2-2.*A3**2)*A4**2+2.*A3**4+(-2.*A2**2-2.*A1**2)
     + *A3**2+2.*A1**2*A2**2)

       QID2=Q2**2*(4.*B9**4+(-8.*B8**2+4.*B5**2+4.*B2**2)*B9**2+(-8.*B5*
     + B6-8.*B2*B3)*B8*B9+4.*B8**4+(4.*B6**2+4.*B3**2)*B8**2+B6**4+(-2.*
     + B5**2+2.*B3**2-2.*B2**2)*B6**2+B5**4+(2.*B2**2-2.*B3**2)*B5**2+B3
     + **4-2.*B2**2*B3**2+B2**4)+Q1**2*(4.*B9**4+(-8.*B7**2+4.*B4**2+4.*
     + B1**2)*B9**2+(-8.*B4*B6-8.*B1*B3)*B7*B9+4.*B7**4+(4.*B6**2+4.*B3*
     + *2)*B7**2+B6**4+(-2.*B4**2+2.*B3**2-2.*B1**2)*B6**2+B4**4+(2.*B1*
     + *2-2.*B3**2)*B4**2+B3**4-2.*B1**2*B3**2+B1**4)+Q1*Q2*(8.*B9**4+(-
     + 8.*B8**2-8.*B7**2+4.*B5**2+4.*B4**2+4.*B2**2+4.*B1**2)*B9**2+((-8
     + .*B5*B6-8.*B2*B3)*B8+(-8.*B4*B6-8.*B1*B3)*B7)*B9+(8.*B7**2+4.*B6*
     + *2-4.*B4**2+4.*B3**2-4.*B1**2)*B8**2+(8.*B4*B5+8.*B1*B2)*B7*B8+(4
     + .*B6**2-4.*B5**2+4.*B3**2-4.*B2**2)*B7**2+2.*B6**4+(-2.*B5**2-2.*
     + B4**2+4.*B3**2-2.*B2**2-2.*B1**2)*B6**2+(2.*B4**2-2.*B3**2+2.*B1*
     + *2)*B5**2+(2.*B2**2-2.*B3**2)*B4**2+2.*B3**4+(-2.*B2**2-2.*B1**2)
     + *B3**2+2.*B1**2*B2**2)

       F1(X2,X3,X4,X5,X6)=-0.5*8.07765E-29*ALSTAT*(QID1+QID2)

C
C CALCULATION OF THE INTEGRATION ARGUMENT:
C

       T11=2.*A7**2-A4**2-A1**2
       T22=2.*A8**2-A5**2-A2**2
       T33=2.*A9**2-A6**2-A3**2
       T12=2.*A7*A8-A4*A5-A1*A2
       T13=2.*A7*A9-A4*A6-A1*A3
       T23=2.*A8*A9-A5*A6-A2*A3


       Z11 = A33*(A7**2*B9**2+(2*A4*A7*B6+2*A1*A7*B3)*B9+A4**2*B6**2+2*A
     +   1*A4*B3*B6+A1**2*B3**2)+A22*(A7**2*B8**2+(2*A4*A7*B5+2*A1*A7*B2
     +   )*B8+A4**2*B5**2+2*A1*A4*B2*B5+A1**2*B2**2)+A11*(A7**2*B7**2+(2
     +   *A4*A7*B4+2*A1*A7*B1)*B7+A4**2*B4**2+2*A1*A4*B1*B4+A1**2*B1**2)

       Z22 = A33*(A8**2*B9**2+(2*A5*A8*B6+2*A2*A8*B3)*B9+A5**2*B6**2+2*A
     +   2*A5*B3*B6+A2**2*B3**2)+A22*(A8**2*B8**2+(2*A5*A8*B5+2*A2*A8*B2
     +   )*B8+A5**2*B5**2+2*A2*A5*B2*B5+A2**2*B2**2)+A11*(A8**2*B7**2+(2
     +   *A5*A8*B4+2*A2*A8*B1)*B7+A5**2*B4**2+2*A2*A5*B1*B4+A2**2*B1**2)

       Z33 = A33*(A9**2*B9**2+(2*A6*A9*B6+2*A3*A9*B3)*B9+A6**2*B6**2+2*A
```

```
+    3*A6*B3*B6+A3**2*B3**2)+A22*(A9**2*B8**2+(2*A6*A9*B5+2*A3*A9*B2
+    )*B8+A6**2*B5**2+2*A3*A6*B2*B5+A3**2*B2**2)+A11*(A9**2*B7**2+(2
+    *A6*A9*B4+2*A3*A9*B1)*B7+A6**2*B4**2+2*A3*A6*B1*B4+A3**2*B1**2)

  Z12 = A33*(A7*A8*B9**2+((A4*A8+A5*A7)*B6+(A1*A8+A2*A7)*B3)*B9+A4*
+    A5*B6**2+(A1*A5+A2*A4)*B3*B6+A1*A2*B3**2)+A22*(A7*A8*B8**2+((A4
+    *A8+A5*A7)*B5+(A1*A8+A2*A7)*B2)*B8+A4*A5*B5**2+(A1*A5+A2*A4)*B2
+    *B5+A1*A2*B2**2)+A11*(A7*A8*B7**2+((A4*A8+A5*A7)*B4+(A1*A8+A2*A
+    7)*B1)*B7+A4*A5*B4**2+(A1*A5+A2*A4)*B1*B4+A1*A2*B1**2)

  Z13 = A33*(A7*A9*B9**2+((A4*A9+A6*A7)*B6+(A1*A9+A3*A7)*B3)*B9+A4*
+    A6*B6**2+(A1*A6+A3*A4)*B3*B6+A1*A3*B3**2)+A22*(A7*A9*B8**2+((A4
+    *A9+A6*A7)*B5+(A1*A9+A3*A7)*B2)*B8+A4*A6*B5**2+(A1*A6+A3*A4)*B2
+    *B5+A1*A3*B2**2)+A11*(A7*A9*B7**2+((A4*A9+A6*A7)*B4+(A1*A9+A3*A
+    7)*B1)*B7+A4*A6*B4**2+(A1*A6+A3*A4)*B1*B4+A1*A3*B1**2)

  Z23 = A33*(A8*A9*B9**2+((A5*A9+A6*A8)*B6+(A2*A9+A3*A8)*B3)*B9+A5*
+    A6*B6**2+(A2*A6+A3*A5)*B3*B6+A2*A3*B3**2)+A22*(A8*A9*B8**2+((A5
+    *A9+A6*A8)*B5+(A2*A9+A3*A8)*B2)*B8+A5*A6*B5**2+(A2*A6+A3*A5)*B2
+    *B5+A2*A3*B2**2)+A11*(A8*A9*B7**2+((A5*A9+A6*A8)*B4+(A2*A9+A3*A
+    8)*B1)*B7+A5*A6*B4**2+(A2*A6+A3*A5)*B1*B4+A2*A3*B1**2)

  W11 = V33*(A7**2*B9**2+(2*A4*A7*B6+2*A1*A7*B3)*B9+A4**2*B6**2+2*A
+    1*A4*B3*B6+A1**2*B3**2)+V22*(A7**2*B8**2+(2*A4*A7*B5+2*A1*A7*B2
+    )*B8+A4**2*B5**2+2*A1*A4*B2*B5+A1**2*B2**2)+V11*(A7**2*B7**2+(2
+    *A4*A7*B4+2*A1*A7*B1)*B7+A4**2*B4**2+2*A1*A4*B1*B4+A1**2*B1**2)

  W22 = V33*(A8**2*B9**2+(2*A5*A8*B6+2*A2*A8*B3)*B9+A5**2*B6**2+2*A
+    2*A5*B3*B6+A2**2*B3**2)+V22*(A8**2*B8**2+(2*A5*A8*B5+2*A2*A8*B2
+    )*B8+A5**2*B5**2+2*A2*A5*B2*B5+A2**2*B2**2)+V11*(A8**2*B7**2+(2
+    *A5*A8*B4+2*A2*A8*B1)*B7+A5**2*B4**2+2*A2*A5*B1*B4+A2**2*B1**2)

  W33 = V33*(A9**2*B9**2+(2*A6*A9*B6+2*A3*A9*B3)*B9+A6**2*B6**2+2*A
+    3*A6*B3*B6+A3**2*B3**2)+V22*(A9**2*B8**2+(2*A6*A9*B5+2*A3*A9*B2
+    )*B8+A6**2*B5**2+2*A3*A6*B2*B5+A3**2*B2**2)+V11*(A9**2*B7**2+(2
+    *A6*A9*B4+2*A3*A9*B1)*B7+A6**2*B4**2+2*A3*A6*B1*B4+A3**2*B1**2)

  W12 = V33*(A7*A8*B9**2+((A4*A8+A5*A7)*B6+(A1*A8+A2*A7)*B3)*B9+A4*
+    A5*B6**2+(A1*A5+A2*A4)*B3*B6+A1*A2*B3**2)+V22*(A7*A8*B8**2+((A4
+    *A8+A5*A7)*B5+(A1*A8+A2*A7)*B2)*B8+A4*A5*B5**2+(A1*A5+A2*A4)*B2
+    *B5+A1*A2*B2**2)+V11*(A7*A8*B7**2+((A4*A8+A5*A7)*B4+(A1*A8+A2*A
+    7)*B1)*B7+A4*A5*B4**2+(A1*A5+A2*A4)*B1*B4+A1*A2*B1**2)

  W13 = V33*(A7*A9*B9**2+((A4*A9+A6*A7)*B6+(A1*A9+A3*A7)*B3)*B9+A4*
+    A6*B6**2+(A1*A6+A3*A4)*B3*B6+A1*A3*B3**2)+V22*(A7*A9*B8**2+((A4
+    *A9+A6*A7)*B5+(A1*A9+A3*A7)*B2)*B8+A4*A6*B5**2+(A1*A6+A3*A4)*B2
+    *B5+A1*A3*B2**2)+V11*(A7*A9*B7**2+((A4*A9+A6*A7)*B4+(A1*A9+A3*A
+    7)*B1)*B7+A4*A6*B4**2+(A1*A6+A3*A4)*B1*B4+A1*A3*B1**2)
```

```
      W23 = V33*(A8*A9*B9**2+((A5*A9+A6*A8)*B6+(A2*A9+A3*A8)*B3)*B9+A5*
     +   A6*B6**2+(A2*A6+A3*A5)*B3*B6+A2*A3*B3**2)+V22*(A8*A9*B8**2+((A5
     +   *A9+A6*A8)*B5+(A2*A9+A3*A8)*B2)*B8+A5*A6*B5**2+(A2*A6+A3*A5)*B2
     +   *B5+A2*A3*B2**2)+V11*(A8*A9*B7**2+((A5*A9+A6*A8)*B4+(A2*A9+A3*A
     +   8)*B1)*B7+A5*A6*B4**2+(A2*A6+A3*A5)*B1*B4+A2*A3*B1**2)


      trm1a=G3333*T33*Z33+G2323*T33*Z33+G1313*T33*Z33+G3333*T23*Z23+2
     1   *G2323*T23*Z23+G2222*T23*Z23+G1313*T23*Z23+G1212*T23*Z23+G232
     2   3*T22*Z22+G2222*T22*Z22+G1212*T22*Z22+G3333*T13*Z13+G2323*T13
     3   *Z13+2*G1313*T13*Z13+G1212*T13*Z13+G1111*T13*Z13+G2323*T12*Z1
     4   2+G2222*T12*Z12+G1313*T12*Z12+2*G1212*T12*Z12+G1111*T12*Z12+G
     5   1313*T11*Z11+G1212*T11*Z11+G1111*T11*Z11


      trm1b=G3333*T33*Z33+G3322*T33*Z33+G3311*T33*Z33+G3333*T23*Z23+G
     1   3322*T23*Z23+G3311*T23*Z23+G2233*T23*Z23+G2222*T23*Z23+G2211*
     2   T23*Z23+G2233*T22*Z22+G2222*T22*Z22+G2211*T22*Z22+G3333*T13*Z
     3   13+G3322*T13*Z13+G3311*T13*Z13+G1133*T13*Z13+G1122*T13*Z13+G1
     4   111*T13*Z13+G2233*T12*Z12+G2222*T12*Z12+G2211*T12*Z12+G1133*T
     5   12*Z12+G1122*T12*Z12+G1111*T12*Z12+G1133*T11*Z11+G1122*T11*Z1
     6   1+G1111*T11*Z11


      trm2a=G3333*T33*Z33+G2323*T33*Z33+G1313*T33*Z33+G3333*T23*Z23+2
     1   *G2323*T23*Z23+G2222*T23*Z23+G1313*T23*Z23+G1212*T23*Z23+G232
     2   3*T22*Z22+G2222*T22*Z22+G1212*T22*Z22+G3333*T13*Z13+G2323*T13
     3   *Z13+2*G1313*T13*Z13+G1212*T13*Z13+G1111*T13*Z13+G2323*T12*Z1
     4   2+G2222*T12*Z12+G1313*T12*Z12+2*G1212*T12*Z12+G1111*T12*Z12+G
     5   1313*T11*Z11+G1212*T11*Z11+G1111*T11*Z11


      trm2b=G3333*T33*Z33+G3322*T33*Z33+G3311*T33*Z33+G3333*T23*Z23+G
     1   3322*T23*Z23+G3311*T23*Z23+G2233*T23*Z23+G2222*T23*Z23+G2211*
     2   T23*Z23+G2233*T22*Z22+G2222*T22*Z22+G2211*T22*Z22+G3333*T13*Z
     3   13+G3322*T13*Z13+G3311*T13*Z13+G1133*T13*Z13+G1122*T13*Z13+G1
     4   111*T13*Z13+G2233*T12*Z12+G2222*T12*Z12+G2211*T12*Z12+G1133*T
     5   12*Z12+G1122*T12*Z12+G1111*T12*Z12+G1133*T11*Z11+G1122*T11*Z1
     6   1+G1111*T11*Z11


      trm3a=G3333*T33*W33+G2323*T33*W33+G1313*T33*W33+G3333*T23*W23+2
     1   *G2323*T23*W23+G2222*T23*W23+G1313*T23*W23+G1212*T23*W23+G232
     2   3*T22*W22+G2222*T22*W22+G1212*T22*W22+G3333*T13*W13+G2323*T13
     3   *W13+2*G1313*T13*W13+G1212*T13*W13+G1111*T13*W13+G2323*T12*W1
     4   2+G2222*T12*W12+G1313*T12*W12+2*G1212*T12*W12+G1111*T12*W12+G
     5   1313*T11*W11+G1212*T11*W11+G1111*T11*W11
```

```
      trm3b=G3333*T33*W33+G2233*T33*W33+G1133*T33*W33+G3333*T23*W23+G
     1   3322*T23*W23+G2233*T23*W23+G2222*T23*W23+G1133*T23*W23+G1122*
     2   T23*W23+G3322*T22*W22+G2222*T22*W22+G1122*T22*W22+G3333*T13*W
     3   13+G3311*T13*W13+G2233*T13*W13+G2211*T13*W13+G1133*T13*W13+G1
     4   111*T13*W13+G3322*T12*W12+G3311*T12*W12+G2222*T12*W12+G2211*T
     5   12*W12+G1122*T12*W12+G1111*T12*W12+G3311*T11*W11+G2211*T11*W1
     6   1+G1111*T11*W11


      TERM=6.*(trm1a+trm2a+2.*trm3a)-2.*(trm1b+trm2b+2.*trm3b)


       FI(X2,X3,X4,X5,X6)=(1/(6480.*3.14159265358979323846**2))*(SI
     + N(BE1(X3))*SIN(BE2(X6)))*TERM


C
C CALCULATION OF THE SHAPE POTENTIAL:
C

       G1(X3,X4,X6)=4.*PARAM2*1.380622E-23*R**12*(SHAPE1*(3.*COS(BE1(X3)
     + )**2+3.*COS(BE2(X6))**2-2.)+SHAPE2*(3.*COS(GA1(X4))**2*SIN(BE1(X3
     + ))**2+3.*COS(GA2(X7))**2*SIN(BE2(X6))**2-2.))


80               CONTINUE
70             CONTINUE
60           CONTINUE
50         CONTINUE
40       CONTINUE

C
C THE INTEGRAL IS CALCULATED:
C

         SS6=0.00
         DO 940 X6=1,16
c       WRITE(6,1911)X6
c1911   FORMAT (1X, 'sub-index (in range 1 to 16) is currently ',I2 )
           SS5=0.00
           DO 950 X5=1,16
             SS4=0.00
             DO 960 X4=1,16
               SS3=0.00
               DO 970 X3=1,16
                 SS2=0.00
                 DO 980 X2=1,16
                   SS1=0.00
                   DO 990 X1=1,64
```

```
C
C SUMMATION OF THE ENERGY TERMS WITH SUBSEQUENT DIVISION BY (-kT):
C

      G3=-1.*(D1(X1)+E1(X2,X3,X4,X5,X6)/SE5(X1)+F1(X2,X3,X4,X5,X6)/SE8(
     + X1)+G1(X3,X4,X6)/SE12(X1)+DDP(X2,X3,X4,X5,X6)/SE3(X1)+DIDP(X2,X3,
     + X4,X5,X6)/SE6(X1)+DQP(X2,X3,X4,X5,X6)/SE4(X1))/TEMPK

      IF(G3.LT.-85) GO TO 5000
      G4=2.71828**G3
      GO TO 5010
5000  G4=0
5010  SS1=SS1+(FI(X2,X3,X4,X5,X6)/(SEP(X1)**1))*G4*COEF2(X1,2)
990               CONTINUE
      SS2=SS2+SS1*COEF1(X2,2)
C
C
980             CONTINUE
      SS3=SS3+SS2*COEF1(X3,2)
C
C
970           CONTINUE
      SS4=SS4+SS3*COEF1(X4,2)
C
C
960         CONTINUE
      SS5=SS5+SS4*COEF1(X5,2)
C
C
950       CONTINUE
      SS6=SS6+SS5*COEF1(X6,2)
C
C
940     CONTINUE
      SS7=SS7+SS6*COEF1(X7,2)

C
C
939   CONTINUE
      ANS=SS7*SEP1*AL11*BE11*GA11*AL21*BE21*GA21*6.022169**2*8.98758**2
     + *1E-36

C
C THE INTEGRAL IS PRINTED TOGETHER WITH MOLECULAR DATA USED
C

      WRITE(4,2266)
```

```
2266   FORMAT(1X,'THE G1A1 TERM CONT TO B(Kerr) FOR ETHENE C2H4')
       WRITE(4,2268)
2268   FORMAT(1X,'AT THE WAVELENGTH 632.8 nm')
       WRITE(4,2267)
2267   FORMAT(1X,'   ')
       WRITE(4,2269)
2269   FORMAT(1X,'   ')
       WRITE(4,1140)ANS
1140   FORMAT(1X,'THE INTEGRAL IS',E15.7)
       WRITE(4,2150)
2150   FORMAT(1X,'INPUT DATA:')
       WRITE(4,2155)TEMP
2155   FORMAT(1X,'TEMPERATURE:       ',F10.5)
       WRITE(4,9260)ALDYN
9260   FORMAT(1X,'MEAN DYNAMIC ALPHA:',F10.5)
       WRITE(4,9261)A11
9261   FORMAT(1X,'DYNAMIC ALPHA11:   ',F10.5)
       WRITE(4,9262)A22
9262   FORMAT(1X,'DYNAMIC ALPHA22:   ',F10.5)
       WRITE(4,9263)A33
9263   FORMAT(1X,'DYNAMIC ALPHA33:   ',F10.5)
       WRITE(4,9264)ALSTAT
9264   FORMAT(1X,'MEAN STATIC ALPHA: ',F10.5)
       WRITE(4,9961)V11
9961   FORMAT(1X,'STATIC ALPHA11:    ',F10.5)
       WRITE(4,9962)V22
9962   FORMAT(1X,'STATIC ALPHA22:    ',F10.5)
       WRITE(4,9963)V33
9963   FORMAT(1X,'STATIC ALPHA33:    ',F10.5)
       WRITE(4,9970)G1111
9970   FORMAT(1X,'DYNAMIC GAMMA1111:    ',F10.5)
       WRITE(4,9971)G2222
9971   FORMAT(1X,'DYNAMIC GAMMA2222:    ',F10.5)
       WRITE(4,9972)G3333
9972   FORMAT(1X,'DYNAMIC GAMMA3333:    ',F10.5)
       WRITE(4,9973)G1122
9973   FORMAT(1X,'DYNAMIC GAMMA1122:    ',F10.5)
       WRITE(4,9974)G2211
9974   FORMAT(1X,'DYNAMIC GAMMA2211:    ',F10.5)
       WRITE(4,9975)G1212
9975   FORMAT(1X,'DYNAMIC GAMMA1212:    ',F10.5)
       WRITE(4,9976)G1133
9976   FORMAT(1X,'DYNAMIC GAMMA1133:    ',F10.5)
       WRITE(4,9977)G3311
9977   FORMAT(1X,'DYNAMIC GAMMA3311:    ',F10.5)
       WRITE(4,9978)G1313
9978   FORMAT(1X,'DYNAMIC GAMMA1313:    ',F10.5)
       WRITE(4,9979)G2233
9979   FORMAT(1X,'DYNAMIC GAMMA2233:    ',F10.5)
```

```
      WRITE(4,9980)G3322
9980  FORMAT(1X,'DYNAMIC GAMMA3322:    ',F10.5)
      WRITE(4,9981)G2323
9981  FORMAT(1X,'DYNAMIC GAMMA2323:    ',F10.5)
      WRITE(4,2190)Q1
2190  FORMAT(1X,'THETA11:           ',F10.5)
      WRITE(4,2241)Q2
2241  FORMAT(1X,'THETA22:           ',F10.5)
      WRITE(4,2210)R
2210  FORMAT(1X,'R(0):                 ',F6.5)
      WRITE(4,2220)SHAPE1
2220  FORMAT(1X,'SHAPE FACTOR 1:    ',F10.5)
      WRITE(4,2221)SHAPE2
2221  FORMAT(1X,'SHAPE FACTOR 2:    ',F10.5)
      WRITE(4,2230)PARAM2
2230  FORMAT(1X,'E/K:                ',F9.5)
      WRITE(4,2235)AMIN1,AMAX1
2235  FORMAT(1X,'MIN AND MAX POINTS OF RANGE (64 INTERVALS):',2(F10.5,3
     + X))
      WRITE(4,2240)
2240  FORMAT(1X,'END BT')
      WRITE(4,2261)
2261  FORMAT(1X,'   ')
      WRITE(4,2262)
2262  FORMAT(1X,'   ')
      WRITE(4,2263)
2263  FORMAT(1X,'   ')
      WRITE(4,2264)
2264  FORMAT(1X,'   ')
      WRITE(4,2265)
2265  FORMAT(1X,'   ')
      close(unit=4)
      END
```

Bibliography

1. J Kerr. A new relation between electricity and light: Dielectrified media birefringent. *Phil. Mag.*, 50:337–348, 1875.

2. M P Bogaard and B J Orr. Electric dipole polarisabilities of atoms and molecules. In A D Buckingham, editor, *International Review of Science, Physical Chemistry, Molecular Structure and Properties*, volume 2 of *Ser. 2*, pages 149–194, Butterworths, London, 1975.

3. C H Kwak and G Y Kim. Rigorous theory of molecular orientational nonlinear optics. *AIP Adv.*, 5:017124, 2015.

4. M Kuzyk, K Singer, and G Stegeman. Theory of molecular nonlinear optics. *Adv. Opt. Photon.*, 5:4–82, 2013.

5. A D Buckingham and J A Pople. Theoretical studies of the Kerr effect I. Deviations from a linear polarization law. *Proc. Phys. Soc. A*, 68:905–909, 1955.

6. A D Buckingham. Theoretical studies of the Kerr effect II. The influence of pressure. *Proc. Phys. Soc. A*, 68:910–919, 1955.

7. A D Buckingham and B J Orr. Kerr effect in methane and its four fluorinated derivatives. *Trans. Faraday. Soc.*, 65:673–681, 1969.

8. A D Buckingham, P A Galwas, and L Fan-Chen. Polarizabilities of interacting polar molecules. *J. Mol. Struct.*, 100:3–12, 1983.

9. V W Couling and C Graham. Second Kerr effect virial coefficients of polar molecules with linear and lower symmetry. *Mol. Phys.*, 93:31–47, 1998.

10. V W Couling and C Graham. Calculation of second Kerr effect virial coefficients of H_2S. *Mol. Phys.*, 98:135–138, 2000.

11. V W Couling, B W Halliburton, R I Keir, and G L D Ritchie. Anisotropic molecular polarizabilities of HCHO, CH_3CHO, and CH_3COCH_3. Rayleigh depolarization ratios of HCHO and CH_3CHO and first and second Kerr virial coefficients of CH_3COCH_3. *J. Phys. Chem. A*, 105:4365–4370, 2001.

12. P Naidoo. *Second Kerr-effect Virial Coefficients of Non-dipolar Molecules with Axial and Lower Symmetry.* Master's thesis, University of KwaZulu-Natal, 2017.

13. E A Donley and D P Shelton. Hyperpolarizabilities measured for interacting molecular pairs. *Chem. Phys. Lett.*, 215:156–162, 1993.

14. E P Concannon. *Hyperpolarizabilities of Interacting Atoms.* PhD thesis, University of Cambridge, 1996.

15. A D Buckingham, E P Concannon, and I D Hands. Hyperpolarizability of Interacting Atoms. *J. Phys. Chem.*, 98:10455–10459, 1994.

16. K L C Hunt. Long-range dipoles, quadrupoles, and hyperpolarizability of interacting inert-gas atoms. *Chem. Phys. Lett.*, 70:336–342, 1980.

17. E A Donley and D P Shelton. Erratum: Hyperpolarizabilities measured for interacting molecular pairs (Chem. Phys. Letters 215 (1993) 156). *Chem. Phys. Lett.*, 228:701, 1994.

18. A D Buckingham and B D Utting. Intermolecular forces. *Ann. Rev. Phys. Chem.*, 21:287–316, 1970.

19. D M Bishop and M Dupuis. The interaction polarizability and interaction second-hyperpolarizability for $He \cdots He$. *Mol. Phys.*, 88:887–898, 1996.

20. X Li, K L C Hunt, J Pipin, and D M Bishop. Long-range, collision-induced hyperpolarizabilities of atoms or centrosymmetric linear molecules: Theory and numerical results for pairs containing H or He. *J. Chem. Phys.*, 105:10954–10968, 1996.

21. B Fernández, C Hättig, H Koch, and A Rizzo. *Ab initio* calculation of the frequency-dependent interaction induced hyperpolarizability of Ar_2. *J. Chem. Phys.*, 110:2872–2882, 1999.

22. C Hättig, H Larsen, J Olsen, P Jørgensen, H Koch, B Fernández, and A Rizzo. The effect of intermolecular interactions on the electric properties of helium and argon. I. *Ab initio* calculation of the interaction induced polarizability and hyperpolarizability in He_2 and Ar_2. *J. Chem. Phys.*, 111:10099–10107, 1999.

23. H Koch, C Hättig, H Larsen, J Olsen, P Jørgensen, B Fernández, and A Rizzo. The effect of intermolecular interactions on the electric properties of helium and argon. II. The dielectric, refractivity, Kerr, and hyperpolarizability second virial coefficients. *J. Chem. Phys.*, 111:10108–10118, 1999.

24. G Maroulis. Computational aspects of interaction hyperpolarizability calculations. A study on $H_2 \cdots H_2$, $Ne \cdots HF$, $Ne \cdots FH$, $He \cdots He$, $Ne \cdots Ne$, $Ar \cdots Ar$, and $Kr \cdots Kr$. *J. Phys. Chem. A*, 104:4772–4779, 2000.

25. J L Cacheiro, B Fernández, D Marchesan, S Coriani, C Hättig, and A Rizzo. Coupled cluster calculations of the ground state potential and interaction induced electric properties of the mixed dimers of helium, neon and argon. *Mol. Phys.*, 102:101–110, 2004.

26. A Rizzo, S Coriani, D Marchesan, J L Cacheiro, B Fernández, and C Hättig. Density dependence of electric properties of binary mixtures of inert gases. *Mol. Phys.*, 104:305–318, 2006.

27. A D Buckingham and B J Orr. Molecular hyperpolarisabilities. *Q. Rev. Chem. Soc.*, 21:195–212, 1967.

28. A D Buckingham. Permanent and induced molecular moments and long-range intermolecular forces. *Adv. Chem. Phys.*, 12:107–142, 1967.

29. A D Buckingham. Molecular quadrupole moments. *Quart. Rev.*, 13:183–214, 1959.

30. L D Barron. *Molecular Light Scattering and Optical Activity.* Cambridge University Press, Cambridge, 2004.

31. R E Raab and O L de Lange. *Multipole Theory in Electromagnetism.* Clarendon Press, Oxford, 2005.

32. D A Imrie. *The Measurement of Electric Quadrupole Moments of Gas Molecules by Induced Birefringence.* PhD thesis, University of Natal, 1993.

33. A Willetts, J E Rice, D M Burland, and D P Shelton. Problems in the comparison of theoretical and experimental hyperpolarizabilities. *J. Chem. Phys.*, 97: 7590–7599, 1992.

34. D P Shelton and J E Rice. Measurements and calculations of the hyperpolarizabilities of atoms and small molecules in the gas phase. *Chem. Rev.*, 94:3–29, 1994.

35. G Otterbein. Kerr effect of benzene and derivatives. *Phys. Z.*, 35:249–265, 1934.

36. A D Buckingham. Frequency dependence of the Kerr constant. *Proc. Roy. Soc. London A*, 267:271–282, (1962).

37. A L Andrews and A D Buckingham. The effect of strong electric and magnetic fields on the depolarization ratios of gases. *Mol. Phys.*, 3:183–189, 1960.

38. A D Buckingham and J A Pople. Electromagnetic properties of compressed gases. *Disc. Faraday Soc.*, 22:17–21, 1956.

39. V W Couling and C Graham. Calculation and measurement of the second light-scattering virial coefficients of nonlinear molecules: a study of ethene. *Mol. Phys.*, 87:779–799, 1996.

40. V W Couling and C Graham. Measurement and interpretation of the second light-scattering virial coefficients of linear and quasi-linear molecules. *Mol. Phys.*, 82:235–244, 1994.

41. V W Couling and C Graham. Depolarized interaction-induced Rayleigh light scattering in gaseous SO_2. *Mol. Phys.*, 96:921–925, 1999.

42. V W Couling and R V Nhlebela. Calculation and measurement of the second light-scattering virial coefficient of $(CH_3)_2O$. *Phys. Chem. Chem. Phys.*, 3:4551–4554, 2001.

43. R R Birss. Macroscopic symmetry in space-time. *Rep. Prog. Phys.*, 26:307–360, 1963.

44. R R Birss. *Symmetry and Magnetism.* North-Holland, Amsterdam, 1966.

45. A D Buckingham, M P Bogaard, D A Dunmur, C P Hobbs, and B J Orr. Kerr effect in some simple non-dipolar gases. *Trans. Faraday Soc.*, 66:1548–1553, 1970.

46. J H Dymond, K N Marsh, R C Wilhoit, and K C Wong. *The Virial Coefficients of Pure Gases and Mixtures.* Springer-Verlag, Berlin, 2002.

47. C Hättig, O Christiansen, and P Jørgensen. Frequency-dependent second hyperpolarizabilities using coupled cluster cubic response theory. *Chem. Phys. Lett.*, 282:139–146, 1998.

48. D E Woon and T H Dunning. Gaussian basis sets for use in correlated molecular calculations. IV. Calculation of static electrical response properties. *J. Chem. Phys.*, 100:2975–2988, 1994.

49. Y Mizrahi and D P Shelton. Dispersion of nonlinear susceptibilities of Ar, N_2 and O_2 measured and compared. *Phys. Rev. Lett.*, 55:696–699, 1985.

50. Y Mizrahi and D P Shelton. Deviations from Kleinman symmetry measured for several simple atoms and molecules. *Phys. Rev. A.*, 31:3145–3154, 1985.

51. F Pawlowski, P Jørgensen, and C Hättig. The second hyperpolarizability of the N_2 molecule calculated using the approximate coupled cluster triples model CC3. *Chem. Phys. Lett.*, 413:272–279, 2005.

52. K Aidas, C Angeli, K L Bak, V Bakken, R Bast, L Boman, O Christiansen, R Cimiraglia, S Coriani, P Dahle, E K Dalskov, U Ekström, T Enevoldsen, J J Eriksen, P Ettenhuber, B Fernández, L Ferrighi, H Fliegl, L Frediani, K Hald, A Halkier, C Hättig, H Heiberg, T Helgaker, A C Hennum, H Hettema, E Hjertenæs, S Høst, I-M Høyvik, M S Iozzi, B Jansík, J H A Jensen, D Jonsson, P Jørgensen, J Kauczor, S Kirpekar, T Kjærgaard, W Klopper, S Knecht, R Kobayashi, H Koch, J Kongsted, A Krapp, K Kristensen, A Ligabue, O B Lutnæs, J I Melo, K V Mikkelsen, R H Myhre, C Neiss, C B Nielsen, P Norman, J Olsen, J M H Olsen, A Osted, M J Packer, F Pawlowski, T B Pedersen, O F Provasi, S Reine, Z Rinkevicius, T A Ruden, K Ruud, V V Rybkin, P Sałek, C C M Samson, A S de Merás, T Saue, S P A Sauer, B Schimmelpfennig, K Sneskov, A H Steindal, K O Sylvester-Hvid, P R Taylor, A M Teale, E I Tellgren, D P Tew, A J Thorvaldsen, L Thøgersen, O Vahtras, M A Watson, D J D Wilson, M Ziolkowski, and H Ågren. The Dalton quantum chemistry program system. *WIREs Comput. Mol. Sci.*, 4:269–284, 2014.

53. D P Shelton. Hyperpolarizability dispersion measured for CO_2. *J. Chem. Phys.*, 85:4234–4239, 1986.

54. I R Gentle, D R Laver, and G L D Ritchie. Second hyperpolarizability and static polarizability anisotropy of carbon dioxide. *J. Phys. Chem.*, 93:3035–3038, 1989.

55. J O Hirschfelder, C F Curtiss, and R B Bird. *Molecular Theory of Gases and Liquids*. Wiley, New York, 1954.

56. C Graham. Calculations of second light-scattering virial coefficients of linear and quasi-linear molecules. *Mol. Phys.*, 77:291–309, 1992.

57. G L D Ritchie, J N Watson, and R I Keir. Temperature dependence of electric field-gradient induced birefringence (Buckingham effect) and molecular quadrupole moment of N_2. Comparison of experiment and theory. *Chem. Phys. Lett.*, 370:376–380, 2003.

58. M P Bogaard, A D Buckingham, R K Pierens, and A H White. Rayleigh scattering depolarization ratio and molecular polarizability anisotropy for gases. *J. Chem. Soc. Faraday Trans. I*, 74:3008–3015, 1978.

59. J W Schmidt and M R Moldover. Dielectric permittivity of eight gases measured with cross capacitors. *Int. J. Thermophys.*, 24:375–403, 2003.

60. U Hohm. Experimental static dipole-dipole polarizabilities of molecules. *J. Mol. Struct.*, 1054–1055:282–292, 2013.

61. W J Meath and A Kumar. Reliable isotropic and anisotropic dipolar dispersion energies, evaluated using constrained dipole oscillator strength techniques, with application to interactions involving H_2, N_2, and the rare gases. *Int. J. Quantum Chem.*, 24:501–520, 1990.

62. S C Read, A D May, and G D Sheldon. The Kerr effect in He, Ne, H_2, and N_2 at room temperature. *Can. J. Phys.*, 75:211–230, 1997.

63. P Nowak, R Kleinrahm, and W Wagner. Measurement and correlation of the (p, ρ, T) relation of nitrogen I. The homogeneous gas and liquid regions in the temperature range from 66 K to 340 K at pressures up to 12 MPa. *J. Chem. Thermodyn.*, 29:1137–1156, 1997.

64. J Klimeck, R Kleinrahm, and W Wagner. An accurate single-sinker densimeter and measurements of the (p, ρ, T) relation of argon and nitrogen in the temperature range from (235 to 520) K at pressures up to 30 MPa. *J. Chem. Thermodyn.*, 30:1571–1588, 1998.

65. R Span and W Wagner. Equations of state for technical applications. II. Results for nonpolar fluids. *Int. J. Thermodyn.*, 24:41–109, 2003.

66. I D Mantilla, D E Cristancho, S Ejaz, and K R Hall. New P–ρ–T data for nitrogen at temperatures from (265 to 400) K at pressures up to 150 MPa. *J. Chem. Eng. Data*, 55:4227–4230, 2010.

67. C M Mthembu. *Experimental Investigation of Electric-field-induced Birefringence in Fluids*. Master's thesis, University of KwaZulu-Natal, 2015.

68. H Sekino and R J Bartlett. Molecular hyperpolarizabilities. *J. Chem. Phys.*, 98:3022–3037, 1993.

69. R Tammer. *Druk- und Temperatur-Abhängigkeit des Kerr-Effektes niedermolekularer Gase*. PhD thesis, Universität Ulm, 1991.

70. P C Balachandran Pillai and V W Couling. Dispersion of the Rayleigh light-scattering virial coefficients and polarisability anisotropy of CO_2. *Mol. Phys.*, 117:289–297, 2019.

71. N Chetty and V W Couling. Measurement of the electric quadrupole moments of CO_2 and OCS. *Mol. Phys.*, 109:655–666, 2011.

72. U Hohm. Frequency-dependence of second refractivity virial coefficients of small molecules between 325 nm and 633 nm. *Mol. Phys.*, 81:157–168, 1994.

73. A Chrissanthopoulos, U Hohm, and U Wachsmuth. Frequency-dependence of the polarizability anisotropy of CO_2 revisited. *J. Mol. Struct.*, 526:323–328, 2000.

74. J C Holste, K R Hall, P T Eubank, G Esper, M Q Watson, W Warowny, D M Bailey, J G Young, and M T J Bellomy. Experimental (P, V_m, T) for pure CO_2 between 220 and 450 K. *J. Chem. Thermodyn.*, 19:1233–1250, 1987.

75. W Duschek, R Kleinrahm, and W Wagner. Measurement and correlation of the (pressure, density, temperature) relation of carbon dioxide I. The homogeneous gas and liquid regions in the temperature range from 217 K to 340 K at pressures up to 9 MPa. *J. Chem. Thermodyn.*, 22:827–840, 1990.

76. I D Mantilla, D E Cristancho, S Ejaz, and K R Hall. $P - \rho - T$ data for carbon dioxide from (310 to 450) K up to 160 MPa. *J. Chem. Eng. Data*, 55:4611–4613, 2010.

77. M A Gomez-Osorio, R A Browne, K R Carvajal Diaz, M Hall, and J C Holste. Density measurements for ethane, carbon dioxide, and methane + nitrogen mixtures from 300 to 470 K up to 137 MPa using a vibrating tube densimeter. *J. Chem. Eng. Data*, 61:2791–2798, 2016.

78. V W Couling and C Graham. Higher-order dipole-dipole, dipole-quadrupole and field gradient contributions to the second light-scattering virial coefficient. *Mol. Phys.*, 79:859–867, 1993.

79. R Tammer and W Hüttner. Kerr effect and polarizability tensor of gaseous ethene. *Mol. Phys.*, 83:579–590, 1994.

80. G Maroulis. A study of basis set and electron correlation effects in the *ab initio* calculation of the electric dipole hyperpolarizability of ethene ($H_2C{=}CH_2$). *J. Chem. Phys.*, 97:4188–4194, 1992.

81. Y Das Gupta, Y Singh, and S Singh. Effect of shape of molecules on transport and equilibrium properties of nonpolar polyatomic gases. *J. Chem. Phys.*, 59: 1999–2006, 1973.

82. W Majer, P Lutzmann, and W Hüttner. The molecular electric quadrupole tensor of ethene from the rotational Zeeman effect of $CH_2{=}CD_2$. *Mol. Phys.*, 83:567–578, 1994.

83. P Claus, R Kleinrahm, and W Wagner. Measurements of the (p, ρ, T) relation of ethylene, ethane, and sulphur hexafluoride in the temperature range from 235 K to 520 K at pressures up to 30 MPa using an accurate single-sinker densimeter. *J. Chem. Thermodyn.*, 35:159–175, 2003.

84. J Smukala, R Span, and W Wagner. New equation of state for ethylene covering the fluid region for temperatures from the melting line to 450 K at pressures up to 300 MPa. *J. Phys. Chem. Ref. Data*, 29:1053–1121, 2000.